COUPLED LOW TEMPERATURE ALGAE HYDROTHERMAL LIQUEFACTION AND CATALYTIC HYDROTREATING TO PRODUCE LOW NITROGEN FUEL INTERMEDIATES

by

WILLIAM V. COSTANZO

(Under the Direction of James Kastner)

ABSTRACT

A four-stage hydrothermal liquefaction and catalytic upgrading process was used to generate a refinery-grade biocrude from algae biomass. Low-temperature liquefaction (PT: 225 °C, 15 min) was implemented to hydrolyze algal proteins and partition nitrogen from the solid phase. The aqueous co-product was analyzed for nutrient and toxin concentrations. The retained solid biomass was subjected to a higher temperature hydrothermal liquefaction (HTL: 350 °C, 60 min). Heterogeneous catalytic hydrodeoxygenation (HDO: 350 °C, 240 min) was conducted using ruthenium (5% on carbon), several forms of cobalt molybdenum catalysts (on aluminum oxide), and a H_2-reduced mixed metal oxide (mainly iron oxide) byproduct known as red mud. The extent of HDO/HDN was limited by low hydrogen concentrations stemming from the consumption of this reactant in a batch atmosphere, and thus the HDO stage was repeated twice per batch, with fresh hydrogen recharged. Implementing all four stages with ruthenium on carbon as catalyst produced the most favorable biocrude, with minimal nitrogen levels and a chemical composition dominated by alkanes and aromatics. Macromolecular degradation pathways were also studied by performing HTL and HDO on model lipids, proteins, and carbohydrates in varying representative ratios.

INDEX WORDS: Hydrothermal Liquefaction, Algae, Bio-oil, Catalytic Hydrotreating

Coupled Low Temperature Algae Hydrothermal Liquefaction and Catalytic Hydrotreating to Produce Low Nitrogen Fuel Intermediates

by

William V. Costanzo

B.S. in Biochemical Engineering, University of Georgia, 2013

M.S. in Biochemical Engineering, University of Georgia, 2015

A Thesis Submitted to the Graduate Faculty

of The University of Georgia in Partial Fulfillment

of the

Requirements for the Degree

Master of Science

Athens, Georgia

2015

COUPLED LOW TEMPERATURE ALGAE HYDROTHERMAL LIQUEFACTION AND CATALYTIC HYDROTREATING TO PRODUCE LOW NITROGEN FUEL INTERMEDIATES

by

WILLIAM V. COSTANZO

Approved:

Major Professor:	James Kastner
Committee:	Sudhagar Mani K.C. Das

Electronic Version Approved:

Julie Coffield
Interim Dean of the Graduate School
The University of Georgia
May 2015

Coupled Low Temperature Algae Hydrothermal Liquefaction and Catalytic Hydrotreating to Produce Low Nitrogen Fuel Intermediates

William V. Costanzo

April 24, 2015

Acknowledgments

My most sincere gratitude to my major professor, Dr. Jim Kastner, for your guidance, your overall prowess, and the trust that you've had in me since my research began. Without all of your motivation and assistance (and pestering!), I would not be nearly as satisfied with my product and with my program as a whole. Thank you, from the bottom of my heart, for directing me and demonstrating firsthand how to be successful.

To Joby Miller: the true workhorse of the College of Engineering. You single-handedly enabled me to do my research by being organized, through your persistence and determination, and with our enjoyable morning conversations. I could not have dreamed of a project this well defined if it had not been for your professionalism and overall mastery of what it looks like to be both a successful scientist and a caring human being.

A special thanks to Justin Weber, for keeping me well-fed every day at lunch (even if I did always have to drive). I've loved having a best friend in my office with whom I can talk about "what-ifs", and I look forward to hearing about your success in the future. To Roger Hilten: thank you for always having the answers (no matter the question). You have been a role model for me since I began here, and I've enjoyed looking to you to see what life and work and love and family should be like. To Andrew Smola: thanks for keeping me safe and organized, even long after you left this place. Your signatures are all around, and it makes me smile thinking of you and your love for logistics... A-OK!

My family has been nothing but supportive since I decided on graduate school. Thank you all for believing in me, pushing me forward, and showing genuine interest in the subject on which I was researching. I love you all so, so much, and I'm incredibly thankful each of you is in my life. Thank you Momma, Pops, and Lou.

A sincere thank you to Dr. Sudhagar Mani, Dr. K.C. Das, and the rest of the College of Engineering for your support and guidance in my program. I have been honored to be a part of an entity growing in the way this place is growing, and I'm excited for what the future holds for it and for you all.

Contents

[1]Costanzo, William and Umakanta Jena, Roger Hilten, KC Das, Jim Kastner. To be submitted to *Bioresource Technology*.

[2]Costanzo, William and Roger Hilten, Jim Kastner. To be submitted to *Bioresource Technology*.

List of Tables

List of Figures

Chapter 1

Project Summary

The eukaryotic group of autotrophs, known more familiarly as algae, possesses very unique characteristics that make it extremely appealing as a source of renewable and sustainable biofuels. This group naturally synthesizes macromolecules (lipids, carbohydrates, and proteins) from CO_2, inorganic nitrogen, and other nutrients that ultimately comprise biocrude oil, a precursor to many modern fuels, without compromising simple growth habitats. Algae are more nutrient-dense than many other bacteria, but not nearly as complex or difficult to mass produce as biomass such as stover or grass. Thus, extensive investigations have been performed to utilize these characteristics to produce biocrude through a high-temperature and high-pressure process known as hydrothermal liquefaction (HTL). Biocrude is an oil-phase mixture of compounds possessing the potential to be used as or to be upgraded to combustible liquid fuels.

Hydrothermal liquefaction employs water in a subcritical state to hydrolyze the macromolecules that algae naturally produce into fuel-like groups, such as long-chain alkanes. The rate of macromolecular hydrolysis increases exponentially as reaction temperatures are increased. In its condensed state, under typical HTL conditions, subcritical water can also act as an acid catalyst, thus enhancing hydrolysis rates. When paired with increased pressures to ensure the water remains subcritical, this process yields bio oil at an extremely competitive rate.

Two issues that currently restrict the widespread implementation of algae biocrude from HTL are the cost of start-to-finish methods of algae cultivation and the generation a stable biocrude product with low nitrogen and oxygen elemental levels. It is desirable for all of the nitrogen to be removed (which is present in the biocrude due to nitrogen-rich protein macromolecules) while retaining as much economic feasibility as possible. To compete with current fuel precursors or to allow co-processing with petroleum intermediates, a significantly better understanding of algae liquefaction kinetics and reaction pathways are needed. To the best of our knowledge, there has been limited research on the impact of protein on the mechanisms of lipid and carbohydrate liquefaction. It is hypothesized that nitrogenated compounds originating from the degradation products of proteins cross-react with the degradation products of lipids and carbohydrates to form suites of unwanted compounds (e.g., pyrrolidines and amides). The compounds in this nitrogenated cross-reaction group, when combusted as part of fuels, become nitrous oxides, a major component in smog and acid rain.

Techniques have been developed to attempt to remove nitrogen prior, during, and after liquefaction in attempts to increase the biocrude quality. These techniques include pretreatment of the algae, for selective protein hydrolysis, and catalytic hydrodenitrogenation (in which metal catalysts are used to remove both oxygen and nitrogen with hydrogen). Although these techniques have been confirmed as successful, the overall effectiveness varies greatly, and depends on the algae strain and pretreatment, HTL conditions, and catalytic upgrading conditions. Because so much variation in algae composition exists and because we lack fundamental knowledge on the simultaneous liquefaction of their three main macromolecular constituents, it becomes difficult to optimize the conversion process in regards to the issues stated above. For example, the optimization for one strain of algae may not be applicable for another because of the differences in their macromolecular compositions, which affects the composition of the biocrude product.

It is thus proposed that a low nitrogen refinery intermediate can be generated from algae through the coupled implementation of both low- and high-temperature liquefaction with catalytic

hydrotreating. In theory, this multistage process could be understood and optimized to allow economic and scientific competition between algae-based biocrude and petroleum-based oils typically used. In addition, a further understanding of the conversion process being undertaken through the systematic evaluation of the liquefaction and upgrading of model macromolecules will aid in process optimization and quality control of the oils being produced. Identifying the pathways of hydrolysis products and predicting the outcome of liquefaction is useful in that researchers can experiment with theoretical combinations of macromolecular ratios in order to find the optimal ratios that coincide with the most economic liquefaction conditions. Results could be used to overcome current limitations of algae liquefaction to liquid fuel processes.

Chapter 2

Background and Literature Analysis

2.1 Thermochemical Conversion Technologies

Two main thermochemical conversion processes exist for converting biomass into high value liquid energy products: pyrolysis and liquefaction. Each of these technologies is effective at producing liquid fuels or the derivatives thereof, and each is presented with advantages and disadvantages. Often, gasification is also classified as a thermochemical conversion process. Although the products of gasification are primarily gases, this process can be paired with a synthesis process such as Fischer-Tropsch Synthesis to product liquid energy products similar to the above mentioned processes.

2.1.1 Pyrolysis

Pyrolysis is the term given to the thermal decomposition of biomass in the absence of oxygen. Whereas normally the feedstock would combust at the temperatures required for this decomposition, pyrolysis operates ensuring insufficient oxygen is present in the reaction space for combustion. The products generated from pyrolysis of biomass vary greatly, and are most dependent upon

the speed of degradation, which is primarily a result of the rate of temperature increase occurring within the feedstock, the reaction temperature, and the reaction (or residence) time.

Slow pyrolysis, often referred to simply as pyrolysis, occurs at temperatures in the 300-700 °C range. The feedstock is heated to the reaction temperature slowly (less than 1 degree per second), and residence times can range from tens of minutes to multiple hours in length. Fast pyrolysis is similar in procedure to slow pyrolysis. This process occurs at a higher temperature (600-1000 °C) at a higher heating rate (tens of degrees per second), which decreases the residence time for decomposition to seconds instead of minutes. Flash pyrolysis is characterized by a sudden drastic heat shock to the feedstock. This type of conversion occurs near 1000 °C, and requires a large enough heating rate (greater than 1000 degrees per second) to allow residence times less than 0.5 seconds (Gungor et al., 2012; Maschio et al., 1992).

Pyrolysis is advantageous in both its fast reaction speed (from relatively low residence times) and its low overhead cost. As an already established conversion process, pyrolysis possesses many resources for large scale production that other technologies currently do not have. However, the cost of drying pyrolysis feedstocks decreases the overall economic feasibility of the process. Another disadvantage comes from the low quality of oil produced through pyrolysis; often, pyrolysis oil contains high concentration of acid compounds and must be upgraded before downstream processing to liquid fuels or other energy-rich compounds.

2.1.2 Gasification

Gasification essentially is controlled combustion of biomass in the presence of air or oxygen that primarily produces gaseous mixtures of CO_2, CO, CH_4, and H_2, called "Syn gas". These products are generated from many types of organic materials as they are subjected to high temperatures (close to 1000 °C) and high residence times (on the order of hours in duration). Fischer-Tropsch Synthesis (FTS) involves a series of reactions with Syn gas substrates that ultimately can yield straight-chain alkanes like the ones most useful for fuel production. Fischer-Tropsch Synthe-

sis occurs at reaction temperatures near 230 °C (considered ”low temperature FTS”) or near 325 °C (”high temperature FTS”) (Leckel, 2009). Figure 2.1 illustrates a typical reaction pathway that would occur through FTS.

One of the major benefits from gasification coupled with Fischer-Tropsch Synthesis is that the liquid product formed often does not need distillation, as it is chemically similar to gasoline. However, only low selectivity is currently possible with synthesis of hydrocarbons in this manner (Laird et al., 2009).

2.1.3 Liquefaction

Liquefaction, often referred to as direct liquefaction, utilizes thermal decomposition in tandem with catalysis to degrade biomass into liquid fuel precursors. Hydrothermal liquefaction is a generalized set of transformation conditions that uses liquid or supercritical water as the conversion agent. This technology is based upon the principles of acid catalysis, through which liquid or supercritical water catalyzes the hydrolysis of complex biomass macromolecules into products that are useful as biofuel precursors (Toor et al., 2011). Specific liquefaction conditions will be discussed in Section 2.2.

One of the main advantages hydrothermal liquefaction processes have over other thermochemical conversion technologies is the economic benefits gained from the ability of wet biomasses to be used directly in HTL. The biomass feedstock must be primarily dry (moisture content below 10%) before it can be used in pyrolysis or gasification, which requires a substantial energy input. Particular to hydrothermal liquefaction, however, is the fact that high reaction pressures are required to maintain liquid or supercritical water and to prevent vaporization (Behrendt et al., 2008).

2.2 Hydrothermal Liquefaction of Algae

Hydrothermal liquefaction is a process that utilizes the unique properties water has in its subcritical or supercritical state to hydrolyze large macromolecules into products that are useful as biofuel precursors (Toor et al., 2011). The rate of macromolecular hydrolysis increases exponentially as reaction temperatures are increased. In its condensed state, under typical HTL conditions, subcritical water can also act as an acid catalyst, thus enhancing hydrolysis rates. When paired with increased pressures to ensure the water remains subcritical, this process yields bio oil at an extremely competitive rate (Alba et al., 2012).

HTL is performed using hot compressed water and appropriate catalysts, since it is a highly reactive medium as it approaches its critical point (374 °C, 22.1 MPa) due to changes in properties such as solubility, density, dielectric constant and reactivity. HTL depolymerizes lipids, proteins and carbohydrates in algae, transforming them into a bio-oil (also referred to as "biocrude" in the literature), water solubles, gas, and solids (char). Multiple reactions occur in three steps, namely, hydrolysis, depolymerization and repolymerization/self-condensation reactions (Yin et al., 2010). Protein molecules are hydrolyzed into amino acids followed by deamination (release of NH_3) and decarboxylation reactions to form complex hydrocarbons (Sato et al., 2004). The bio-oil is a dark viscous liquid with an energy value 70-95% of that of petroleum fuel oil (Brown et al., 2010; Dote et al., 1998; Minowa et al., 1998). Thus, HTL converts organic constituents of algae into a liquid bio-oil that in theory can be refined to gasoline/diesel-like fuels. However, due to the large amount of proteins present in the starting algae biomass, the bio-oil has a large abundance of nitrogen heterocyclic compounds leading to higher amount of nitrogen in the bio-oil which causes potential problems in the subsequent upgrading process. The various nitrogen compounds generated in the HTL product bio-oil are nitrogen heterocyclics (pyridine, pyrrole, pyrrolidine, piperdine, and indole) and non-heterocyclics such as open-chain amines and amides (hexadecanenitrile, and hexadecanamides) (Anastasakis and Ross, 2011; Biller and Ross, 2011; Brown et al., 2010; Jena et al.,

2011a; Ross et al., 2010). Also, the presence of polypetides and proteins lead to the high molecular weight compounds in the bio-oil in the range of 2,000-10,000 g mol^{-1} (Alba et al., 2012). The rest of the components result in low (100 to 300 g mol^{-1}) and medium (400 to 500 g mol^{-1}) molecular weight compounds. Additionally, nitrogen in the bio-oil will pose potential problem in further upgrading and use of this product, since it leads to poisoning of the catalyst and deactivation of catalysts (Laurent and Delmon, 1993).

Studies have shown that variances in the HTL conditions have effects on the phase yields and the quality of the oil generated (Biller and Ross, 2011; Jena et al., 2011a). Jena et al. (2011a) demonstrated that *Spirulina* generates oil at the optimized HTL conditions of 350 °C held for 1 hour. A series of liquefaction experiments performed by our lab on three separate algal strains (*Spirulina*, *Nannochloropsis*, and a UGA Consortium) verified that an HTL-only experiment appears optimized when performed at 350 °C held for 1 hour. Naturally, the amount and quality of the oil generated depends heavily on the composition of the strain used as feedstock. Our research has shown, however, that liquefaction of each of the three strains yielded approximately 25% oil (a percentage of the dry/ash-free algae fed).

Because the model compounds being used in this work contain no cell wall resistances or ash inhibition, a 30 minute holding time will be used instead. It is hypothesized that the depolymerization of the macromolecules that ultimately forms the biocrude oil will occur more quickly due to the decreased thermal and mass resistances brought from the lack of cell walls or ash-forming minerals. See Section 2.5 for discussions on previous work conducted using model compounds to mimic HTL of algae.

2.3 Catalytic Conversion and Upgrading of Algal Oil

Algae oil generated from hydrothermal liquefaction naturally contains nitrogen stemming from the algae protein that comprises a majority of the algal mass. Before this algae biocrude can

be utilized as a fuel precursor, the biocrude must be upgraded. Specifically, fatty acids undergo decarboxylation to form alkanes, and nitrogenated heteroatoms must be denitrogenated altogether. Nitrogen is a major component in smog when present in combustion-based fuels.

One approach for this upgrading is through the use of solid catalysts that replace unwanted nitrogen and oxygen with hydrogen. Hydrode-oxygenation and -nitrogenation, respectively, occur at high temperatures in the presence of hydrogen gas. The heterogeneous catalysts utilized are typically composed of precious metals or metal oxides, and decarboxylate (generate CO_2 by cleaving and replacing it with hydrogen) the varying oil compounds to "upgrade" the quality of the oil as a whole. Since the oil quality is often judged on the percent nitrogen and oxygen, removing these elements in a catalytic fashion is useful in making the oil a viable product (Duan and Savage, 2010; Savage and Duan, 2011).

Bai et al. (2014) performed a catalytic screening study in which algae oil generated from the liquefaction of *Chlorella* was subjected to a two-stage upgrading process: a high-temperature upgrading stage using hydrogen gas without catalyst (350 °C for 4 hours), and a supercritical upgrading stage using varying types of heterogeneous catalysts (400 °C for 4 hours; 10% catalyst loading by weight). It was determined that although the hydrogen treatment favorably reduced the nitrogen content of the bio-oil and increased its flowability, every catalyst tested achieved greater desirable changes. Specifically, across a range of 14 commercial catalysts, including precious metal catalysts, sulfided metal catalysts, zeolites, and varying supports, their work demonstrated that ruthenium (5% wt. on carbon) and Raney nickel, used in conjunction, produced the best results. Their two-stage process reduced the nitrogen content of the bio-oil from 8.0% to 2.0% (by mass).

Our lab has experimented with several heterogeneous catalysts: Ruthenium metal, suspended in 5% on carbon, a sulfided cobalt-molybdenum catalyst (suspended on alumina), and a metal oxide catalyst that is a byproduct of the mining industry called reduced red mud. The metal oxide groups found in red mud (mainly iron oxide) remove oxygen using the reverse Mars-van Krevelen

mechanism (Karimi et al., 2010; Sushil and Batra, 2008). This mechanism requires oxygen-vacant sites on the catalyst's surface that are structured to bind oxygen, allowing the hydrogen chemisorption to occur more quickly (kinetically); these vacant sites are formed by passing hydrogen gas over the catalyst at high temperatures (300 °C).

Catalytic hydrodeoxygenation has become a popular step in most oil-generation processes, such as bio-oil stemming from the pyrolysis of biomass. Similar to algae liquefaction, HDO of oil derived from biomass occurs using heterogeneous precious metal catalysts. Some of the more popular metals are nickel, ruthenium, palladium, cobalt, and titanium (Bai et al., 2014; Gunawan et al., 2013; Na et al., 2012; Olcese et al., 2013; Zacher et al., 2014). Often, these HDO stages are performed for as long as 4 hours, and they are performed at similar temperatures and pressures as liquefaction (see Section 2.2).

Several reaction mechanisms exist for oxygen and nitrogen removal. These mechanisms are promoted and enhanced by the presence of the catalysts in the reaction slurry. One mechanism for the removal of oxygen is *decarboxylation* in which a carboxyl group is cleaved to form carbon dioxide and a hydrocarbon, as shown in Figures 2.2 and 7.1. Hydrocarbons are valuable compounds in the fuel and chemical industries, so the upgrading of bio oil by decarboxylation is a necessary step for bio oil to be of the same quality as petroleum oil (Zacher et al., 2014). A similar mechanism, *decarbonylation*, creates hydrocarbons from the cleaving of the carbonyl group of aldehydes (thus producing carbon monoxide with the hydrocarbon); Figure 2.3 illustrates an example mechanism, which could potentially occur on algae fatty acids (see Figure 7.1).

The most common mechanism for nitrogen removal is *deamination* in which an amine group (NH_3) is cleaved from the parent chain, producing ammonia. Often, this deamination is catalyzed by water, and replaces the amine group with a double-bonded oxygen, requiring further transformation. Figure 2.4 illustrates the first step in this mechanism in which the amine group is cleaved. Similar to the removal of the amine group, amide groups (amines with a carboxylic acid group

attached) are removed during denitrogenation catalytically by a mechanism nearly identical to deamination (Brown, 1991).

2.4 Large-Scale Production of Algae Feedstock

2.4.1 Algae Production Technology

In order for algae bio oil to become a wide-scale replacement for petroleum oil, an ample amount of algae feedstock must be grown and harvested. As a photosynthetic organism, algae require sunlight and carbon dioxide in order to grow (similar to *Kingdom Plantae* organisms). Algae also require nitrogen and phosphorus, along with several minerals (such as calcium and manganese). These nutrients, in accordance with the procedure followed at the University of Georgia Bioconversion Research and Education Center, are mixed according to the BG-11 growth media recipe (shown in Table 2.1).

For growth of algae with a specific molecular or macromolecular composition, a photobioreactor is typically used (Figure 2.5). This reactor type is adept at controlling the exact environment in which the algae is grown, including nutrient concentration, sunlight concentration, stirring speed, cell density, temperature, and concentration of dissolved gases. Because of this controlled nature, photobioreactors can maintain a biomass concentration of up to 5 g/L and have a harvesting turnover time as short as 2 weeks (both of which are more efficient than mass producing bodies such as raceway ponds) (Demirbas, 2010). Photobioreactors also have the advantage of recapturing unused nutrients from wastewater.

Photobioreactors, although experimentally desirable, are not economically feasible for large scale growth of algae. It has been shown that open raceway ponds, cyclic paddle-stirred tracks of liquid media (Figure 2.6), have the capacity to produce algae at the necessary rate (Becker, 2007; Demirbas, 2010; Devi et al., 1981; Oliveira et al., 1999; Torzillo et al., 1986). These ponds utilize

natural sunlight (unlike the artificial light provided in photobioreactors) to allow less expensive algae growth. The stirred nature of the ponds provides some dissolution of carbon dioxide, with the remaining necessities bubbled from the side of the tank. This system is continuous, allowing for uninterrupted harvesting of matured algae while providing fresh nutrients for immature algae. These ponds usually are limited to a 30 centimeter depth, so as to not limit the sunlight reaching the bottom of the tanks; large scale tanks, because of this limitation, are often 2000 square meters in area (Demirbas, 2010).

A consortium of three algal strains (*UGA Consortium* henceforth), namely *Chlorella sorokiniana*, *Chlorella minutissima*, and *Scenedesmus bijuga*, were grown and harvested for use in this study as well. A monoculture inocula of the constituent strains were first grown in 20 L carboys under controlled conditions in a growth chamber at 25 $\pm$ 1 °C for 12 h with alternating light-dark cycles; the light intensity was 100 μmoles m^{-2} s^{-1} with continuous air bubbling. The final consortium was prepared by mixing equal proportions (v/v) of each individual strain and then using it as inoculum at 10% v/v for outdoor cultivation in raceway ponds under green house facilities at an algae bioenergy lab of UGA. The raceway ponds are constructed of HDPE plastic and are 1.32 m wide, 2.18 m long, and 0.61 m deep with a working volume of approximately 500 L at 0.17 m water depth. Standard algae growth medium BG 11 was used in fresh water for cultivation (Jena et al., 2011b). Supplemental CO_2 was derived from a commercial 10% CO_2 storage cylinder and used as a carbon source and for pH control. The UGA designed carbonation column (Putt et al., 2011) was used for CO_2 mass transfer. Once the cell density in raceways reached 500 mg/L, the biomass was harvested using a continuous centrifuge and dried at 55 °C until constant weight was observed after multiple weighing. The dried biomass was packed in zip-lock bags and stored at 4 °C until further use. Subsequently, the dried microalgae was ground to a fine powder using a heavy-duty laboratory knife mill (Retsch SM 2000, Germany) with a screen size of 0.5 mm. The knife mills cutting blade rotor (1690 rpm, 60 Hz) was powered by a 1.5 kW electric motor.

2.4.2 Algae Harvesting Technology

Once the algal cells have completed the exponential and lipid-accumulation phases of their growth (Becker, 2007; Torzillo et al., 1986), they are ready to be harvested for use in industry (for fuel or other commodities such as cosmetics or food supplements). Since liquefaction accepts wet biomass, no drying step is required (although it is often performed for storage purposes).

The outlet streams from the algae production bodies are typically either centrifuged or flocculated (by dissolved air or metal chloride chemical) (Demirbas, 2010; McGarry and Tongkasame, 1971; Sandbank and Shelef, 1987). In either case, the purpose of the harvesting step is to concentrate the biomass, to recycle unused nutrients in the wastewater, and to remove unwanted particulate before the feedstock reaches the conversion stage.

2.5 Hydrothermal Liquefaction of Model Macromolecules

Liquefaction of Model Lipids

Liquefaction of lipids operates under the mechanism of water acid-catalyzed hydrolysis of triglycerides to ultimately form free fatty acids. There is evidence that the major products of this hydrolysis are intact fatty acids such as oleic and palmitic acid, depending heavily on the triglyceride being used as feedstock. Liquefaction of sunflower oil in subcritical water, for example, yields 14-, 16-, and 18-carbon saturated free fatty acid chains (Biller and Ross, 2011; Changi, 2012; Mazaheri et al., 2010; Peng et al., 2013). Three moles of fatty acids and one mole of glycerol are yielded from the hydrolysis of a triglyceride. A more detailed pathway investigation was performed and is presented herein (in Section 7.2).

The model lipid being used in these experiments is palm oil. Justification for this selection can be found in section 3.2 on page 35. It is hypothesized that palm oil, which is primarily composed

of triglycerides containing palmitic and oleic acid, will hydrolyze to yield these two acids as free fatty acid chains.

Liquefaction of Model Carbohydrates

Liquefaction of carbohydrates involves the hydrolysis and removal of many of the hydroxy groups bound to the cyclic rings that define most carbohydrates. The extent of this hydroxide removal varies greatly with the liquefaction conditions. In some cases, the carbohydrate ring was completely dehydroxylated to form benzene (Biller and Ross, 2011); in others, cyclic ketones (such as cyclohexanone and cyclopentanone) were formed (Changi, 2012; Salimath et al., 1987). A more detailed pathway investigation was performed and is presented herein (in Section 7.2).

The model carbohydrate being used in these experiments is starch (in a powdered form, from potatoes). Justification for this selection can be found in section 3.2 on page 35. It has been demonstrated that isolated starch can be hydrolyzed and undergo a series of reactions to form cyclohexanone, benzene, indenone, and ethanone (Biller and Ross, 2011).

Liquefaction of Model Proteins

The liquefaction of proteins is difficult to characterize because of the vast array of possibilities that exist for the formation of proteins. Most proteins are comprised of a combination of amino acids, and it can be assumed the first stage in protein hydrolysis (via liquefaction) is cleaving of the peptide bond that joins amino acids together (Changi, 2012; Dote et al., 1998; Simo et al., 2005). A more detailed pathway investigation was performed and is presented herein (in Section 7.2).

The liquefaction of amino acids involves the cleaving of the amine group and the side chain group (in the case of cyclic side chains). The products, and phase solubility, of the liquefaction of amino acids varies. Dote et al. (1998) reports, in Table 2.2, that most amino acids do not hydrolyze to form water insoluble (or oil-forming) compounds. Less than 10 percent of all amino acids except tryptophan become products in the oil phase; 66% of tryptophan becomes oil-forming

compounds. It has also been reported that liquefaction of whole proteins (such as egg albumin or soya protein) hydrolyze to form groups such as phenols, indole, pyrrols, and piperdine (Biller and Ross, 2011; Brown et al., 2010; Rogalinski et al., 2005, 2008; Stein, 1949). Proteins are the only nitrogen source in these experiments, so it can be said that any nitrogenated products (such as the groups listed above) must have a reaction pathway stemming from proteins and amino acids.

The model protein being used in these experiments is albumin protein sourced from chicken egg. Biller et al. (2011) reports that isolated egg albumin can be hydrolyzed to form phenols, pyrrols, indole, and piperdine, along with a suite of other nitrogenated cyclic groups.

It is important to notice the amino acid Tryptophan is converted to biocrude at a proportion nearly 10 times higher than any other amino acid. Tryptophan has a double-ring structure, possibly explaining the presence of the multitude of nitrogenated cyclic groups reported from the liquefaction of protein.

2.6 Kinetic Analysis and Arrhenius Relationship

The biocrude forms as each individual macromolecule is hydrolyzed and degraded through a series of irreversible reactions. Figure 2.7 illustrates the stepwise pathways through which the large components of algae become biocrude "degradation products". Macromolecule A hydrolyzes to product B via reaction kinetics involving the constant k_1 (which is only constant with isothermal conditions); B further hydrolyzes to a series of degradation products C, which include multiple groups of compounds.

These pathways can be modeled kinetically and mathematically (Rogalinski et al., 2005, 2008). Equation 2.1 shows how the concentration change of reactants over time is affected by the concentrations themselves and the rate constant k. Reactant A is only consumed, causing the rate differential to be a single term; reactant B is both consumed (to C) and generated (by A), causing the rate differential to be two terms.

$$\frac{-dC_A}{dt} = k_1 C_A \quad and \quad \frac{-dC_B}{dt} = k_2 C_B - k_1 C_A \tag{2.1}$$

HTL being performed in batch is not isothermal, so the k "constant" is actually a function of temperature. The relationship between k and temperature is given by the Arrhenius Equation (Eq. 2.2), which is dependent on the frequency factor (A) and activation energy (E_A). These constants are unique for each reaction, making k (denoted by k_n) unique as well.

$$k_n = A e^{\frac{-E_a}{RT}} \tag{2.2}$$

Combining equations 2.1 and 2.2 leads to the relationship between reaction rate, reactant concentration, and temperature. Equation 2.3 shows this relationship for reactant B.

$$\frac{-dC_B}{dt} = [A_B e^{\frac{-E_{a_B}}{RT}}] * C_B - [A_A e^{\frac{-E_{a_A}}{RT}}] * C_A \tag{2.3}$$

Since both the temperature and concentration of reactants are functions of time, a series of coupled ordinary differential equations ($\frac{-dC}{dt}$ and $\frac{dT}{dt}$) can be regressed in a non-linear manner to determine the Arrhenius constants A and E_a.

The net reaction rate of B is partially affect by the drive B has to be consumed and form a degradation product (C). As B is given more options to be consumed, its consumption rate will increase; C is not a single product, but multiple *groups* of products. Thus, it is often practiced that the overall kinetics of a pathway is measured based upon its middle reactant (in this case, reactant B because it is both generated and consumed) (Rogalinski et al., 2005, 2008).

Cross reactions occur when the B compound of one pathway reacts with the B compound from a separate pathway. It is hypothesized that these cross reactions are what cause the formation of undesired nitrogenated compounds in algae biocrude such as pyrrolidines and long chain amides. A few of these nitrogenated compounds are shown in Figure 2.8. The compounds are similar in structure, but not congruent, to desirable groups (such as long chain alkanes); research is being

performed to explore catalytic hydrodenitrification of these nitrogenated groups to upgrade the algae biocrude (Biller et al., 2011; Duan and Savage, 2010).

2.7 Economic Analysis of Liquid Fuels from Whole Algae

The algae-to-fuel conversion process can be broadly grouped into two sections: feedstock development and conversion. Feedstock development includes algae growth (water and nutrient supplementation, raceway motors, auxiliary carbon dioxide or light) and harvesting (flocculation, filtration, centrifugation, transportation, and storage). Conversion includes hydrothermal liquefaction (electrical consumption, reaction configuration, and separations) and catalytic upgrading (catalytic materials and upkeep solvents, separation solvents, electrical consumption, post-processing, handling, and transportation or storage). An extensive theoretical analysis of the algae-to-fuel process as a whole has recently been conducted, showing that algae can be used to produce a gallon of gasoline equivalent (gge) at a price of 4.49 $/gge (Jones et al., 2014).

The research conducted by Jones et al. (2014) demonstrated that algae conversion via HTL possesses the necessary economic capacities to be a feasible technology for the production of liquid fuels. Specifically, they showed that feedstock development accounts for nearly 74% of the gge price listed above (3.31 of the 4.49 $/gge); this assumes the feedstock costs 430 $/US ton of dry/ash-free algae. A large portion of this cost is in nutrient supplementation, mainly nitrogen and phosphorus. This provides evidence that the cost of algae feedstock development can be drastically reduced if a method for nutrient recycling was implemented.

All of the conversion process, including purchasing and maintaining the precious metal catalysts and operating the reactors at high temperatures, account for only 12% of the gge price. Jones et al. (2014) estimated the capital cost to be $ 467,900,000 for a conversion facility producing 122 gal/ton algae. Nearly 25% of this capital cost is for the conversion equipment and reactor configu-

rations. The cost of this facility would be coupled with an after-tax return-on-investment (ROI) of 10%.

2.8 Figures and Tables

$$(2n+1)H_2 + nCO \rightarrow C_nH_{(2n+2)} + nH_2O$$

Figure 2.1: Generalized reaction scheme for Fischer-Tropsch Synthesis (n typically 10 to 20).

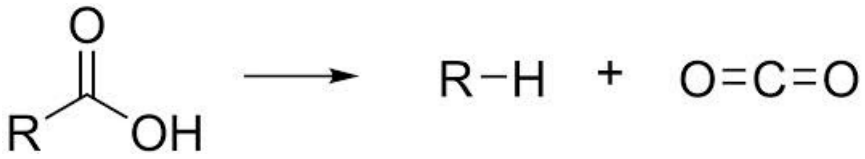

Figure 2.2: Mechanism of decarboxylation.

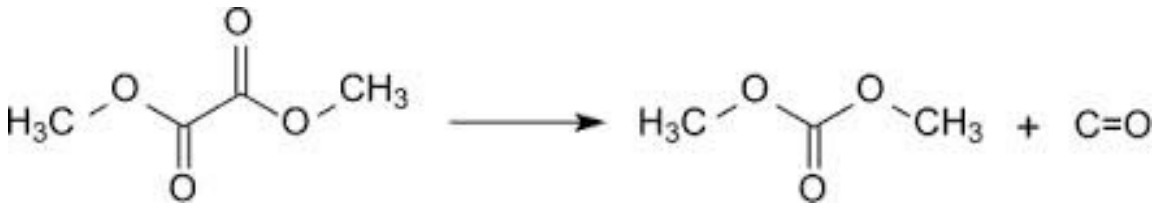

Figure 2.3: Mechanism of decarbonylation.

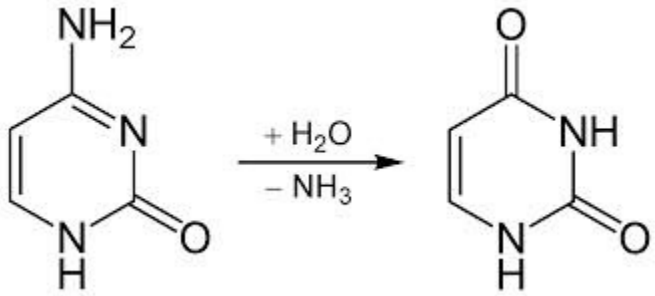

Figure 2.4: Mechanism of deamination.

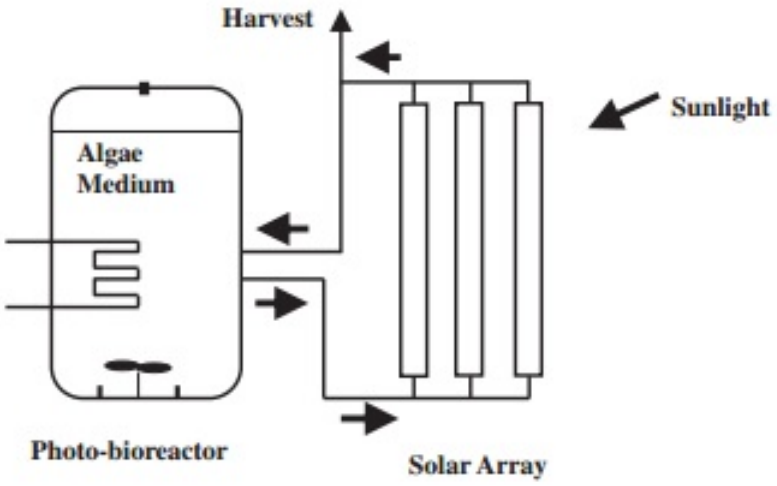

Figure 2.5: A tubular photobioreactor (Demirbas, 2010).

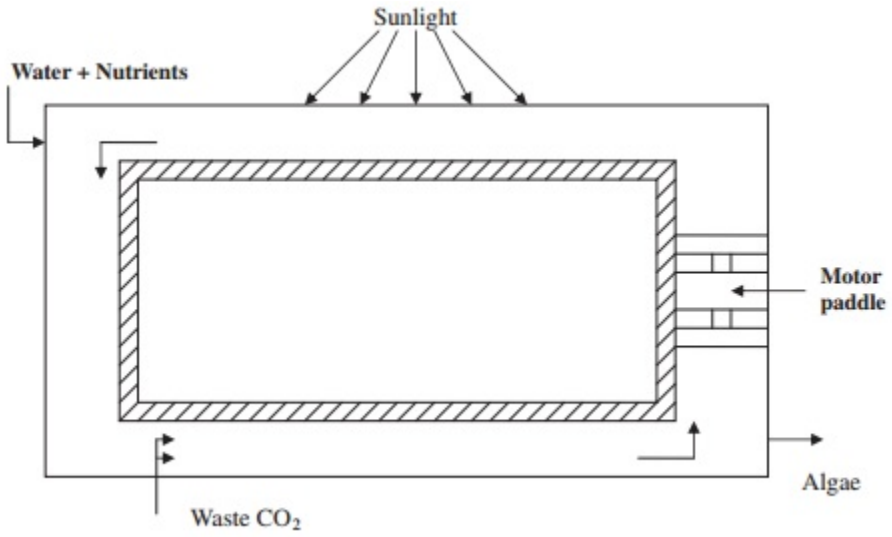

Figure 2.6: An open raceway pond (Demirbas, 2010).

$$A \rightarrow B \rightarrow C$$

$$Protein \rightarrow Amino\ Acid \rightarrow Degradation\ Products$$

$$Triglyceride \rightarrow Diglyceride + FFA \rightarrow\rightarrow Degradation\ Products$$

$$Starch \rightarrow Glucose \rightarrow Degradation\ Products$$

Figure 2.7: Proposed pathways for macromolecular hydrolysis.

Each macromolecule begins one of these pathways; the *degradation products* are a suite of compounds.

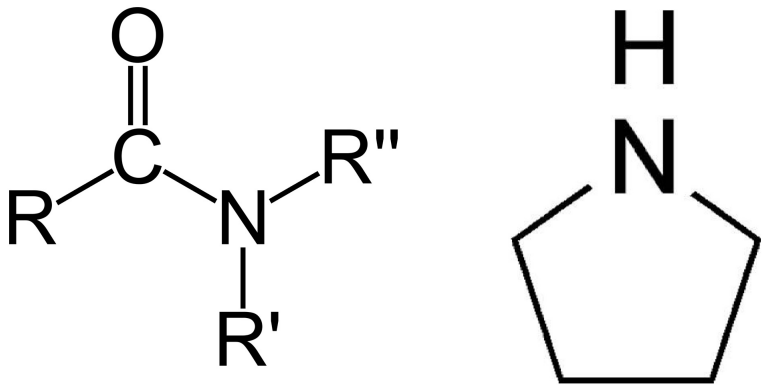

Figure 2.8: Examples of nitrogenated compounds in non-upgraded algae biocrude from HTL (peptide and pyrrolidine).

Table 2.1: BG-11 Growth Media Recipe (Jena et al., 2011b).

Ingredients	**mg/L**
Sodium nitrate	1500.0
Dipotassium hydrogen phosphate	31.4
Magnesium Sulphate	36.0
Calcium chloride dihydrate	36.7
Sodium carbonate	20.0
Disodium magnesium EDTA	1.0
Citric acid	5.6
Ferric ammonium citrate	6.0

Table 2.2: Oil yield from liquefaction of various amino acids (Dote et al., 1998).

Amino Acid	*Oil Yield (%)*	*N in oil (%)*	*Amino Acid*	*Oil Yield (%)*	*N in oil (%)*
Glycine	0.2	0.9	Lysine	1.4	3.7
Alanine	0.3	2.2	Glutamine	0.6	1.2
Serine	4.0	7.7	Glutamic acid	0.2	0.0
Proline	0.2	0.0	Methionine	2.3	3.6
Valine	3.2	13.3	Histidine	0.2	9.7
Threonine	2.3	5.2	Phenylalanine	9.6	4.8
Leucine	7.7	10.4	Arginine	0.4	5.5
i-leucine	5.7	10.4	Tyrosine	0.2	1.5
Asparagine	1.3	5.6	Tryptophan	66.4	10.3
Aspartic acid	1.7	4.0			

*Means of two analyses, reproducible to ±0.1%

Chapter 3

Rationale

3.1 Scope of Work

It is well understood that a clean, renewable, and sustainable source of fuel is needed since currently used fossil fuels are dwindling in supply, and the portions that are remaining are harmful to the environment and are difficult to harvest. Thus, a precursor for fuels that is both simple and renewable to create as well as passive in its effect on the Earth is required.

The need for alternative fuel sources is an issue that no longer can be subordinate. Petroleum fuel, in particular, is dwindling in supply and is causing global disputes because of economic complications and domestication of production. For this reason, a fuel source is needed that is economically feasible, manageably and domestically producible, and environmentally conserving. Many options for bio-fuels exist that satisfy a portion of these requirements in different ways, but very few of these options satisfy of them simultaneously in the way that bio-oil production from algae does.

It has been demonstrated that algae can be converted to a biofuel precursor called biocrude through a high-temperature and high-pressure reaction with sub-critical water called hydrothermal liquefaction (HTL). Past research has shown that algae can be effectively converted to biocrude via

HTL (Toor et al., 2011), but little is known about the reaction pathways through which the varying macromolecules in algae (lipids, carbohydrates, proteins) hydrolyze to form the biocrude products (which number in the thousands).

It is thus my motivation to explore these hydrolysis pathways. By performing HTL on representative model lipids, carbohydrates, and proteins (both isolated and in combination) it can be shown which biocrude products are formed from which macromolecule or molecules. Understanding these pathways is a crucial step in eliminated undesired products such as nitrogenated aromatics or long chain amides. In addition, the kinetics of these pathways can be characterized to better understand how the liquefaction conditions affect the biocrude product quality.

Through the research being performed, it is desired that algae biocrude via HTL become a competitive source for fuel precursors. This project aims to model the pathways through which algae becomes biocrude, and through the model, more effective methods for selective production of compounds can be achieved. Comprehensive knowledge of how undesired products are formed is a major step towards eliminating these products in the biocrude, thus upgrading the biocrude and further allowing it to be used with, and instead of, fossil fuels. By understanding the impact of the ratio of algae macromolecules and their cross-reactions on the biocrude product formed from HTL, future research will be able to work towards developing an algae that contains the potential optimized (yet not existing) ratio of lipid, protein, and carbohydrate that will enable algae biofuels to be a competitive and promising source for bioenergy.

Several approaches to removing nitrogen and proteins from feedstocks such as algae have already been examined. Barreiro et al. (2014) examined the effects of enzymatic hydrolysis of proteins on HTL of two algal strains (*Nannochloropsis* and *Scenedesmus*). Through use of cell rupturing coupled with endoprotease (Alcalase) and exoprotease (Flavourzyme), they were able to extract 44.3% and 62% of the protein from each strain, respectively. This translated to a favorable decrease in the nitrogen content of the bio-oil generated from HTL. For example, when HTL was performed at 350 °C after use of the enzyme for 6 hours, the nitrogen content of the bio-oil decreased from

5.1% to 4.2% in *Nannochloropsis*, with a similar trend observed in *Scenedesmus*. This can be compared to the direct HTL performed without pretreatment in this study on *Nannochloropsis* (see Section 5.3.2) in which the biocrude generated contained a nitrogen content of 6.6%. Although the percent bio-oil yield was similar between HTL on raw algae and protein-extracted algae, Barreiro reported that the enzymatic hydrolysis removed 53.5% of the initial *Nannochloropsis* mass and 80.9% of the initial *Scenedesmus* mass. This shows that the enzymes hydrolyze more than just proteins, which likely correlates to a significant decrease in the overall biocrude yield. Also, this enzymatic hydrolysis required at least 2 hours of processing time, with the most favorable results requiring 6 hours (Garcia et al., 2012). Although energy-saving, this process is very time intensive, making its widescale use more difficult to implement.

Another technique that has been investigated is the effect of alkali and organic acids on high temperature HTL (Ross et al., 2010). In this study, 1 M alkali or organic acids (Na_2CO_3, KOH, HCOOH, and CH_3COOH) were added to the HTL reaction of *Spirulina* and *Chlorella* microalgal strains at 300 and 350 °C. The average nitrogen content reported in the biocrude generated was 4.7% with alkali acids and 5.3% with organic acids; this was coupled with a maximum biocrude yield of 27.3% in *Chlorella* and 20.0% in *Spirulina* (at 350 °C using Na_2CO_3). This is marginally different from the results Jena et al. (2011a) reported on a similar HTL of *Spirulina* study with no acid catalysts, in which HTL conducted at 350 °C for 1 hour generated a biocrude containing a nitrogen content of 6.3% at a yield of 39.9%. Similarly, our direct HTL of *Spirulina* conducted in this study (see Section 5.3.2) generated a biocrude containing a nitrogen content of 7.1% at a yield of 29.34%. The use of acid catalysts such as these seems to be effective in increasing the quality of the biocrude by removing nitrogen, but the presence of the catalysts may become problematic for downstream processing, requiring additional input energy for separation of the acids before distillation of the biocrude. It thus appears beneficial to create nitrogen removal without the addition of external catalysts, enzymes, or reagents.

Garcia-Moscoso et al. (2013) examined a continuous flash hydrolysis method that utilized subcritical water to hydrolyze *Scenedesmus* proteins rapidly. They report that subjecting an algae slurry (approx. 1% algae by mass, in water) to subcritical hydrolysis temperatures for a little as 10 seconds can extract up to 66% (at 305 °C) of the nitrogen initially present in the algae feedstock. They also demonstrate an increase in the nitrogen removal as temperatures increase from 205 to 305 °C; however, this increase in nitrogen removal is coupled with a decrease in the biomass retained, decreasing from 52.1% at 205 °C to 24.0% at 325 °C. One issue with the study conducted by Garcia-Moscoso is the scale at which their continuous setup was operated. They demonstrated successful flash hydrolysis on the 3 mL scale using a 1% algae slurry (by mass); heat transfer and flowability become major concerns when discussing the scalability of a process, especially when the mechanism of hydrolysis depends on rapid heat transfer.

Chakraborty et al. (2012) proposed a sequential hydrothermal extraction that utilizes both low-temperature (160 °C) and high-temperature (300 °C) hydrothermal liquefaction on *Chlorella sorokiniana* microalgae both to reduce nitrogen present in the generated bio-oil and to extract value-added polysaccharides. Through their two-stage batch process, they reduced the nitrogen present in their bio-oil from 1.14% using direct HTL to 0.78% using sequential HTL. Their algae feedstock was grown heterotrophically in fermentors, which yielded a low nitrogen feedstock (2.91% initially). The addition of the low-temperature HTL decreased the bio-oil yield from 27.8% in direct HTL to 23.4%. Miao et al. (2014) tested a similar sequential HTL of yeast (180 °C followed by 220 °C). Through their two-stage batch process, they reduced the nitrogen present in their bio-oil from 1.13% using direct HTL to 0.51% using sequential HTL; their yeast feedstock contained a nitrogen content of 2.65%, which is significantly lower than many algal feedstocks due to the high protein content normally found in algae. This two-stage process had very little effect on the biocrude yield, which was approx. 58.3% for both direct and sequential HTL. In both Chakraborty et al. (2012) and Miao et al. (2014), the feedstocks studied were grown under ideal conditions. Realistically, large-scale production of fuel precursors must stem from feedstocks

grown under the most economically feasible conditions, balancing optimization of feedstock characteristics with economics and energy inputs.

This study was developed to evaluate the use of a low-temperature hydrothermal pretreatment (PT) on mass-produced algae feedstocks and the effect of that pretreatment on biocrude generated from high-temperature liquefaction. In principle, utilization of a low-temperature hydrothermal pretreatment could hydrolyze proteins without significantly hydrolyzing lipids or carbohydrates, causing the degradation products to become water soluble and removing nitrogen from the solid phase (Abdelmoez et al., 2007; Fujii et al., 2006; Lamoolphak et al., 2006; Rogalinski et al., 2005, 2008). The solids retained from the hydrothermal pretreatment could then be utilized as a low-nitrogen feedstock for high-temperature hydrothermal liquefaction to produce biocrude with a favorable elemental composition. The aqueous co-product stream, now nitrogen-rich from the protein and nitrogen extraction, will be evaluated for characteristics that would allow it to be used as a nutrient recycle stream for future algae growth (Alba et al., 2013; Biller et al., 2012; Jena et al., 2011b; Minowa and Sawayama, 1999). Nitrogen (typically as ammonium or nitrate) and other nutrients present in the aqueous stream (such as phosphorus and potassium) could be used to supplement the cultivation of algae feedstocks.

Moreover, even with the reduction in nitrogen from the pretreatment stage, the nitrogen content of the subsequent biocrude is too high for direct use as a refinery input. This, coupled with an abundance of oxygen in the biocrude, makes it unsuitable for co-processing with petroleum oil. Typically, refinery oils based from petroleum contain 0.5-6% oxygen and 0.1-1.5% nitrogen (Manning and Thompson, 1995; Mederos et al., 2012; Olsen, 2014). It is thus common practice to upgrade the biocrude generated through heterogeneous catalytic hydrodeoxygenation and hydrodenitrogenation (Galadima and Muraza, 2014; Tran et al., 2010).

Bai et al. (2014) performed a catalytic screening study in which algae oil generated from the liquefaction of *Chlorella* was subjected to a two-stage upgrading process: a high-temperature upgrading stage using hydrogen gas without catalyst (350 °C for 4 hours), and a supercritical up-

grading stage using varying types of heterogeneous catalysts (400 °C for 4 hours; 10% catalyst loading by weight). It was determined that although the hydrogen treatment favorably reduced the nitrogen content of the bio-oil and increased its flowability, every catalyst tested achieved greater desirable changes. Specifically, across a range of 14 commercial catalysts, including precious metal catalysts, sulfided metal catalysts, zeolites, and varying supports, their work demonstrated that ruthenium (5% wt. on carbon) and Raney nickel, used in conjunction, produced the best results. Their two-stage process reduced the nitrogen content of the bio-oil from 8.0% to 2.0% (by mass).

Savage and Duan (2011) conducted a study on the relative importance of temperature (430 to 530 °C), time (2 to 6 hours), catalyst loading (5 to 20%), and catalyst type on the quality of algae bio-oil after the catalytic upgrading stage. Using either Mo_2C, HZSM-5, or Pt/C catalyst, they determined which parameter of the catalytic hydrodeoxygenation (HDO) stage had the most relevant effect on the elemental quality, the compound quality, and the higher heating value of *Nannochloropsis* hydrothermal liquefaction (HTL) biocrude upgraded in supercritical water. Their work demonstrated that temperature had the greatest relative importance for every biocrude characteristic analyzed, with higher temperatures (530 °C), times (6 hours) and catalyst loading (20%) correlating to more favorable quality. Their evidence showed that at an HDO temperature of 530 °C, however, more of the carbon was distributed to the gas and coke phases than to the oil phase. This suggested that 530 °C was likely too severe a treatment temperature if liquid fuel precursors are the desired product. Supercritical temperatures, in general, are inherently more energy demanding, requiring additional energy inputs to maintain.

This study was designed firstly to determine if subcritical HDO temperatures (350 °C) are suitable for generating refinery quality bio-oil if paired with low- and high-temperature hydrothermal liquefaction. Literary evidence suggests that using a lower temperature during HDO will maximize the bio-oil yield: a necessary qualification for the technology to be considered for scale-up (Bai et al., 2014; Galadima and Muraza, 2014; Tran et al., 2010). To better mimic the continuous

reaction setting likely to be utilized on the larger scale, catalytic HDO will be performed on the entire HTL liquid and solid product (including the aqueous phase) (Elliott et al., 2013; Jazrawi et al., 2013). Moreover, Bai et al. (2014) and Savage and Duan (2011) both suggested that catalyst performance is heavily affected by the algae strain being used and the conditions of the upgrading stage. For that reason, multiple catalysts will be evaluated in this study. Ruthenium (5% on carbon, Ru/C) will be the control catalyst used, since its performance has already been demonstrated as a top candidate for this process (Bai et al., 2014). Cobalt molybdenum (CoMo) will be evaluated in several forms, as it is a primary candidate for co-processing with petroleum oil. Sulfided CoMo is regularly used in petroleum refining, and will thus be evaluated; since algae biocrude is naturally low in sulfur concentrations, a hydrogen-reduced CoMo will also be evaluated. In addition, a hydrogen reduced mixed metal oxide catalyst known as red mud (primarily iron oxide, RRM) will be evaluated, as it is potentially an inexpensive alternative to precious metal catalysts since it is a waste product from the mining industry. Several explorative evaluations of the activity of RRM as an HDO catalyst in the presence of hydrogen have been performed on model compounds (Balakrishnan et al., 2011; Sushil and Batra, 2008).

3.2 Selection of Model Macromolecules

Rather than performing HTL only on model whole algae cells, a series of reactions will be tested involving varying combinations of model macromolecules. These ratios are meant to provide insight on product formation in a way that systematically identifies pathways while simultaneously providing kinetics for these pathways. Model compounds will be selected in a manner that best represents a wide range of algal strains; these compounds will be selected based on the constituents that compose them. The lipid will be selected on free fatty acid composition, the protein on amino acid composition, and the carbohydrate on simple sugar composition.

For lipid selection, a survey of *Spirulina platensis* was performed in which the free fatty acid composition was determined. Literature indicates that lipids generated by this species are primarily composed of the C_{16} free fatty acid, palmitic acid (Oliveira et al., 1999; Torzillo et al., 1986). Figure 3.1 shows that the lipids of *Spirulina* contain palmitic acid at nearly 50 percent. Since palmitic acid was the highest lipid component, this was the major characteristic for determining an appropriate model lipid. Figures 3.2 and 3.3 indicate that palm oil is an obtainable lipid that contains the necessary proportions of free fatty acids (mainly, palmitic acid) (Carpenter et al., 1976; Man et al., 1999). The palm oil will be sourced from palm fruit.

Figure 3.4 on page 41 illustrates the simple sugar (monosaccharide) composition of 16 different algal strains (Brown, 1991). In the strains listed, the majority of the simple sugar weight contained by the algae is in the form of glucose; these percentages range from 21 to 87.5 percent. Since most algae surveyed follow this pattern, the model carbohydrate being chosen is one containing glucose as its primary monosaccharide (Brown, 1991; Salimath et al., 1987). Starch fits the criteria effectively, as it is composed of a glucose polymer. The starch will be sourced from potatoes.

Algal proteins were initially surveyed for amino acid composition; a model protein was to be selected based up similarities between that protein, and the average amino acid make-up of algal strains as a whole. As Figure 3.5 on page 42 illustrates, there is no clear, representable amino acid composition that can be accurately modeled; each algae species surveyed had a different amino acid composition (Babadzhanov et al., 2004; Brown, 1991; Torzillo et al., 1986). This criteria was thus dropped, and was not used to select a model protein. Instead, a model protein was selected based on more generalized characteristics and prior research performed on the model protein.

The highest frequency protein found in algae are part of a water-soluble group of photosynthetic proteins called *Biliproteins* (Simo et al., 2005). This protein group, comprised of *allophycocyanin and c-phycocyanin*, was found to have properties that can be modeled by most high-production proteins. Albumin was thus selected because of the knowledge already amassed in literature and

because of its macro-qualities (such as solubility) that make it similar to algae *Biliproteins* (Stein, 1949). The albumin will be sourced from chicken eggs.

3.3 Figures and Tables

Table 3.1: Free fatty acid composition of *Spirulina sp.* (Torzillo et al., 1986).

	$C_{16:0}$	$C_{16:1\,\Delta 9}$	$C_{18:1\Delta 9}$	$C_{18:2\Delta 9,12}$	$C_{18:3\Delta 6,9,12}$
Photobioreactor	52.3	4.2	3.8	23.0	13.8
Open Pond	48.0	6.5	3.0	21.5	18.1

Table 3.2: Free fatty acid composition of palm oil (Man et al., 1999).

	Fatty Acid Composition (%)				
Fatty Acid	CPO[a]	RBD palm oil	RBD olein	RBD stearin	Superolein
Saturated					
M	0.93	0.92	0.89	1.21	0.81
P	45.48	46.3	41.54	61.21	38.47
S	3.49	3.52	3.51	4	3.14
Total	49.91	50.74	45.94	66.42	42.42
Unsaturated					
O	40.17	39.58	43.63	27.54	35.77
L	9.92	9.68	10.43	6.05	11.81
Total	50.09	49.26	54.06	33.59	57.58

[a]CPO, crude palm oil; RBD, refined, bleached, deodorized; M, myristic; P, palmitic
S, stearic; O, oleic; L, linoleic

Table 3.3: Free fatty acid composition of various vegetable oils (Carpenter et al., 1976).

Oil	14:0	16:0	16:1	18:0	18:1	18:2	18:3	Unknown
	Weight percent of total fatty acid methyl esters							
Wesson SBO/CSO	0.1	12.1	0.1	4.2	33.4	46.7	3	0.4
Nu-Made SBO/CSO	0.1	10.8	0.2	5	35	44.1	3.4	1.4
Giant SBO	0	10.1	--	4.8	40.8	40.8	2.7	0.8
Crisco SBO	0	8.9	--	3.9	47.2	36.7	2.7	0.6
Kraft SBO	0	10	--	5	45.8	36.6	2	0.6
Hollywood SBO	0	10.6	--	4.1	24.7	52.6	7.6	0.4
Ann Page CO	--	11.4	--	2.2	26.1	58.5	1.4	0.4
Nu-Made CO	--	11.3	--	2.2	26.4	58.3	1.2	0.6
Marola CO	--	11.5	--	1.8	25.1	60.5	0.6	0.5
Saffola SFO	0.1	6.4	--	2.3	11.6	79.3	--	0.3
Hollywood SFO	0.1	6.5	--	2.4	11.2	79.5	--	0.3
Planters PO	--	10.2	--	2.4	47.1	33.2	--	7.1
Progresso OO	--	10.5	0.8	3.1	78.6	6.2	0.5	0.3
Golden Harvest AKO	--	5.2	0.8	1.2	58.7	33.4	0.7	0

SBO = Soybean Oil; CSO = Cottonseed Oil; CO = Corn Oil; SFO = Safflower Oil; PO = Peanut Oil; OO = Olive Oil; AKO = Apricot Kernel Oil

Table 3.4: Sugar composition (weight percentage) of several algae species (Brown, 1991).

Sugar	Bacilliariophyceae						Chlorophyceae	
	C. calcitrans	*C. gracilis*	*N. closterium*	*P. tricornutum*	*S. costatum*	*T. pseudonana*	*D. tertiolecta*	*N. atomus*
Arabinose	0.20	0.33	2.40	0.15	1.4	0.19	0.65	0.16
Fructose	14.3	6.9	12.8	4.3	3.4	2.8	0.0	7.9
Galatose	20.5	14.9	18.4	8.9	7.0	5.4	1.1	10.6
Glucose	54.7	57.9	32.6	21.0	62.0	82.4	85.3	55.2
Mannose	2.0	5.5	16.8	45.9	11.4	5.0	4.5	5.0
Rhannose	3.3	6.0	7.7	8.6	6.6	1.3	5.5	13.3
Ribose	3.3	3.5	2.1	3.7	5.4	1.4	2.0	1.0
Xylose	1.7	5.1	7.0	7.5	2.8	1.6	1.0	6.6

Sugar	Cryptophyceae	Eustigmatophyceae	Prasinophyceae		Prymnesiophyceae		
	C. salina	*N. oculata*	*T. chul*	*T. succica*	*I. galbana*	*P. hutheri*	*P. salina*
Arabinose	0.08	0	0.41	0.9	5.7	11.7	1.6
Fructose	3	4.4	0	0	0.6	3.6	0.51
Galatose	2.7	3.8	11.3	15.7	19	12.9	4.4
Glucose	87.5	68.2	84.7	74.8	76.5	42.6	81
Mannose	2.3	6.1	1.8	3	3.6	13.2	5.1
Rhannose	0	8.3	0.04	0.97	0.3	2.1	0
Ribose	2.5	4.6	1.8	4.5	2	3.5	2.5
Xylose	1.6	4.4	0	0	2.3	10.3	48

Table 3.5: Amino acid composition of several algae species (Brown, 1991).

Amino Acid	Bacilliariophyceae						Chlorophyceae		Cryptophyceae
	C. calcitrans	*C. gracilis*	*N. closterium*	*P. tricornutum*	*S. costatum*	*T. pseudonana*	*D. tertiolecta*	*N. atomus*	*C. salina*
Essential									
Arginine	6.4	6.6	7.1	6.6	6.4	6.3	6.8	5.9	6.7
Histidine	1.9	2.4	1.4	1.7	1.6	1.6	2.1	1.8	1.8
Isoleucine	5.5	5.8	5	4.9	5.2	5.5	4.8	3.4	4.1
Leucine	82	7.2	8.1	7.7	8.3	8.4	8.4	7.5	7.8
Lysine	6.3	5.1	5.7	5.6	5.7	5.9	6	5.2	6.1
Methionine	2.6	2.4	1.6	1.9	2.2	2.2	1.4	1.9	2.4
Phenylalanine	6.7	7.1	6.9	6.6	6.4	6.8	6.7	5.5	5.5
Proline	5.6	6.3	4.6	6.3	4.9	4.8	6.5	13.1	5.4
Threonine	4.5	5.9	5.5	5.4	5.11	5.2	4.7	4	5.4
Tryptophan	1.4	1.6	1.4	1.6	1.3	0.87	1.5	1.1	1.3
Valine	5.9	6.2	6.2	5.9	6.3	6.1	6.2	5.9	6.1
Non-essential									
Alanine	7.2	6.9	6.9	7.2	7.3	7.4	8	8.2	7.9
Aspartate	9.8	8	8.8	8.6	10.1	9.7	9	8.3	9.5
Cystine	0.42	0.52	0.58	0.38	0.4	0.53	0.44	0.55	0.63
Glutamate	10.5	9.4	10.6	11.2	10.4	10.4	10.3	11.4	10.9
Glycine	5.9	5.1	6	5.8	6.4	6.2	6	6.3	5.8
Hydroxy-proline	0.18	0.33	1.4	0.31	0.23	0.23	0.15	0.3	0.04
Ornithine	0.21	0.33	0.52	1.4	0.39	0.21	0.35	0.25	0.28
Serine	5.8	6.6	6.6	5.9	6.1	6.8	5.2	4.8	5.9
Tyrosine	4.5	5.4	3.9	4.1	4.5	4.2	5	3.9	5.6

Chapter 4

Experimental Approach

4.1 Methodology and Experimentation

4.1.1 Materials

Freeze-dried *Spirulina* was obtained from Earthrise Nutritionals LLC (Calipatria, CA), and *Nannochloropsis* was obtained from Reed Mariculture (”Nanno 3600”, strain CCMP525). A consortium of three algal strains (*UGA Consortium* henceforth), namely *Chlorella sorokiniana*, *Chlorella minutissima*, and *Scenedesmus bijuga*, were grown and harvested for use in this study as well. A monoculture inocula of the constituent strains were first grown in 20 L carboys under controlled conditions in a growth chamber at 25 $\pm$ 1 °C for 12 h with alternating light-dark cycles; the light intensity was 100 μmoles m^{-2} s^{-1} with continuous air bubbling. The final consortium was prepared by mixing equal proportions (v/v) of each individual strain and then using it as inoculum at 10% v/v for outdoor cultivation in raceway ponds under green house facilities at an algae bioenergy lab of UGA. The raceway ponds are constructed of HDPE plastic and are 1.32 m wide, 2.18 m long, and 0.61 m deep with a working volume of approximately 500 L at 0.17 m water depth. Standard algae growth medium BG11 was used in fresh water for cultivation. Supplemental CO_2

was derived from a commercial 10% CO_2 storage cylinder and used as a carbon source and for pH control. The UGA designed carbonation column (Putt et al., 2011) was used for CO_2 mass transfer. Once the cell density in raceways reached 500 mg/L, the biomass was harvested using a continuous centrifuge and dried at 55 °C until constant weight was observed after multiple weighing. The dried biomass was packed in zip-lock bags and stored at 4 °C until further use. Subsequently, the dried microalgae was ground to a fine powder using a heavy-duty laboratory knife mill (Retsch SM 2000, Germany) with a screen size of 0.5 mm. The knife mills cutting blade rotor (1690 rpm, 60 Hz) was powered by a 1.5 kW electric motor.

Ruthenium (5% on carbon w/w, 20 um particle size, *Ru/C*) and a cobalt oxide (3.4-4.5%) molybdenum oxide (11.5-14.5%) on alumina (Al_2O_3) catalyst (2.5 mm trilobe, *CoMo*) were obtained from commercial sources. The $CoMo/Al_2O_3$ catalyst was reduced in the presence of flowing hydrogen (100%) at 400 °C in a tubular packed bed reactor (1 in. ID); 100 mL min^{-1} of hydrogen gas was passed over the catalyst for 2 hours (*CoMo-H_2*). In addition, pre-sulfided $CoMo/Al_2O_3$ catalyst (2-7% Co-S and 5-25% Mo-S, trilobe 2.5 mm, *CoMo-S*) was obtained from EureCat (EU). A mixed metal oxide catalyst (Red Mud) was obtained from Rio Tinto (Alcan, Canada). This catalyst was dried (105 °C), crushed, and sieved ($0.5 < d_p < 2$, mm). The red mud particles were reduced in the presence of flowing hydrogen (100%) at 300 °C in a tubular packed bed reactor (1 in. ID); 90 mL min^{-1} of hydrogen gas was passed over the catalyst for 20 hours (*RRM*).

4.1.2 Apparatus and Experimental Procedure

The low temperature liquefaction pretreatment (*PT*, 125 to 225 °C) was performed in a batch reactor (Parr 5000 Multi Reactor System, 75 mL vessel). Vessels were charged with 7 g of algae and 32 g of deionized water, and were sealed using a PTFE gasket. The system contains six separate vessels, each with its own PTFE magnetic stir bar (300 RPM) and band heater in an aluminum block (250 W); the heating rate of each reactor is approximately 10 °C min^{-1}. The residence time is taken from the point the reactor reaches temperature. Vessels were pressurized

with 300 psi (20.7 bar) helium prior to heating to ensure liquid water throughout the reaction. Once the residence time was complete (ranging from 0.5 to 30 minutes), the vessels were removed from the heating block, and the bottom sections of the vessels (below the screw cap) were submerged in a water bath. At ambient temperatures, the vessels were depressurized and weighed to determine the mass of gas produced from the reaction.

The whole product from the low temperature liquefaction stage was transferred without additional solvent into a 50 mL centrifuge tube and centrifuged in a Sorvall Super T21 centrifuge at 10000 RPM for 20 minutes. The aqueous phase was decanted off and weighed, and the remaining solids were resuspended in a fresh aliquot of deionized water (enough to make the slurry 47 g total). For solid analysis, solids were dried after centrifugation and decanting at 105 °C for 4 hours.

High temperature liquefaction (*HTL*, 350 °C) was performed in a different batch reactor (Parr 4598 Micro-Stirred Reactor, 100 mL vessel). Vessels were charged with either 7 g of algae and 40 g of deionized water, or with the resuspended solid slurry. Vessels were sealed using a consumable Parr Grafoil gasket (flat flexible graphite). The mixture was stirred using a 4-blade impeller powered by a magnetic stirrer (model no. A1120HC6, 100 W variable speed) at 300 RPM. Vessels are heated using a ceramic fiber external jacket (700 W); the heating rate is approximately 14 °C min^{-1}. The residence time is taken from the point of PID leveling that is characterized by a noticeable and sizable decrease in the heating rate, occurring approximately 10 degrees below the set point. High temperature liquefaction was performed at 350 °C for 60 minutes. Vessels were pressurized with 500 psi (34.5 bar) helium prior to heating to ensure liquid water throughout the reaction. Once the residence time was complete, the external jacket was lowered and removed, and the vessel was cooled using a fan. At ambient temperatures, the vessels were depressurized and weighed to determine the mass of gas produced from the reaction. The whole product was transferred without additional solvent into a 50 mL centrifuge tube for storage.

Catalytic hydrodeoxygenation (*HDO*, 350 °C) was performed in the Parr 4598 Micro-Stirred Reactor following the procedure listed above. The vessels were charged with catalyst while being charged with the reaction slurry, and 750 psi (51.7 bar) of hydrogen gas was used to fill the headspace. The headspace was purged with hydrogen gas for 1 minute prior to pressurization. Reactions were conducted for 4 hours, stirring at either 300 or 500 RPM.

Separate experimentation was performed at the Desert Research Institute (DRI) to determine if protein separation and nitrogen reduction during the low-temperature liquefaction pretreatment (175 to 250 °C) could be achieved at very short residence times (less than 5 minutes) if batch heat-up times were minimized. DRI's two-chamber reactors operate by preheating the reaction water prior to addition of biomass (see Figure 5.1). The reaction water in the reactor is heated to the desired temperature, and a ball valve is opened to drop biomass into the hot reaction chamber; the biomass (inside a screen) is reacted for the desired time, then the entire reactor is quenched in an ice bath. Approximately 5 g algae biomass (*UGA Consortium* only) and 40 mL deionized water were used. At the end of the experimental trial, the reactor was ice-cooled and the gaseous products were vented to the atmosphere. Centrifugation, decanting, and solid drying were performed before analysis of phases, as stated above.

4.1.3 Extraction of Primary Oil via Methylene Chloride

Following high temperature liquefaction or catalytic HDO, 40 mL of dichloromethane (DCM) was added to the whole product and mixed. This solution was filtered under vacuum through Whatman #4 filter paper (pore size 20-25 um), and the cake was rinsed with 15 mL of additional DCM. The cake was weighed wet, dried at 105 °C for 4 hours, and weighed again to determine wet and dry solid yield, and estimated solid water content. The filtrate was transferred into a separatory funnel (150 mL) and was allowed to phase separate for 15 minutes. The bottom phase (oil, solubilized in DCM) was decanted off, and 1 g of anhydrone (magnesium perchlorate) was added to the decanted phase. The interface between the phases (approximately 1 cm) was discarded, and the

top layer (aqueous phase) was sampled and stored. The DCM/oil phase was filtered again under vacuum with 10 mL DCM used to rinse the anhydrone cake. The filtrate was transferred to a rotary evaporator (Rotovap) flask. The flask was then rotated under vacuum pressure (40 mbar) in a 36 °C water bath for 30-45 minutes until all DCM was removed; the remaining product was weighed to determine the mass of bio-crude. Since the solvent-free bio-crude is very viscous, two different storage techniques were used: a subsample was scooped from the flask using a scoopula for analyses that require solvent-free product, and the remaining bio-crude in the flask was resuspended in DCM (approximately 6:1 DCM:oil by mass).

4.1.4 Sample Workup and Analytical Methods

Yield and Elemental Removal

Phase yields are determined based on a weight percentage of some reference weight. Most yields are referenced against the weight of dry/ash-free (daf) feedstock charged to the reaction. In the case of multi-stage conversion, yield is based upon the daf feedstock weight charged to the first stage.

The nitrogen removal was calculated on a weight basis based on the initial amount of nitrogen in the dry/ash-free feedstock, according to Eq. 6.2.

$$\%Nitrogen\ Removal = \frac{(\%N * DAF\ wt.)_{feedstock} - (\%N * wt.)_{product}}{(\%N * DAF\ wt.)_{feedstock}} * 100 \tag{4.1}$$

CHNS-O Elemental Analysis (Ultimate)

The elemental composition (C, H, N, and S) of the samples was measured using a Thermo-Scientific Flash 2000 elemental analyzer according to the ASTM D5291 standard method; solvent-free oils and dry solids were used in this analysis. Oxygen was found by subtraction, assuming

these 5 elements comprise 100% of the sample. Issues with the catalytically upgraded biocrude being overly volatile during sample weighing were overcome by using two tin capsules (instead of one) and by loading and analyzing each replicate individually (rather than loading the device carousel fully). The higher heating value (HHV) of bio-crude was estimated using the elemental composition and the Dulong formula, Eq. 6.1 (Corbitt, 1999).

$$0.3383 * \%C + 1.422 * (\%H - (\%O/8)) \quad [MJ/kg] \tag{4.2}$$

Gas Chromatography-Mass Spectrometry (GC/MS)

Gas Chromatography/Mass Spectrometry (GC/MS) was performed on an Agilent GC-MSD (Hewlett-Packard 5973 and 6890) with an HP5 MS Capillary Column (30 m x 0.25 um x 0.25 um). Separation was achieved using a temperature-programmed method of 40 °C, held for 4 minutes, with a 5 °C min^{-1} ramp until 275 °C was reached, held for 5 minutes; the inlet was held at 260 °C, the split ratio was 50:1, the injection volume was 1 uL, the helium carrier gas flow was 0.8 mL min^{-1}, and the MS scan was 30-400 m.u.

Standard curves were constructed on model compounds using 1-hexanol as an internal standard, in triplicate. Known concentrations of model compounds were mixed with a consistent concentration of 1-hexanol, and a linear correlation was found, describing the relationship between the model concentration and the ratio of the model peak area and the 1-hexanol peak area. Unknown compound concentrations were measured by adding the same 1-hexanol concentration used to construct standard curves to the unknown and performing the GC/MS method described above. The peak area ratio linear correlation was used for compounds for which a standard curve had been constructed.

Gas Chromatrography-Thermal Conductivity Detection (GC-TCD)

Gas Chromatrography-Thermal Conductivity Detection (GC-TCD) was performed on a Carboxen 1000 with a 60/80 SS Packed Column (15 ft x 1/8 in). Separation was achieved using a temperature-programmed method of 35 °C, held for 5 minutes, with a 20 °C min^{-1} ramp until 200 °C, held for 5.75 minutes; the inlet was held at 100 °C, the detector at 140 °C, and the injection volume was 50 uL gas sample.

Gas Chromatography-Flame Ionization Detection (GC-FID)

Gas Chromatography-Flame Ionization Detection (GC-FID) was performed on an HP Innowax column (30 m x 0.25 mm x 0.25 mm) with an HP 5890 Series II detector. Separation was achieved using a temperature-programmed method of 45 °C, held for 2.5 minutes, with a 10 °C min^{-1} ramp until 200 °C, held for 8 minutes; the inlet was held at 240 °C, and the detector was held at 250 °C.

High Pressure Liquid Chromatography (HPLC)

High Pressure Liquid Chromatography (HPLC) was performed on a Shimadzu LC-20 AT equipped with a RID-10A refractive index detector and a Coragel 64-H transgenomic analytical column (7.8 x 300 mm); the flow was 0.6 mL min^{-1} for a 55 minute run time, the sample volume was 5 uL, the mobile phase was 4 mN sulfuric acid, and the samples were analyzed at 6.89 MPa and 60 °C. About 2 mL of the oil was diluted with DI water at 1:1 ratio and centrifuged at 5000 rpm for 30 min, and then decanted. The supernatant was filtered through a 0.45 um filter into 2 mL auto-sampling vials. The sample was injected into the column using the LC-20 AT Shimadzu auto-injector.

Thermal Gravimetric Analysis (TGA) and Proximate Analysis

Proximate analysis was performed using Thermal Gravimetric Analysis (TGA) on a LECO TGA 701. The moisture step was performed with a 6 °C min^{-1} ramp from 25 to 107 °C in a nitrogen atmosphere, the volatiles step was performed with a 43 °C min^{-1} ramp from 107 to 950 °C in a nitrogen atmosphere with crucible lids on, and the ash step was performed with a 15 °C min^{-1} ramp from 600 to 750 °C in an oxygen atmosphere.

Total Acid Number (TAN)

Total Acid Number was determined according to the ASTM D974-12 standard method, in which sample dissolved in a solution of toluene, isopropanol, and water (500:495:5, by mass) is titrated with potassium hydroxide titrant (dissolved in isopropanol, molarity approx. 0.11 M) until the indicator solution (p-naphtholbenzein) drastically changes color. Total Acid Number is typically reported as milligrams of KOH required to neutralize one gram sample (mg KOH (g $oil)^{-1}$).

Water Content

Water content was determined using a Mettler Toledo DL31 Karl Fischer Titrator. Water content was measured on a weight percentage basis using sample suspended in Hydranal, titrated with CombiTitrant 5 Keto.

Bradford Protein Assay

The concentration of whole proteins was found by performing Bradford Protein Assay using 0.15 M NaCl, Coomassie Blue Dye, and UV-Vis spectroscopy; bovine serum albumin was used as a standard (Bradford, 1976).

Simulated Distillation (SimDist)

Simulated Distillation was performed on a Mettler-Toledo TGA/SDTA 851e. The following temperature-programmed volatilization was used: 25 °C initially, followed by a 10 °C min^{-1} ramp to 625 °C. 40 uL aluminum crucibles containing approximately 2 mg of sample were used for analysis; the inert gas flow was 50 mL min^{-1} of nitrogen.

In addition, the boiling point distribution was simulated using GC/MS. The total peak area percentage for each identified compound was determined, and a direct correlation between retention time and boiling point was used. The boiling point distribution was constructed using the cumulative peak area percentage as compounds increased in both retention time and boiling point.

Catalyst Preparation and Characterization

Tar bound to the catalysts after reaction was weighed via rinsing. A known mass of used catalyst was rinsed with a 1:1:1 (by volume) mixture of toluene, acetone, and methanol, and was filtered under vacuum through Whatman #4 filter paper (pore size 20-25 um) until the rinsate became clear in color. The rinsed catalyst was then dried at 105 °C for 1 hour, and the mass lost through rinsing is considered tar. Tar is reported as a percent based per gram of catalyst, as shown in Equation 6.3.

$$Tar\ Removal(\%) = \frac{mass_{tar\ removed}}{mass_{catalyst}} \tag{4.3}$$

Surface area of the catalysts were measured by N_2 adsorption over a relative pressure range (P/P_0) of 0.05-0.35 using a 7-point BET analysis equation (Quantachrome AUTOSORB-1C, USA). Pore size distribution, average pore radius, and total pore volume were estimated from N_2 desorption curves using BJH analysis. All samples were degassed ranging from 250 to 300 °C for 3-4 hours prior to analysis.

Catalyst coke weight was determined using a Mettler-Toledo TGA/SDTA 851e. The temperature-programmed method was 25 °C, followed by a 10 °C min^{-1} ramp to 800 °C. 5 mg of sample was used, and the temperature profile occurred in an air atmosphere. For carbon-supported catalysts, the coke weight was determined compared to the mass loss observed from temperature-programmed combustion of an unused catalyst control.

Nitrogen and Ammonium Ion Concentrations

Total nitrogen was determined using the Persulfate Digestion Method (Hach Method 10072; Hach Co., USA). Ammonium (NH_4^+) concentrations were determined using a Thermo Scientific Orion Star A329 probe and meter.

Aqueous Phase Nutrient Concentrations

pH was determined using potentiometry performed on an Orion 520A Digital pH meter (Orion Research Inc., USA). Elemental concentrations (such as phosphorus, calcium, and magnesium) were determined using inductively coupled plasma (ICP) spectography (EPA Method 200.7) performed on a Thermo Jarrell-Ash 61E ICP (Thermo Elemental, USA).

4.2 Experimental Plan

4.2.1 Low Temperature Liquefaction Pretreatment: Optimization Studies

A series of low temperature liquefaction conditions were tested to determine the effects of liquefaction temperature and holding time on the nitrogen partitioning and solid retention of three algal strains (*Spirulina*, *UGA Consortium*, and *Nannochloropsis*). Table 4.1 shows the different combinations of experimental conditions. In short, liquefaction was performed at 125, 175, and 225 °C across holding times ranging from 0.5 to 30 minutes. The heating rate (approx. 10 °C

min^{-1}), solid loading (20% by mass), stir speed (300 RPM), and initial pressure (34.5 bar He) were all held constant.

The conditions were ranked based on their ability both to remove nitrogen from the solid phase and to retain total mass in the solid phase. In the event these two criteria are inversely related, nitrogen partitioning was held at a higher priority.

4.2.2 Two-Stage Conversion: Low- and High-Temperature Liquefaction

In order to determine the effect of the liquefaction pretreatment on biocrude generated from high-temperature liquefaction, the same series of experimental conditions used to optimize the low-temperature liquefaction stage were repeated (see Table 4.1), and the retained solids were resuspended in deionized water for use in high-temperature liquefaction. High-temperature liquefaction was performed at 350 °C for 1 hour, as these conditions promote the maximum biocrude yield (Jena et al., 2011a). High-temperature liquefaction control trials were also performed (without pretreatment) for comparative purposes. 54 trials were conducted in this study.

4.2.3 Catalytic Upgrading Implementation

The bio-oil generated from either single-stage or two-stage liquefaction requires upgrading in order to reach an elemental composition suitable for co-processing with current refinery inputs. Firstly, the effect of each individual stage (Pretreatment, HTL, HDO) on the final biocrude product was determined. Three strains of algae were tested against two catalyst types (Ru/C and RRM) and two catalyst loadings (10% and 30%). Table 4.2 contains the different combinations of experimental conditions. HDO was conducted on the entire HTL product, and the reaction temperature (350 °C), holding time (4 hours), heating rate (15 °C min^{-1}), stir speed (300 RPM), and initial pressure (51.7 bar) were all held constant; any pretreatment conducted utilized the optimized conditions

determined in the previous study. Figure 4.1 illustrates the complete 3-stage conversion, including separation techniques utilized.

The biocrude was analyzed for elemental content and qualitative chemical comparisons (via GC/MS). In addition, the hydrogen consumption (which is an indication of HDO reaction rate and catalytic activity) was measured via GC-TCD.

4.2.4 Catalytic Upgrading Optimization: Agitation Rate, Repeated Batch, and Catalyst Reuse

The catalytic upgrading stage was then optimized across several of its variables. First, the effect of the agitation rate on the catalytic activity (measured by hydrogen consumption and the quality of the oil generated) on a three-stage conversion process (PT/HTL/HDO) was determined; two strains (*UGA Consortium* and *Nannochloropsis* were tested across two additional agitation rates (500 and 700 RPM, compared to 300 RPM originally used). The catalyst type and loading were determined based on the most positive results found in the HDO implementation study; all other conditions were congruent to those used previously. 4 trials were conducted in this study.

After all of the above experiments had been conducted, an issue with the nature of the batch reactors arose: the amount of hydrogen that could be safely charged to the reactor prior to the HDO stage was being consumed, and thus the reaction itself was hydrogen limited. In a continuous reactor system, the hydrogen concentration would be constant regardless of the time-on-stream. It was thus decided that the HDO reaction would be repeated (hereafter referred to as *Repeated Batch, RB*). The 4-hour HDO stage would be conducted as normal, but the reactor, once cooled, would have its headspace flushed and recharged with 100% hydrogen (51.7 bar). The 4-hour HDO would then be conducted again before the contents removed and processed. Select combinations of strains and catalysts (Ru/C, RRM, CoMo-H_2, and CoMo-S) were tested, as shown in Table 4.3; as a confirmation, some of the repeated batch trials were conducted at a pretreatment temperature

other than what was found optimal (175 °C, as opposed to the optimized 225 °C). 11 trials were conducted in this study.

The effects of the Repeated Batch stage on the biocrude quality were determined, as well as a comparison between the various catalysts used.

In addition, a study was conducted to determine the longevity of the catalysts being used. As a representative study, the catalyst used for the repeated batch of *UGA Consortium* was reused in a second repeated batch on freshly made oil. This catalyst reuse study was compared to the effectiveness of fresh catalyst to determine the time-on-stream effects.

4.2.5 Hydrothermal Liquefaction of Model Macromolecules

The macromolecular ratios were mixed proportionally in water (by weight) so that the final mixture contains 80 percent water and 20 percent macromolecules. The working volume of the batch reactors to be used (Parr 4598 Micro-Stirred Batch Pressure Reactor and 4875 Pressure Reactor) was 50 and 500 mL, respectively. Each mixture was then sealed and pressurized with gas (helium for HTL, hydrogen for HDO) to an initial pressure of 500 psig or 750 psig, respectively. ParrCom software was used to control and monitor the vessel internal temperature and pressure, and the RPM of the internal impellers. The external heating jacket was engaged, and the ParrCom PID control raised the internal vessel temperature to 350 °C. The heating rate was constant across all sets (approximately 15 degrees per minute), and the stirrer was set to 300 RPM (significant enough to prevent mass transfer or heat transfer limitations).

Once the temperature reaches its PID ”leveling point”, indicated by a sharp decrease in heating rate, the 30-minute holding time began; this ”leveling point” normally occurred near 340 °C. For the large scale batches, 5 mL subsamples will be taken every 5 minutes without any pressure loss. Subsamples will be taken during heat up and holding. Upon subsampling, the subsample will be immediately quenched to room temperature by immersion in an ice bath. This quench

of temperature will be rapid enough to consider the cooling period insignificant compared to the heating and holding times, and thus it will be ignored.

Each sample or subsample was allowed to phase separate gravimetrically, causing an aqueous layer, an oil layer, and a solid layer to form. It will be assumed the solid layer was solely nonreacted macromolecules and solid formation, so no analysis was performed. For each of the other two layers, analyses that determined the concentration of reactants *A* and *B* for each macromolecule were performed (see Figure 2.7). Protein and amino acid concentrations will be determined using the Braford protein assay technique and reverse phase chromatography (Rogalinski et al., 2005). Reverse phase chromatography involves delayed solvent flow through a selective column that emits distinguishable peaks based upon the amino acid concentration. Starch and glucose concentrations will be determined using the Phenol Sulfuric Acid method and High Performance Liquid Chromatography (HPLC). Lipid concentrations will be determined using various solvent extractions (i.e. hexane). GC-MS will also be performed on each of the phases for each of the sets in order to identify the degradation products.

Table 4.4 contains the sets of ratios investigated (Becker, 2007; Brown et al., 2010; MILNER and HAROLD, 1948; Oliveira et al., 1999). The sets of macromolecules were performed in sequence (in duplicate or triplicate), with analysis performed in between each set. It is hypothesized that when comparing the products of the isolated macromolecules (identified by GC-MS) with the products typically seen in algae HTL bio-oil, some of the algal products will be missing. It is through the combination and cross-reaction of macromolecules that these additional suites of compounds will be formed.

The kinetics of each of the pathways can be modeled mathematically using first order reaction kinetics and the Arrhenius equation (see Equations 2.1 and 2.2 on page 16). The concentration changes over time (with respect to changing temperature) will undergo non-linear regression in Polymath software to determine the Arrhenius constants A and E_a respectively. These constants will be unique for each of the reactants in each of the pathways, so six different sets of constants

will be calculated for each of the primary and secondary reactants. Since the reactions taking place are not isothermal (due to batch heating conditions), k will not be calculated; instead, coupled differential equations will be used to map the change in k as a function of both time and temperature.

Through the kinetics developed, any ratio of macromolecules can be modeled, allowing the researchers to see the interaction of compounds and the results of liquefaction without having to physically mix or react the molecules. Table 4.4 shows nine defined ratios that will be used to determine the kinetic model of HTL of these macromolecules. The kinetic model will be used to calculate an optimized ratio of macromolecules that is predicted to yield the greatest amount of desirable bio-crude products while minimizing the yield of undesirable products. Once predicted, this ratio will be experimented with the model compounds in a manner similar to the previous sets; this experimentation is used to confirm the kinetic model.

One potential pitfall is the limitation model compounds have in representing the *entire* algal cell. More specifically, the kinetics of a mixture of model compounds, even in the same proportions as found in an algal cell, may differ because of unrepresented factors such as cell wall resistances, mineral micronutrients, and nucleic acids. It is assumed that these additional factors will be insignificant compared to the defining factors that drive hydrolysis. However, variances between the model HTL and algal HTL could be due to mass and heat transfer resistances through the cell wall and additional compounds being formed from the non-modeled algal compounds. It is hypothesized that the latter issue will be easily identifiable (i.e. a chlorinated compound found in algal oil is not likely to be a degradation product from the model macromolecules being utilized).

It is also important to mention that a low percentage of the algae will not convert to any portion of bio-oil; this unusable portion is called ”ash”. The ash percentages of each modeled algae have been embedded in the ratios themselves. It is hypothesized that these ash compounds do not inhibit or affect the hydrolysis, and thus they can be ignored.

4.2.6 Hydrodeoxygenation of Model Macromolecules

As mentioned, it is often advantageous to upgrade the product of HTL using catalysts in the presence of hydrogen gas. The catalyzed removal of both oxygen and nitrogen is beneficial to increasing the quality of the biocrude being produced. Once the liquefaction pathways had been identified, the process was shifted to a two-stage process in which the product of the liquefaction was subjected to a second, hydrodeoxygenation, step. It is ideal for the biocrude product, after HDO has been performed, to be composed primarily of hydrocarbons (either in a long-chain form, dodecane, or a cyclic form, cyclohexane).

This hydrodeoxygenation (HDO) step was performed on the product of the HTL step in its entirety; the only new additions to the vessel once the liquefaction has completed was hydrogen gas and the catalyst itself. The headspace was pressurized with hydrogen to 750 psig after the vessel had been purged with hydrogen, ensuring the headspace was filled entirely and purely with hydrogen. This pressure was used to ensure no mass transfer limitations exist between the hydrogen, the catalyst, and the biocrude compounds.

The catalyst selected for use in this stage is Ruthenium, suspended 5 % on carbon. This catalysts was added in a proportion of 30 % of the solid weight being reacted; 3 grams of catalyst was used for every 10 grams of dry solid initially added to the reactor (Bai et al., 2014).

The reaction was heated similar to the operation procedure presented in 4.1.2. Upon reaching the PID leveling point, the HDO was allowed to continue for 4 hours. The cooldown, processing, and extraction procedures are congruent to those listed for the HTL of the model compounds.

The macromolecular ratios were systematically varied (to achieve every combination) according to Table 4.4 on page 64. It was the goal of this phase of experimentation to demonstrate how even the cross products of algal liquefaction can be upgraded to create desired fuel precursor compounds.

It should be noted that the catalytic upgrading of algal oil is a process that is difficult to optimize. For this reason, it is not anticipated for *every* undesired compounds found in the HTL product to be eliminated and converted to a desirable product once HDO concludes.

4.3 Figures and Tables

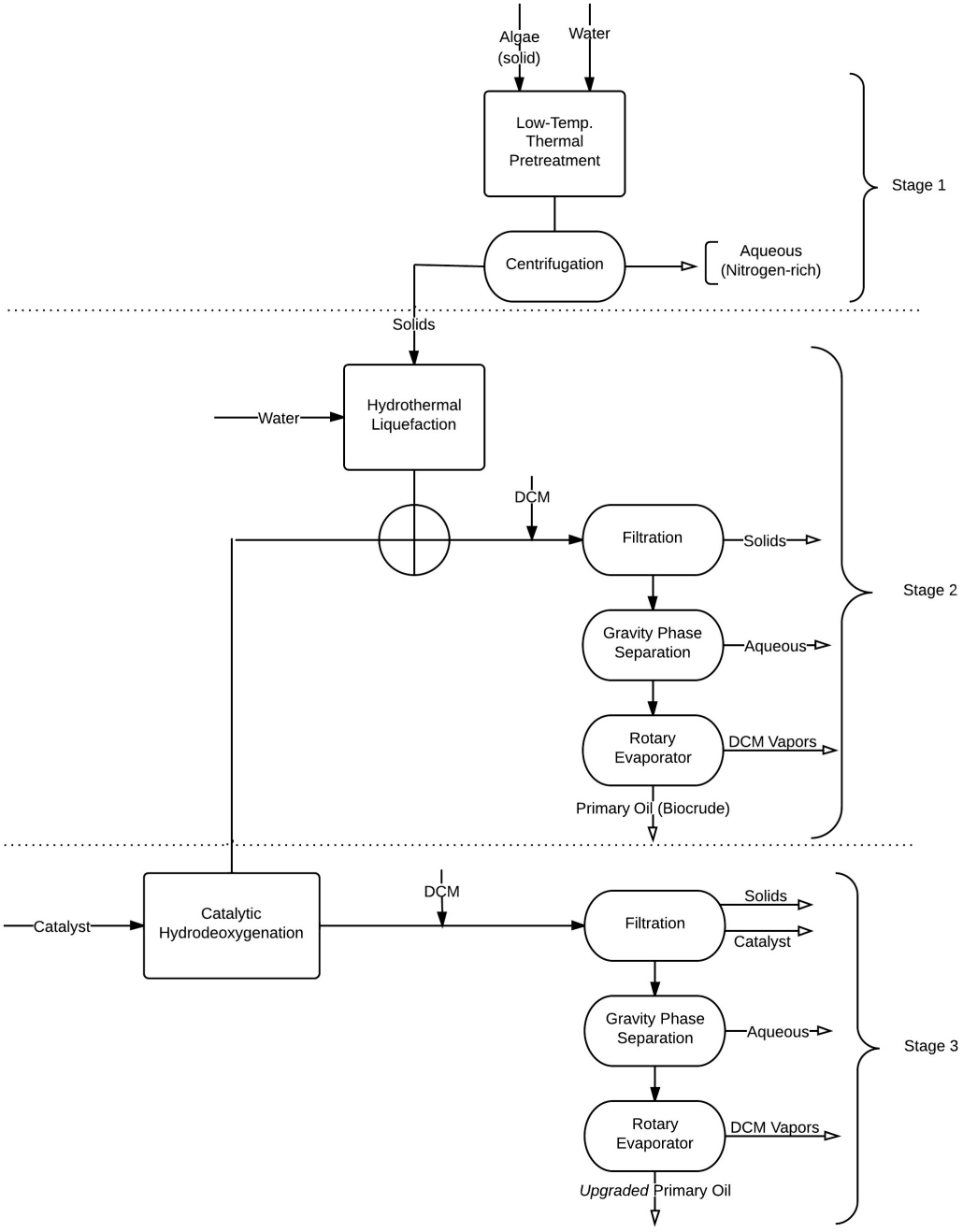

Figure 4.1: Overall schematic of three-stage conversion of algae to upgraded biocrude.

Table 4.1: Experimental Plan: Pretreatment Optimization.

Temperature	Holding Time	Strains	Number of Experiments	
(°C)	(min.)		(per strain)	(total)
125-225	0.5-30	3	18	**54**

Table 4.2: Experimental Plan: Catalytic HDO Implementation

Catalyst Types	Strains	Stage Combinations	Catalyst Loadings	Number of Experiments	
				(per strain)	(total)
2	3	4	2	16	**48**
Ru/C, RRM		HTL/HDO, PT/HTL/HDO, PT/HDO, HDO	10%, 30%		

Table 4.3: Experimental Plan: Repeated Batch.

Catalyst	Strain	PT Temperature (°C)
Ru/C	Nanno	225
	Nanno	175
	UGA	225
	UGA	175
	Spiru	225
	Spiru	175
CoMo-S	Nanno	225
	UGA	225
	Spiru	225
CoMo-H_2	Nanno	225
RRM	Nanno	225

Table 4.4: Weight ratio combinations of model macromolecules subjected to HTL.

Lipid	Carbohydrate	Protein	Reference
1	0	0	Lipid Only
0	1	0	Carbohydrate Only
0	0	1	Protein Only
1	0	1	Lipid/Protein
0	1	1	Carbohydrate/Protein
1	1	0	Lipid/Carbohydrate
1	1	1	Equal Parts
8	16	60	*Spirulina* model
28	12	52	*Nannochloropsis* model

Chapter 5

Evaluation of Low Temperature Hydrothermal Liquefaction of Algae for Low Nitrogen Biocrude Generation and Nutrient Recycling Potential[1]

[1]Costanzo, William and Umakanta Jena, Roger Hilten, KC Das, Jim Kastner. To be submitted to *Bioresource Technology*.

Abstract

A two-stage hydrothermal liquefaction process was used for the simultaneous production of low nitrogen biocrude from algae biomass and an aqueous co-product stream for algae cultivation. The first step involved a low temperature liquefaction pretreatment (PT: 125-225 °C, 0.5-30 minutes) to hydrolyze algal proteins and partition nitrogen out of the solid phase. The aqueous co-product was separated and analyzed for nutrient and toxin concentrations. The retained solid biomass was subjected to a higher temperature hydrothermal liquefaction (HTL) in the second step at 350 °C for 60 minutes. The low temperature pretreatment was found most effective at higher temperatures and holding times (225 °C, 15 minutes), partitioning 45% of the nitrogen present in the cultivated algae feedstock out of the solid phase while retaining 59% of the solid mass. Trials conducted in two-chamber reactors demonstrated increasing the reactor heating rate allows the same nitrogen partitioning with shorter residence times (54.4% N-reduction with conditions of 225 °C, 5 minutes). When paired with high-temperature HTL, this pretreatment improved the elemental content of the biocrude by increasing the total nitrogen removed, as compared to HTL alone. The aqueous co-product stream was analyzed for nutrient availability and it showed potential for further algae cultivation because of its high nitrogen and phosphorus levels, moderate pH, and low inhibitory compound concentrations.

5.1 Introduction

The Energy Independence and Security Act of 2007 (EISA) requires the United States to produce 36 billion gallons of renewable fuels from biomass sources by 2022. In support, the U.S. Department of Energy (DOE) has set a goal to promote energy diversity and independence in its strategic plan. Consequently, the DOE Biomass Program emphasizes four key priorities: 1) reduction of dependence on foreign oil, 2) promotion of diverse, sustainable, domestic energy resources,

3) reduction of carbon emissions and 4) establishment of a domestic biomass industry (EERE-2010-BT-CE-0014). Meeting the renewable fuel goals of EISA 2007 will require the production of liquid biofuels from a large and diverse volume of sustainable feedstocks.

Producing liquid fuels from the renewable sources such as biomass is critical to energy security and sustainability, and alternative sources of liquid fuels will protect the economic growth of the U.S. by eliminating the uncertainties caused by fluctuating petroleum prices. Algae as a source of liquid fuel production are attractive since they are renewable, grow rapidly even in adverse conditions, and reduce net greenhouse gas emissions by utilizing CO_2. Although algal biomass production has been commercialized in the recent years (Becker, 2007; Demirbas, 2010; Devi et al., 1981; McGarry and Tongkasame, 1971; Oliveira et al., 1999; Sandbank and Shelef, 1987; Torzillo et al., 1986), downstream processing and conversion of algal biomass to fuels is a significant bottleneck in commercialization according to the recent evaluations (NABT Roadmap, 2008). There has been limited focus on the conversion of algal biomass into liquid fuels, except for biodiesel production via transesterification process. Liquid fuels produced from algal biomass via transesterification is limited to high lipid algal species and requires algae monocultures and biomass drying, which lead to higher production costs. Drying is a highly energy intensive process and negatively affects the economy of the whole process. Thus, a conversion process that directly converts the wet algae biomass into liquid hydrocarbons is required. Such a product could then be catalytically upgraded to a product similar to gas oil or refinery intermediate. One such conversion technology is ”thermochemical or hydrothermal liquefaction” or ”TCL or HTL”, where algae biomass is pressure heated in hot compressed water (at 5-20 bar or 75-300 psi, and 280-380 °C) to generate biocrude, gases, water solubles and a solid residue (Toor et al., 2011). The biocrude is subsequently separated from the rest of the products and catalytically upgraded to a product similar to that of other petroleum intermediate streams.

HTL and pyrolysis are two thermochemical conversion processes that directly convert biomass into liquid hydrocarbons. Previous comparative evaluation of HTL and pyrolysis processes for

biocrude production from microalgae biomass indicate that HTL is energetically more efficient for liquid fuel production than the pyrolysis process, resulting in 29% higher biocrude yield and 32% more energy recovery (Jena and Das, 2011). Also, past studies indicate that HTL biocrude is more energy dense and shows higher thermal and oxidative stabilities than the biocrude produced from pyrolysis (Jena and Das, 2011). To reduce overall energy and cost input, it is necessary to process algae without complete drying (unlike pyrolysis), which can be accomplished by hydrothermal liquefaction (HTL) process. HTL is performed using hot compressed water, since it is a highly reactive medium as it approaches its critical point (374 °C, 218 atm or 3203 psi) due to changes in properties such as solubility, density, dielectric constant and reactivity. HTL depolymerizes lipids, proteins and carbohydrates in algae, transforming them into a bio-oil (also referred to as "biocrude" in the literature), water soluble products, gas, and solids (char). Multiple reactions occur in three steps, namely, hydrolysis, depolymerization and repolymerization/self-condensation reactions (Yin et al., 2010). Protein molecules are hydrolyzed into amino acids followed by deamination (release of NH_3) and decarboxylation reactions to form complex hydrocarbons (Sato et al., 2004). Bio-oil is a dark viscous liquid and has an energy value at 70-95% of that of petroleum fuel oil (Brown et al., 2010; Dote et al., 1998; Minowa et al., 1998). Thus, HTL converts organic constituents of algae into a liquid bio-oil that in theory can be refined to gasoline/diesel-like fuels. However, due to the large amount of proteins present in most of the algae biomass, the biocrude has a large abundance of nitrogen heterocyclic compounds, which pose potential problems in the subsequent upgrading processes; nitrogen in the biocrude will pose potential problems, since it leads to catalyst poisoning and deactivation (Laurent and Delmon, 1993). The various nitrogen compounds generated in the HTL product biocrude are nitrogen heterocyclics (e.g. pyridine, pyrrole, pyrrolidine, piperdine, and indole) and non-heterocyclics such as long-chain amines and amides (hexadecanenitrile and hexadecanamides) (Anastasakis and Ross, 2011; Biller and Ross, 2011; Brown et al., 2010; Jena et al., 2011a; Ross et al., 2010). Also, the presence of polypetides and proteins lead to high molecular weight compounds in the biocrude in the range of 2,000-10,000

g mol^{-1} (Alba et al., 2012). The rest of the components result in low (100 to 300 g mol^{-1}) and medium (400 to 500 g mol^{-1}) molecular weight compounds.

Several approaches to removing nitrogen and proteins from feedstocks such as algae have been examined. Barreiro et al. (2014) examined the effects of enzymatic hydrolysis of proteins on HTL of two algal strains (*Nannochloropsis* and *Scenedesmus*). Through use of cell rupturing coupled with endoprotease (Alcalase) and exoprotease (Flavourzyme), they were able to extract 44.3% and 62% of the protein from each strain, respectively. This resulted in a net decrease in the nitrogen content of the bio-oil generated from HTL from 5.1% to 4.2% in *Nannochloropsis* at 350 °C, with a similar trend observed in *Scenedesmus* (compared to HTL without protein hydrolysis). Although the percent bio-oil yield was similar between HTL on raw algae and protein-extracted algae, Barreiro reported that the enzymatic hydrolysis removed 53.5% of the initial *Nannochloropsis* mass and 80.9% of the initial *Scenedesmus* mass. This shows that the enzymes hydrolyze more than just proteins, which likely correlates to a significant decrease in the overall biocrude yield. Also, this enzymatic hydrolysis required at least 2 hours of processing time, with the most favorable results requiring 6 hours (Garcia et al., 2012). Although this method does not require additional heat input, this process is very time intensive, making its scale-up more difficult to implement. Another technique that has been investigated for reducing nitrogen content is the addition of alkali and organic acids in high temperature HTL (Ross et al., 2010). In this study, 1 M alkali or organic acids (Na_2CO_3, KOH, HCOOH, and CH_3COOH) were added to the HTL reaction of *Spirulina* and *Chlorella* microalgal strains at 300 and 350 °C. The average nitrogen content in the resulting biocrude was 4.7% for the HTL with alkali acids and 5.3% for HTL with organic acids; this was coupled with a maximum biocrude yield of 27.3% in *Chlorella* and 20.0% in *Spirulina* (at 350 °C using Na_2CO_3). This is marginally lower from the results Jena et al. (2011a) reported on a similar HTL of *Spirulina* study with no acid catalysts, in which HTL conducted at 350 °C for 1 hour generated a biocrude containing a nitrogen content of 6.3% at a yield of 39.9%. The use of acid catalysts seems to be effective in increasing the quality of the biocrude by removing nitrogen,

but the presence of the catalysts may become problematic for downstream processing, requiring additional input energy for separation of the acids before distillation of the biocrude. Hence, there is a need for alternative ways of removing nitrogen without the addition of external reagents such as catalysts, enzymes, or acids. Garcia-Moscoso et al. (2013) examined a continuous flash hydrolysis method that utilized subcritical water to hydrolyze *Scenedesmus* proteins rapidly. They report that subjecting an algae slurry (approx. 1% algae by mass, in water) to subcritical hydrolysis temperatures for a little as 10 seconds can extract up to 66% (at 305 °C) of the nitrogen initially present in the algae feedstock. They also demonstrated an increase in the nitrogen removal as temperatures increased from 205 to 305 °C. However, this increase in nitrogen removal was coupled with a decrease in the biomass retained, decreasing from 52.1% at 205 °C to 24.0% at 325 °C. They demonstrated successful continuous flash hydrolysis on the 3 mL scale using a 1% algae slurry (by mass). However, heat transfer and flowability become major concerns when discussing the scalability of a process, especially when the solid content is increased and the mechanism of hydrolysis depends on rapid heat transfer.

Chakraborty et al. (2012) proposed a sequential hydrothermal extraction that utilizes both low-temperature (160 °C) and high-temperature (300 °C) hydrothermal liquefaction on *Chlorella sorokiniana* microalgae both to reduce nitrogen present in the generated bio-oil and to extract value-added polysaccharides. Through their two-stage batch process, they reduced the nitrogen present in their bio-oil from 1.14% using direct HTL to 0.78% using sequential HTL. Their algae feedstock was grown heterotrophically in fermentors, which yielded a low nitrogen feedstock (2.91%, initially). The addition of the low-temperature HTL decreased the bio-oil yield from 27.8% in direct HTL to 23.4%. Miao et al. (2014) tested a similar sequential HTL of yeast (180 °C followed by 220 °C). Through their two-stage batch process, they reduced the nitrogen present in their bio-oil from 1.13% using direct HTL to 0.51% using sequential HTL; their yeast feedstock contained a nitrogen content of 2.65%, which is significantly lower than many algal feedstocks due to the high protein content normally found in algae. This two-stage process had very little

effect on the biocrude yield, which was approx. 58.3% for both direct and sequential HTL. In both Chakraborty et al. (2012) and Miao et al. (2014), the feedstocks studied were grown under ideal conditions. Realistically, large-scale production of fuel precursors must stem from feedstocks grown under the most economically feasible conditions, balancing optimization of feedstock characteristics with economics and energy inputs.

Converting algae to fuel intermediates via HTL is appealing because of the production rate of the feedstock and the energy economy of the process, especially since it utilizes a wet feedstock. Lack of a suitable method for reduction of nitrogen in HTL bio-oil can limit the widespread implementation of the HTL technology. Although techniques involving enzymatic or alkaline reactions are effective to a certain extent in treating algae biomass prior to HTL, they require costly downstream separations. Utilization of a low-temperature liquefaction pretreatment has been suggested, but studies on its effect on mass-produced algae feedstocks has yet to be determined. In principle, utilization of a pretreatment such as this could hydrolyze proteins without significantly hydrolyzing lipids or carbohydrates, causing the degradation products to become water soluble and removing nitrogen from the solid phase (Abdelmoez et al., 2007; Fujii et al., 2006; Lamoolphak et al., 2006; Rogalinski et al., 2005, 2008). The solids retained from the hydrothermal pretreatment could then be utilized as a low-nitrogen feedstock for high-temperature hydrothermal liquefaction to produce biocrude with a favorable elemental composition. Now nitrogen-rich from the protein and nitrogen extraction, the aqueous co-product phase from the pretreatment can be evaluated for characteristics that would allow it to be used as a nutrient recycle stream for future algae growth (Alba et al., 2013; Biller et al., 2012; Jena et al., 2011b; Minowa and Sawayama, 1999). Also, it is desirable to know the effects of this pretreatment stage on the bio-oil ultimately produced via HTL of this algae, which is not very well known presently. Moreover, evidence suggests algae bio-oil is only economically feasible if the aqueous co-products generated from HTL are recycled for nutrient supplementation for the cultivation of algae (Chisti, 2013).

This study was developed to evaluate the use of a low-temperature hydrothermal pretreatment (PT) as a nitrogen removal method on mass-produced algae feedstocks and the effect of that pretreatment on biocrude generated from high-temperature liquefaction in the next step. This study also conducts the detailed characterization of the aqueous co-product stream from the pretreatment stage. Nitrogen (typically as ammonium or nitrate) and other nutrients present in the aqueous stream (such as phosphorus and potassium) could be used to supplement the cultivation of algae feedstocks.

5.2 Experimental

5.2.1 Materials

Freeze-dried *Spirulina platensis* was obtained from Earthrise Nutritionals LLC (Calipatria, CA), and *Nannochloropsis sp.* was obtained from Reed Mariculture ("Nanno 3600", strain CCMP525). A consortium of three algal strains (*UGA Consortium* henceforth), namely *Chlorella sorokiniana*, *Chlorella minutissima*, and *Scenedesmus bijuga*, were grown and harvested for use in this study as well.

5.2.2 Algae Growth

A monoculture inocula of the constituent strains were first grown in 20 L carboys under controlled conditions in a growth chamber at 25 $\pm$ 1 °C for 12 h with alternating light-dark cycles; the light intensity was 100 μmoles m^{-2} s^{-1} with continuous air bubbling. The final consortium was prepared by mixing equal proportions (v/v) of each individual strain and then using it as inoculum at 10% v/v for outdoor cultivation in raceway ponds under green house facilities at an algae bioenergy lab of UGA. The raceway ponds were constructed of HDPE plastic and were 1.32 m wide, 2.18 m long, and 0.61 m deep with a working volume of approximately 500 L at 0.17 m water

depth. Standard algae growth medium BG 11 was used in fresh water for cultivation (Jena et al., 2011b). Supplemental CO_2 was derived from a commercial 10% CO_2 storage cylinder and used as a carbon source and for pH control. The UGA designed carbonation column (Putt et al., 2011) was used for CO_2 mass transfer. Once the cell density in raceways reached 500 mg L^{-1}, the biomass was harvested using a continuous centrifuge and dried at 55 °C until constant weight was observed after multiple weighing. The dried biomass was packed in zip-lock bags and stored at 4 °C until further use. Subsequently, the dried microalgae was ground to a fine powder using a heavy-duty laboratory knife mill (Retsch SM 2000, Germany) with a screen size of 0.5 mm. The knife mills cutting blade rotor (1690 rpm, 60 Hz) was powered by a 1.5 kW electric motor.

5.2.3 Liquefaction Apparatus and Experimental Procedure

Reactor Operation

Figure 5.2 illustrates the entire conversion process, including analytical methods performed. The low temperature liquefaction pretreatment (*PT*, 125 to 225 °C) was performed in a batch reactor (Parr 5000 Multi Reactor System, 75 mL vessel). Vessels were charged with 7 g of algae and 32 g of deionized water, and were sealed using a PTFE gasket. The system contained six separate vessels, each with its own PTFE magnetic stir bar (300 RPM) and band heater in an aluminum block (250 W); the heating rate of each reactor was approximately 10 °C min^{-1}, equating to heat up times of 9, 14, and 21 minutes (for 125, 175, and 225 °C, respectively). Vessels were pressurized with 300 psi (20.7 bar) helium prior to heating to ensure liquid water throughout the reaction. The residence time was taken from the point the reactor reaches temperature until the reactor was removed from the heating well. Once the residence time was complete (ranging from 0.5 to 30 minutes), the vessels were removed from the heating block, and the bottom sections of the vessels (below the screw cap) were submerged in a water bath. At ambient temperatures, the vessels were depressurized.

The whole product from the low temperature liquefaction stage was transferred without additional solvent into a 50 mL centrifuge tube and centrifuged (Sorvall Super T21) at 10,000 RPM for 20 minutes. The aqueous phase was decanted off and weighed, and the remaining solids were resuspended in a fresh aliquot of deionized water (enough to make the slurry 47 g total). For solid analysis, solids were dried after centrifugation and decanting at 105 °C for 4 hours.

High temperature liquefaction (*HTL*, 350 °C) was performed in a different batch reactor (Parr 4598 Micro-Stirred Reactor, 100 mL vessel). Vessels were charged with either 7 g of algae and 40 g of deionized water, or with the resuspended solid slurry. Vessels were sealed using a consumable Parr Grafoil gasket (flat flexible graphite). The mixture was stirred using a 4-blade impeller powered by a magnetic stirrer (model no. A1120HC6, 100 W variable speed) at 300 RPM. Vessels were heated using a ceramic fiber external jacket (700 W); the heating rate was approximately 14 °C min^{-1}. The residence time was begun from the point of PID leveling characterized by a noticeable and sizable decrease in the heating rate, occurring approximately 10 degrees below the set point. High temperature liquefaction was performed at 350 °C for 60 minutes. Vessels were pressurized with 500 psi (34.5 bar) helium prior to heating to ensure liquid water throughout the reaction. Once the residence time was complete, the external jacket was lowered and removed, and the vessel was cooled using a fan. At ambient temperatures, the vessels were depressurized and weighed to determine the mass of gas produced from the reaction. The whole product was transferred without additional solvent into a 50 mL centrifuge tube for storage.

Separate experimentation was performed at the Desert Research Institute (DRI) to determine if protein separation and nitrogen reduction during the low-temperature liquefaction pretreatment (175 to 250 °C) could be achieved at very short residence times (less than 5 minutes) with rapid batch heat-up times. DRI's two-chamber reactors operate by preheating the reaction water prior to addition of biomass. The reaction water in the reactor was heated to the desired temperature, and a ball valve was opened to drop biomass into the hot reaction chamber; the heat-up time of the biomass is nearly instantaneous (see Figure 5.1 for reactor configuration). The biomass

(inside a screen) was reacted for the desired time, then the entire reactor was quenched in an ice bath. Approximately 5 g algae biomass (*UGA Consortium* only) and 40 mL deionized water were used. At the end of the experimental trial, the reactor was ice-cooled and the gaseous products were vented to the atmosphere. Centrifugation, decanting, and solid drying were performed before analysis of phases, as stated above.

Phase Separation and Biocrude Extraction Procedure

Following high temperature liquefaction, 40 mL of dichloromethane (DCM) was added to the whole product and mixed. This solution was filtered under vacuum through Whatman #4 filter paper (pore size 20-25 um), and the cake was was rinsed with 15 mL of additional DCM. The cake was weighed wet, dried at 105 °C for 4 hours, and weighed again to determine wet and dry solid yield, and estimated solid water content. The filtrate was then transferred into a separatory funnel (150 mL) and was allowed to phase separate for 15 minutes. The bottom phase (biocrude solubilized in DCM) was decanted off, and 1 g of anhydrone (magnesium perchlorate) was added to the decanted phase to absorb residual water. The top phase (aqueous) was decanted separately and stored, with the interface between the phases not saved. The DCM phase was filtered under vacuum with 10 mL DCM used to rinse the anhydrone cake. The filtrate was transferred to a rotary evaporator (Rotovap) flask. The flask was then rotated under vacuum pressure (40 mbar) in a 36 °C water bath for 30-45 minutes until all DCM was removed; the remaining product was weighed to determine the mass of bio-crude. Since the solvent-free bio-crude was very viscous, two different storage techniques were used: a subsample was removed from the flask using a scoopula for analyses that require solvent-free product, and the remaining bio-crude in the flask was resuspended in DCM (approximately 6:1 DCM:biocrude by mass).

5.2.4 Sample Workup and Analysis

The elemental composition (C, H, N, and S) of the dried solids and biocrude was measured using a Thermo-Scientific Flash 2000 elemental analyzer according to the ASTM D5291 standard method. The concentration of whole proteins in the aqueous phase was found by performing Bradford Protein Assay using Coomassie Blue and UV-Vis spectroscopy (595 nm, measured on a Beckman DU 650 spectrophotometer). Proximate analysis was performed on dried solids using thermogravimetric analysis (TGA) on a LECO TGA 701. The moisture step was performed with a 6 °C min^{-1} ramp from 25 to 107 °C in a nitrogen atmosphere, the volatiles step was performed with a 43 °C min^{-1} ramp from 107 to 950 °C in a nitrogen atmosphere with crucible lids on, and the ash step was performed with a 15 °C min^{-1} ramp from 600 to 750 °C in an oxygen atmosphere.

Gas Chromatography-Mass Spectrometry (GC/MS) was performed on the aqueous phase and biocrude on an Agilent GC-MSD (Hewlett-Packard 5973 and 6890) with an HP5 MS Capillary Column (30 m x 0.25 um x 0.25 um). Separation was achieved using a temperature-programmed method of 40 °C, held for 4 minutes, with a 5 °C min^{-1} ramp until 275 °C was reached, held for 5 minutes; the inlet was held at 260 °C, the split ratio was 50:1, the injection volume was 1 uL, the helium carrier gas flow was 0.8 mL min^{-1}, and the MS scan was 30-400 m.u. Standard curves were constructed using model compounds and 1-hexanol as an internal standard, in triplicate.

High Pressure Liquid Chromatography (HPLC) was performed on the aqueous phase a Shimadzu LC-20 AT equipped with a RID-10A refractive index detector and a Coragel 64-H transgenomic analytical column (7.8 x 300 mm); the flow was 0.6 mL min^{-1} for a 55 minute run time, the sample volume was 5 uL, the mobile phase was 4 mN sulfuric acid, and the samples were analyzed at 6.89 MPa and 60 °C. About 2 mL of the sample was diluted with DI water at 1:1 ratio and centrifuged at 5000 rpm for 30 min, and then decanted. The supernatant was filtered through a 0.45 m filter into 2 mL auto-sampling vials. The sample was injected into the column using the

LC-20 AT Shimadzu auto-injector. Samples were identified using standard curves constructed on isolated model compounds.

The higher heating value (HHV) of biocrude was estimated using the elemental composition and the Dulong formula [Eq. 6.1] (Corbitt, 1999). The nitrogen removal was calculated on a weight basis based on the initial amount of nitrogen in the dry/ash-free feedstock and in the retained mass after pretreatment, according to Eq. 6.2. Total nitrogen in the aqueous phase was determined using the Persulfate Digestion Method (Hach Method 10072; Hach Co., USA). Ammonium (NH_4^+) concentrations in the aqueous phase were determined using a Thermo Scientific Orion Star A329 probe and meter. pH was determined using potentiometry performed on an Orion 520A Digital pH meter (Orion Research Inc., USA). Elemental concentrations in the aqueous phase (such as phosphorus, calcium, and magnesium) were determined using inductively coupled plasma (ICP) spectography (EPA Method 200.7) performed on a Thermo Jarrell-Ash 61E ICP (Thermo Elemental, USA).

$$0.3383 * \%C + 1.422 * (\%H - (\%O/8)) \quad [MJ\ kg^{-1}] \tag{5.1}$$

$$\%Nitrogen\ Removal = \frac{(\%N * DAF\ wt.)_{feedstock} - (\%N * wt.)_{product}}{(\%N * DAF\ wt.)_{feedstock}} * 100 \tag{5.2}$$

5.3 Results and Discussion

5.3.1 Low Temperature Pretreatment Stage

Nitrogen Partitioning from Solid Phase

Table 5.1 provides the proximate and ultimate analysis of the algae feedstocks used. The nitrogen content of two of the algae strains was above 10% (*Spirulina* and *Nannochloropsis*, at 10.8% and 10.1% respectively), and the *UGA Consortium* feedstock had a nitrogen content of

7.6%. In general, lower nitrogen content in the feedstock is a favorable criteria for obtaining a low-nitrogen biocrude. There is a correlation between the nitrogen content and the protein content of the feedstocks (as seen in the biochemical composition of the feedstocks provided in Table 5.2). The *UGA Consortium* had a protein content of 33%, compared to 48% and 45.8% in *Spirulina* and *Nannochloropsis*, respectively. The lipid content varied from 0.5% to 18% and was highest in *Nannochloropsis*. The carbohydrate content was similar between the three feedstocks, ranging from 14% to 17%.

The dry solid retention and nitrogen partitioning caused by the series of low temperature liquefaction pretreatment stages tested are illustrated in Figure 5.3. Liquefaction was performed on slurries containing the each of the three feedstocks at 125, 175, and 225 °C with holding times ranging from 0.5 to 30 minutes. Across all three strains, the reduction in the nitrogen content of the solid phase increased with temperature, yet for two of the strains (*Nannochloropsis* and *UGA Consortium*) was independent of holding time. A PT temperature of 225 °C and a holding time of 15 minutes or greater resulted in the largest reduction in solid phase nitrogen content for all strains. At these conditions, the reduction in nitrogen in *Nannochloropsis* was 62.0%, in *Spirulina* was 65.4%, and in *UGA Consortium* was 44.6% (Figures 5.3a, 5.3c, and 5.3e) as compared to the nitrogen content of the respective feedstocks. The discrepancy between strains could be due to the abnormally fibrous cell wall *Spirulina platensis* possesses, making protein degradation and partitioning limited by cell wall degradation (Van Eykelenburg, 1977). However, as the liquefaction temperature increased, the solid yield decreased (Figures 5.3b, 5.3d, and 6.1b), ultimately leading to a reduction in biocrude yield (see Section 5.3.2). At a reaction temperature of 225 °C and with a holding time of 15 minutes, the solid retention observed in *Nannochloropsis* was 46.6%, in *Spirulina* was 39.4%, and in *UGA Consortium* was 59.0%, as reported on the dry/ash-free weight of the feedstocks charged to the reactors. At higher temperatures, the proteins within the algal cells degrade, and the nitrogenated degradation products, being water soluble, partition out of the solids into the aqueous phase. Unconverted mass from the low temperature liquefaction is retained as

solids. There appeared to be an inversely proportional relationship between the amount of nitrogen partitioned and the solids retained.

The dry solid retention and nitrogen partitioning generated by short residence time batch reactors through the series of low temperature and short residence liquefaction stages are illustrated in Figure 5.4. Liquefaction was performed on slurries containing *UGA Consortium* feedstock at 175, 200, 225, and 250 °C with holding times ranging from 1 to 5 minutes. Similar to liquefaction performed with long heat-up times (on the order of 15 minutes), the reduction in the nitrogen content of the solid phase increased with temperature, yet was independent of holding time. A PT temperature of 250 °C and a holding time of 5 minutes resulted in the largest reduction in solid phase nitrogen content. At these conditions, the reduction in nitrogen was 66.7% (Figure 5.4a). A PT temperature of 225 °C and a holding time of 5 minutes resulted in a nitrogen reduction of 54.4%, which is comparable to the nitrogen removal achieved in traditional heat-up liquefaction of *UGA Consortium* of 38.2%. This comparison demonstrates that nitrogen partitioning can be obtained through shorter residence time liquefaction, if heat-up times are reduced. The nitrogen partitioning appears to be impacted by the rate of heat transfer to the algae biomass; a higher rate of heat transfer correlates with a higher nitrogen partitioning. However, as the liquefaction temperature increased, the solid yield decreased (Figure 5.4b). At a reaction temperature of 250 °C and with a holding time of 5 minutes, the solid retention observed through DRI's two-chamber reactor was 38.5% of the dry/ash-free weight of feedstock charged to the reactor. Like traditional heat-up liquefaction, there appeared to be an inversely proportional relationship between the amount of nitrogen partitioned and of solids retained in the short residence time studies. Through use of the two-chamber reactors, a pretreatment temperature of 225 °C and a holding time of 5 minutes resulted in a solid retention of 49.2%, compared to 63.4% achieved through traditional heat-up liquefaction using the same conditions. Although using the two-chamber reactor to eliminate heat-up time proved effective for partitioning additional nitrogen, its use also reduced the amount of

solids retained from the low temperature pretreatment, which would ultimately lead to a reduction in biocrude yield.

Simultaneously, the liquefaction temperatures can cause cell lysing, allowing the whole proteins to partition from the algal cells into the aqueous phase. Figure 5.5 illustrates the protein concentration measured in the aqueous phase following the low temperature liquefaction stage. Across all three strains, the whole protein partitioning was highest at 175 °C, while independent of holding time across all three strains. At a reaction temperature of 175 °C, the average protein concentration in the aqueous phase across all holding times tested was 9.5 g/L for *Nannochloropsis*, 7.5 g/L for *Spirulina*, and 2.5 g/L for *UGA Consortium*. This local maxima of protein concentration is likely due to the balance between cell lysing and protein hydrolysis; cells lyse effectively at 175 °C, but more nitrogen is partitioned at 225 °C due to the protein hydrolysis that occurs at the above temperature. Since *UGA Consortium* had a lower starting protein content, it is logical that the protein concentration upon removal was lower as compared to the two feedstocks containing higher protein contents (see Table 5.2 for biochemical composition of the feedstocks).

Nutrient Analysis on the Aqueous Co-Product and Opportunity for Recycling

In order to determine the feasibility of recycling the aqueous phase co-product for algae cultivation, GC/MS and HPLC analyses were performed on this fraction. These analyses were performed on the aqueous phase recovered from liquefaction of *UGA Consortium* at 225 °C for 15 minutes, but are representative for all strains and all liquefaction conditions. In the GC/MS chromatogram (Figure 5.6), compounds left to right are acetic acid, methyl-pyrazine, 2,5-dimethyl-pyrimidine, 2-ethyl-5-methyl-pyrazine, 3-ethyl-2,5-dimethyl-pyrazine, and hexahydro-3-(2-methylpropyl)-pyrrolo[1,2-a]pyrazine-1,4-dione. The majority of these peaks can be characterized by their nitrogenated heteroatoms, indicating protein hydrolysis and nitrogen partitioning occurred.

These analyses indicated low levels of acetic acid and no presence of potentially inhibitory compounds, such as phenol, for any strain or low temperature liquefaction conditions (Biller et al., 2012). Quantifying the peaks via HPLC (matched with standard curves) indicated acetic acid levels at 1.6 to 3.2 g L^{-1}, with higher levels correlated to higher reaction temperature and time (Table 5.3). Alba et al. (2013) demonstrated successful algae cultivation using a diluted HTL aqueous steam that originally contained acetic acid at a concentration of 3.95 g L^{-1}; the dilution lowered the acetic acid concentration to 0.025 g L^{-1} using a dilution factor of 160. This implied that the acetic acid levels found in the aqueous co-product from the low-temperature pretreatment were suitable for supplemental algae cultivation. Separation and recovery of the aqueous phase after the low temperature liquefaction stage generated a stream high in protein with low levels of algae growth inhibitors, and reduced the nitrogen level in the subsequently derived biocrude.

Total nitrogen, ammonium, total phosphorus, and pH for the aqueous phase co-products generated are shown in Table 5.3. The samples obtained from the PT stage performed at varying reaction conditions were characterized by a pH ranging from 4.7-6.8. More acidic pH aqueous phases were generated under conditions of lower residence time, with 125 °C having the most acidic pH of the three temperatures analyzed (likely from acetic acid). These pH values are lower than the pH of growth media commonly used for algae cultivation (typically 7.5), and may need to be adjusted before the aqueous phase can be utilized (Alba et al., 2013; Jena et al., 2011b). The aqueous phase from all experiments had total nitrogen (TN) and ammonium (NH_4^+) at concentrations near 9 and 2.5 g L^{-1}, respectively. The concentration of total nitrogen and ammonium increased with increasing reaction temperature and duration.

Aqueous phase co-products obtained from the PT experiments performed with short heat-up times (through use of the two-chamber reactors at DRI) were characterized by a neutral or alkaline pH (7.0-7.8) for all experimental conditions except for the lower temperature runs at 175 °C, which resulted in a pH ranging from 5.6-6.0 (see Table 5.3). The aqueous phase from all experiments of this type had total nitrogen (TN) and ammonia nitrogen at concentrations of 0.5 and 0.1 g L^{-1},

respectively. This indicates that proteins in the algal feedstock were hydrolyzed and fragmented to a lesser extent with a faster heating rate, potentially due to the fact that agitation was not performed during HTL using the short residence time reactor system. One-third to half of the Total-N constituted ammonia-N. Also, the aqueous phase was characterized by significant amounts of total phosphorous (TP) (13-154 mg L^{-1}). Due to partitioning of N and P of the algae biomass into the PT aqueous phase, this byproduct can be further used for additional algae growth and other plant growth. Also, the aqueous phase was characterized by the presence of organic carbon (not shown, 548-5749 mg L^{-1}).

Typically, algae cultivation is supplemented using growth medium. BG-11 medium contains 250 mg L^{-1} total nitrogen and 10 mg L^{-1} total phosphorus (Jena et al., 2011b). COMBO growth medium requires 10 times less of each nutrient, and 3N-BBM+V requires 15 times more phosphorus (Alba et al., 2013; Biller et al., 2012). Analysis indicated that pretreatment conditions of 225 °C and 15 minutes generate an aqueous co-product, containing 10 g L^{-1} total nitrogen, 2.7 g L^{-1} ammonium and 322 mg L^{-1} total phosphorus, that can be further diluted for cultivation of algae. Previously reported work indicated that aqueous co-products generated from traditional high temperature HTL, which are chemically similar to ours, can cultivate algae and compete with fresh growth media if diluted correctly (Alba et al., 2013; Biller et al., 2012; Jena et al., 2011b). Algae are sensitive to nutrient concentrations, and algae growth can be inhibited by unsuitably high or low concentrations of nutrients, even of nutrients required for growth. Jena et al. (2011b) successfully cultivated *Chlorella* by diluting an HTL aqueous stream by a factor of 100 (TN of 100 mg L^{-1}); Biller et al. (2012) demonstrated similar results on several strains by diluting a factor of 400 (TN of 25 mg L^{-1}). The HTL aqueous stream generated by Alba et al. (2013) (using *Desmodesmus*) contained significantly less total nitrogen than the stream generated in this experiment (only 3.4 g L^{-1}, compared to 8.7 to 10 g L^{-1}), and our aqueous stream would require a dilution of a factor of 750 (TN of 13 mg L^{-1}) to have similar concentrations as the media ultimately used. The requirement of diluting the aqueous co-product is economically beneficial since the volume of aqueous

co-product is drastically less than the volume of water required to cultivate algae. On the industrial scale, nitrogen, phosphorus, and other micronutrients must be supplied, often in excess (Demirbas, 2010; Grima et al., 2009).

Table 5.4 provides the nutrient concentration present in the aqueous co-product generated from the pretreatment of *UGA Consortium* at 225 °C for 15 minutes. Chen et al. (2011) demonstrated that the overall growth of *Dunaliella* is adversely affected by the absence of Fe, Co, Mn, Mo, and P nutrients (in the order of most profound effect when absent). Their work indicated that each of these nutrients served a purpose in algae cultivation, and are beneficial in the aqueous co-product generated. Similarly, Alba et al. (2013) concluded their study was limited by the absence of key micronutrients, such as Mg, which are responsible for metabolic and enzymatic activities such as photosynthesis and vitamin synthesis. In their work, the aqueous co-product used for cultivation contained 29.3 ppm Mg; the co-product generated from our work contains nearly 5 times that amount (145.4 ppm), but would still be 400% below the required level if diluted by a factor of 100, as is likely required (Jena et al., 2011b). Nickel has been shown to have inhibitory affects on algae growth when present in concentrations as low as 0.85 ppb (Biller et al., 2012). Since the aqueous co-product generated will be diluted by at least a factor of 100 before use in cultivation (Jena et al., 2011b), it is likely the 0.14 ppm originally present in the co-product will be diluted to safe levels (at least 1.4 ppb) before use.

5.3.2 Effects of Pretreatment Stage on Biocrude Quality

Two-stage liquefaction was performed with the first stage (low temperature pretreatment) having a reaction temperature of 225 °C and a residence time of 15 minutes, with nitrogen removal being the primary project goal. Figure 5.7 illustrates the effect of the low temperature liquefaction on the chemical composition of biocrude generated from high temperature liquefaction viewed through a comparison of GC/MS profiles. In the chromatogram for biocrude generated without the low temperature pretreatment (Figure 5.7a), retention times between 5 and 25 minutes contain

a cluster of peaks characterized by nitrogenated and oxygenated rings (e.g. methyl-pyrazine). It is clear from the second chromatogram (Figure 5.7b) that implementation of the low temperature pretreatment eliminated the vast majority of these early peaks, most of which were undesirable compounds in biocrude because they contain nitrogen or oxygen. The peaks with retention times beyond 25 minutes appeared to be affected, but to a lesser extent, by the low temperature pretreatment stage. These peaks were mainly long chain hydrocarbons that were either unsaturated or contain nitrogenated groups at the chains' end (hexadecanamide, 1-pentadecene) or fatty acids stemming from hydrolysis of triglycerides (hexadecanoic acid). Compounds such as these are favorable for drop-in fuel precursors because they can be catalytically upgraded into saturated long chain hydrocarbons (Galadima and Muraza, 2014; Tran et al., 2010).

Biocrude generated from single stage high temperature liquefaction of *UGA Consortium* resulted in an 81.2% total reduction in net nitrogen from the feedstock (Figure 5.8). That is, 18.8% (100% minus 81.2%, the total reduction from the feedstock provided above) of the total nitrogen present in the feedstock ended up in the biocrude, equating to the biocrude having an elemental composition of 5.8% nitrogen (by weight). Implementation of the low temperature liquefaction stage (225 °C, 15 minutes) as a pretreatment to the biomass entering the high temperature liquefaction stage resulted in an additional 6.5% reduction in nitrogen from the feedstock (totaling 87.7%, "Addl. RFF" in Figure 5.8). However, the elemental composition of the biocrude from two-stage HTL still contained 5.8% nitrogen, and the biocrude yield decreased from 26.7% in the single stage HTL to 17.4% in the two-stage HTL. In *Nannochloropsis*, implementation of the low temperature pretreatment stage brought the total nitrogen reduction in the biocrude to 93.0%, up from 84.5% in biocrude generated from high temperature HTL only, but resulted in a reduction in the biocrude yield from 23.7 to 13.8%. *Spirulina* exhibited a similar trend, with the addition of the pretreatment stage resulting in an increase in the nitrogen reduction (to 96.0% from 82.8%) and a decrease in the biocrude yield (to 8.6% from 29.3%).

5.4 Conclusion

The results indicate that nitrogen removal can be achieved through low temperature hydrothermal liquefaction. An increase in temperature and in the heating rate corresponded to an increase in nitrogen partitioning across all strains; the amount partitioned was moderately independent of reaction duration, with higher durations corresponding to increased partitioning. The amount of solids retained was inversely related to the amount of nitrogen partitioned. It was demonstrated that the addition of the pretreatment caused a quality improvement in the composition of the bio-crude subsequently produced via HTL. In addition, the aqueous co-product generated from the pretreatment stage contains ample nutrients and minimal inhibitory compounds, making it suitable for algae cultivation.

5.5 Figures and Tables

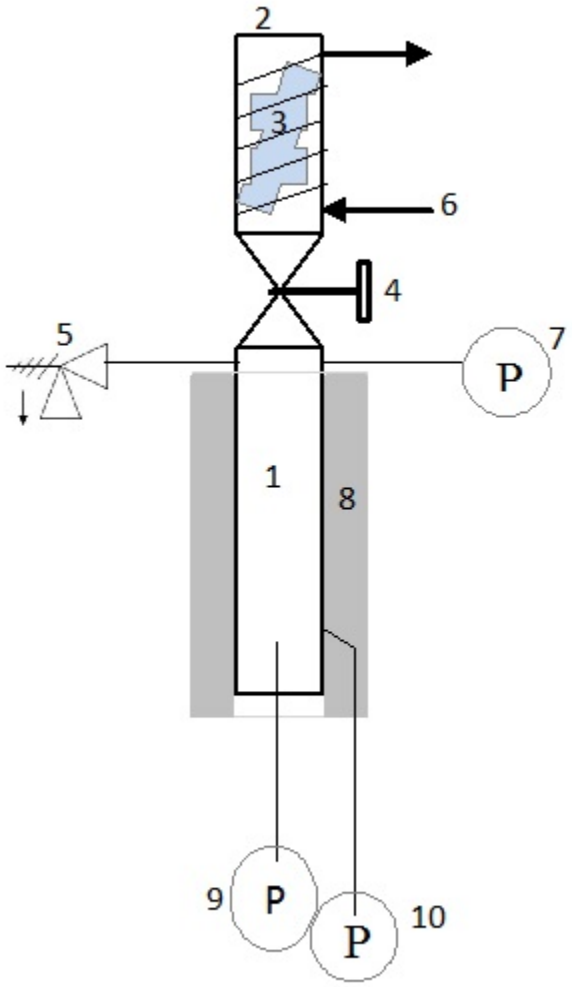

Figure 5.1: Schematic of two-chamber reactor configuration used in rapid heat-up low temperature liquefaction trials.

(1) Bottom chamber; (2) Top chamber; (3) Biomass cartridge; (4) Ball valve; (5) Pressure relief valve; (6) Water-cooling coil; (7) Pressure gauge; (8) Radiant heater; (9) Temperature indicator; (10) PID temperature controller.

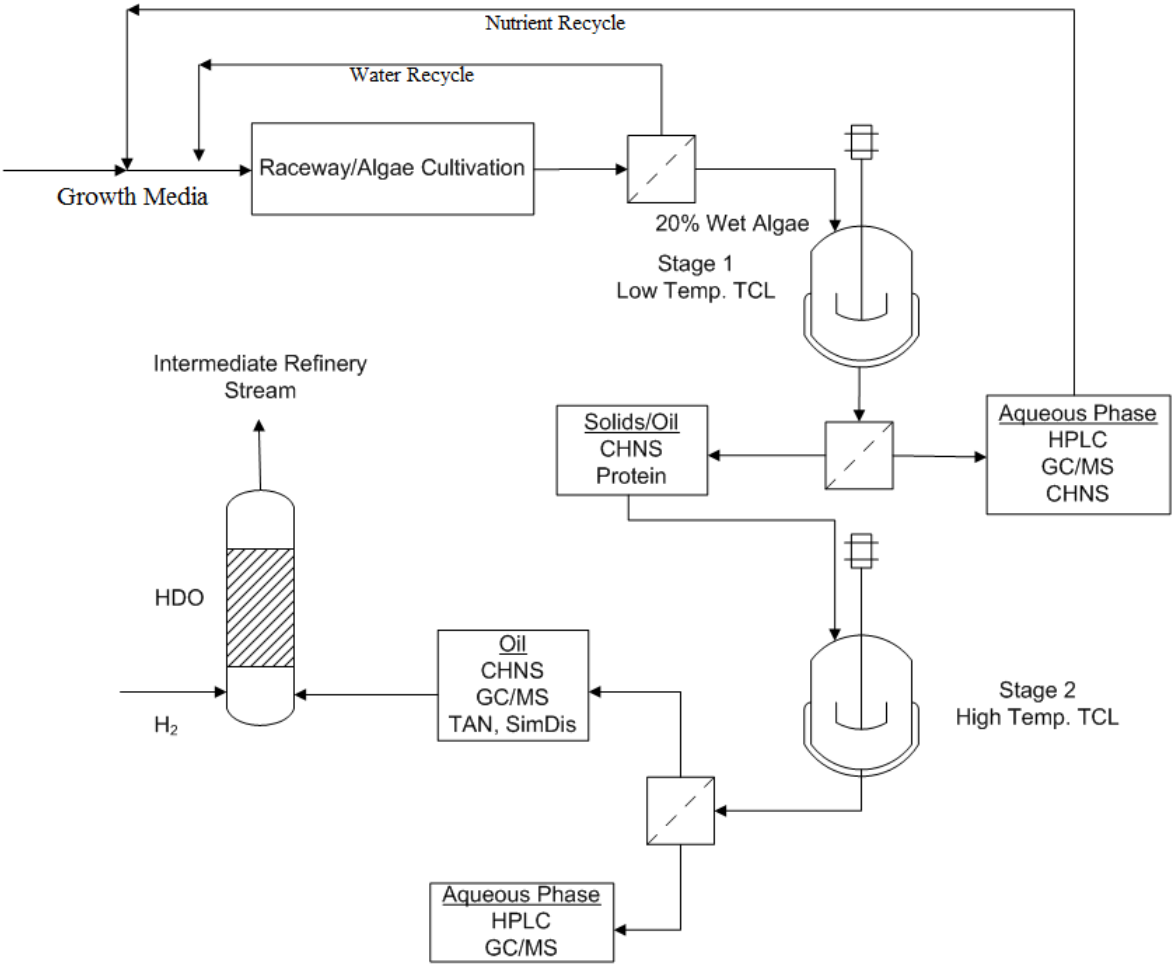

Figure 5.2: Process flow diagram for experimental steps and analytical procedures for the conversion of algae to liquid fuel.

Note - TCL is equivalent to HTL in our procedures, and catalytic upgrading (HDO) is not included in this study.SimDis: Simulated Distillation, TAN: Total Acid Number.

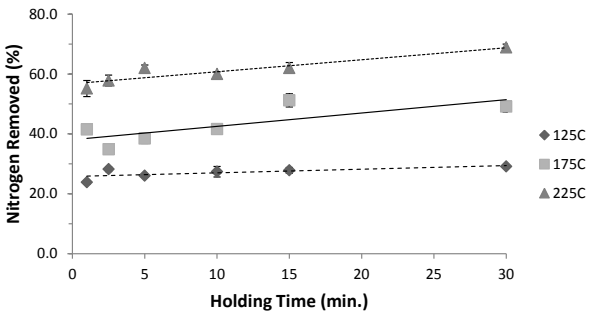

(a) Nitrogen partitioning of *Nannochloropsis*.

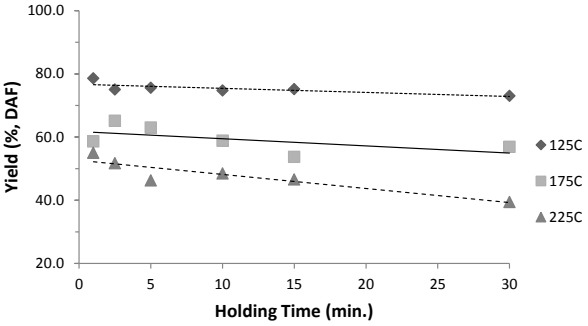

(b) Solid retention of *Nannochloropsis*.

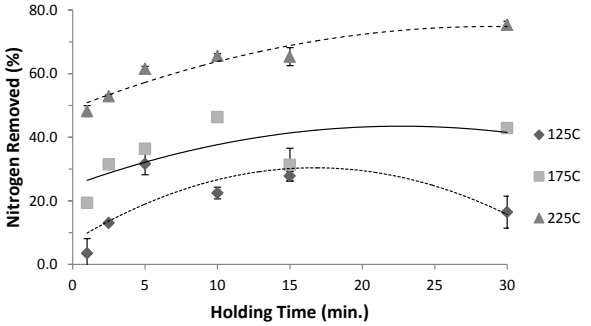

(c) Nitrogen partitioning of *Spirulina*.

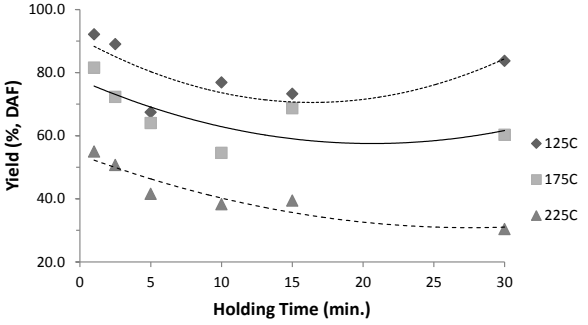

(d) Solid retention of *Spirulina*.

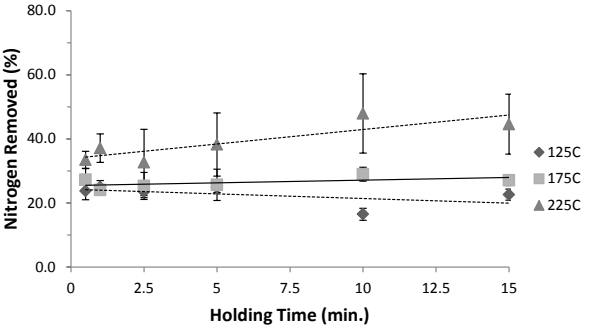

(e) Nitrogen partitioning of *UGA Consortium*.

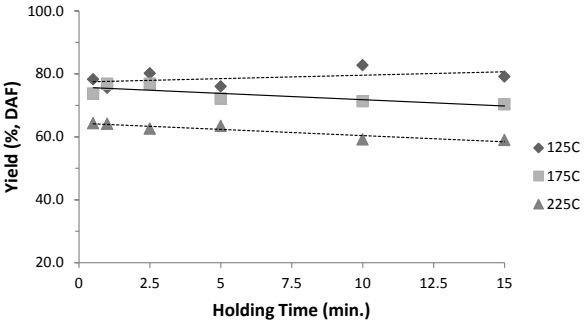

(f) Solid retention of *UGA Consortium*.

Figure 5.3: Effects of temperature and reaction duration of pretreatment stage on nitrogen partitioning (% removal from solid phase, w/w) and solid retention (dry/ash-free yield %) using traditional heat-up batch reactor system.

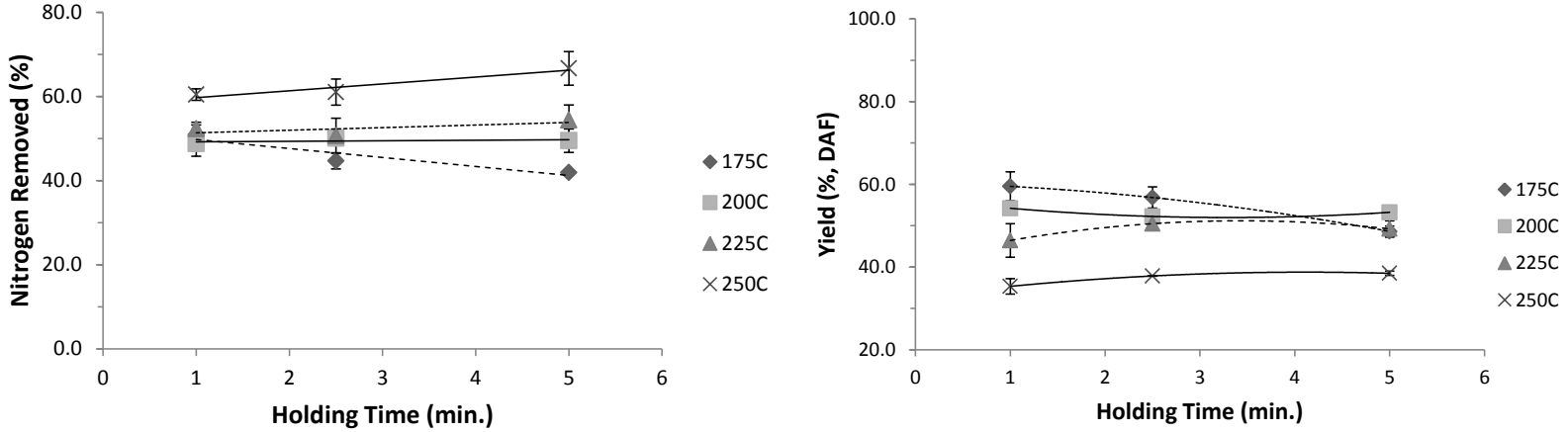

(a) Nitrogen partitioning of *UGA Consortium*.

(b) Solid retention of *UGA Consortium*.

Figure 5.4: Effects of temperature and reaction duration of pretreatment stage on nitrogen partitioning (% removal from solid phase, w/w) and solid retention (dry/ash-free yield %) using the rapid heat-up two-chamber batch system.

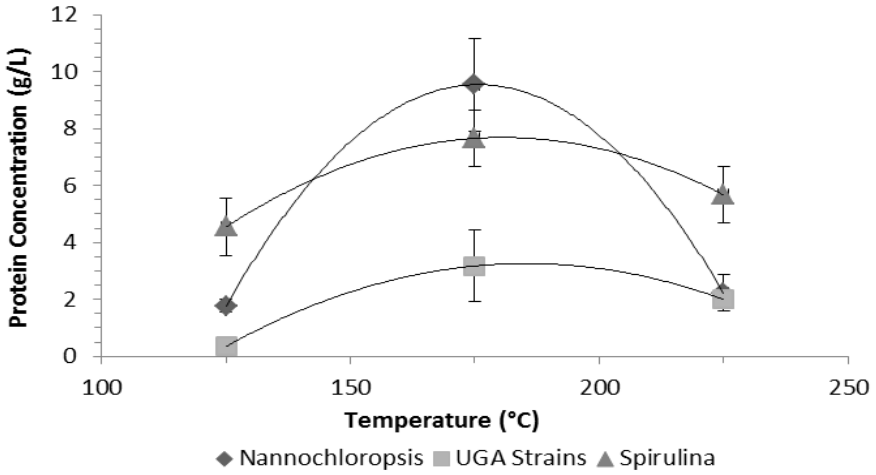

Figure 5.5: Effect of pretreatment temperature on protein levels released to the aqueous phase after subcritical hydrolysis (Bradford protein assay).

The error bars are one standard deviation of protein concentration at all measured retention times.

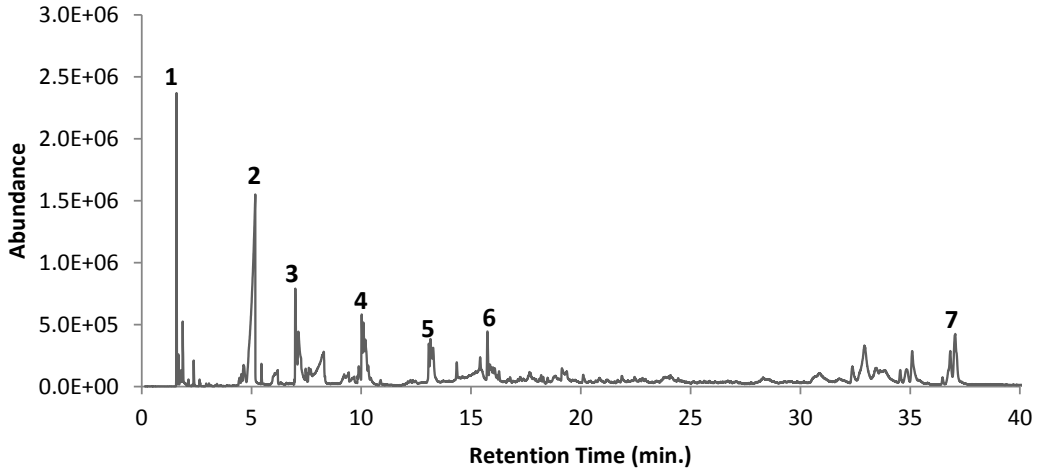

Figure 5.6: GC/MS analysis of aqueous co-product generated from low-temperature liquefaction of *UGA Consortium* (PT: 225 °C, 15 min).

Chromatograms were similar for the other strains under the same PT conditions. Identified compounds are (1) carbon dioxide, (2) acetic acid, (3) methyl-pyrazine, (4) 2,5-dimethyl-pyrazine, (5) 2-ethyl-5-methyl-pyrazine, (6) 3-ethyl-2,5-dimethyl-pyrazine, (7) hexahydro-3-(2-methylpropyl)-pyrrolo[1,2-a]pyrazine-1,4-dione.

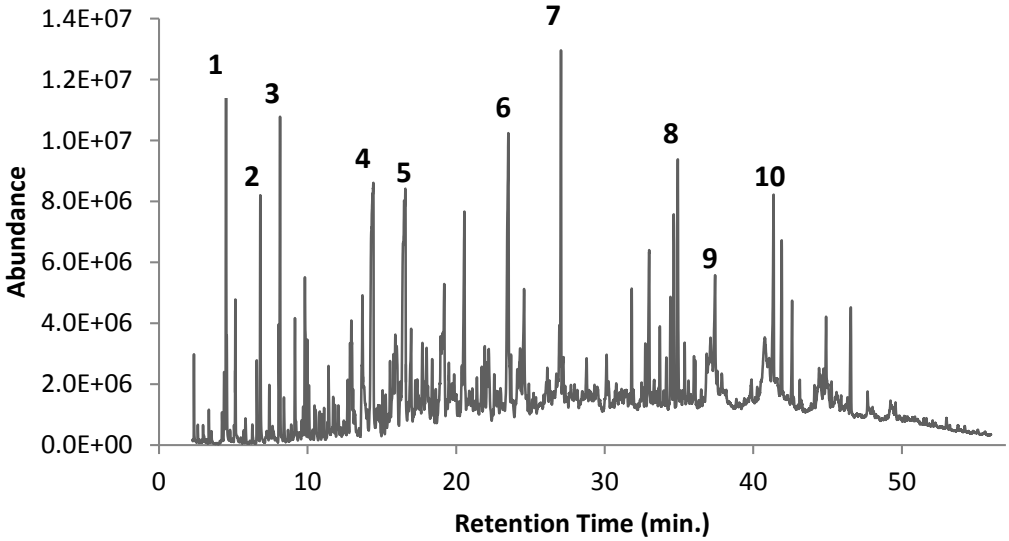

(a) Single stage high temperature liquefaction only (HTL: 350 °C, 60 min).

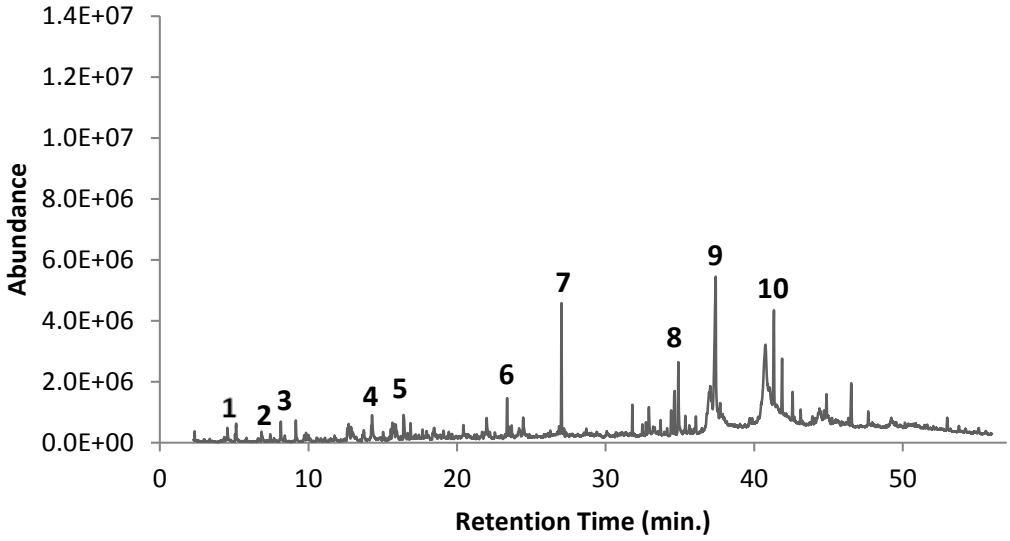

(b) Two stage low- and high-temperature liquefaction (PT: 225 °C, 15 min; HTL: 350 °C, 60 min).

Figure 5.7: GC/MS analysis of *UGA Consortium* biocrude.

Chromatograms were similar for the other strains under the same conditions. Identified compounds are (1) pyrazine, (2) methyl-pyrazine, (3) ethyl benzene, (4) 1-methyl-2-pyrrolidinone, (5) 1-ethyl-2-pyrrolidinone, (6) 1-methyl-piperidine, (7) 1-pentadecene, (8) 3,7,11,15-tetramethyl-2-hexadecene, (9) hexadecanoic acid, (10) hexadecanamide.

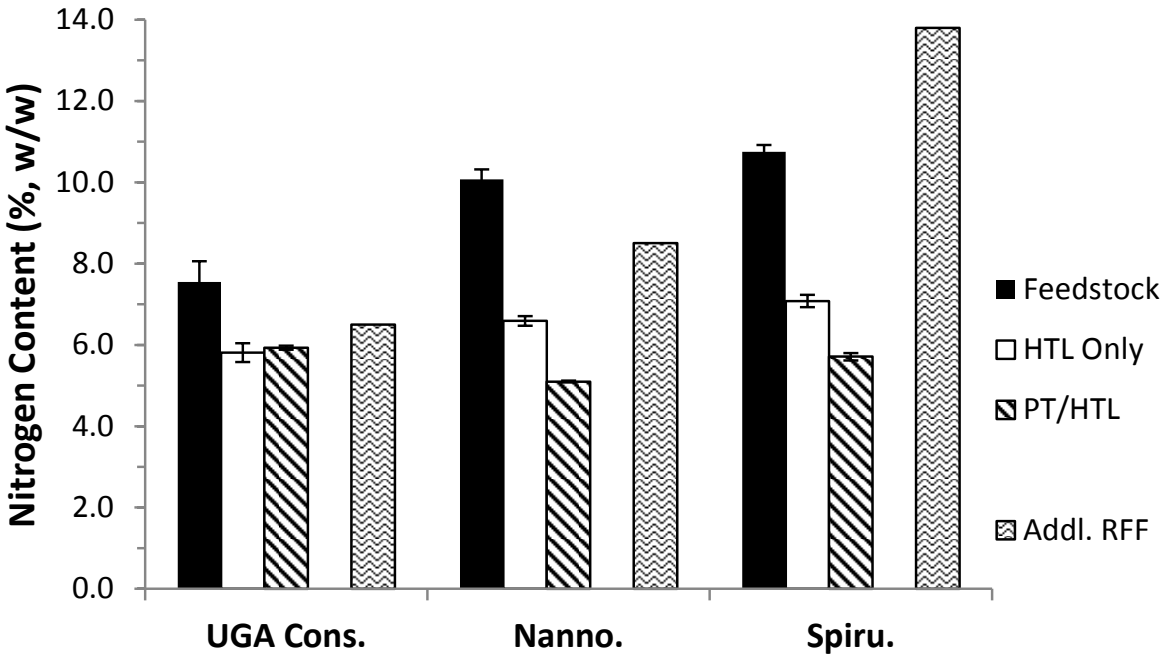

Figure 5.8: Nitrogen content (% w/w) in algae feedstocks and biocrude generated from either single stage high-temperature liquefaction or two stage low- and high-temperature liquefaction (PT: 225 °C, 15 min; HDO: 350 °C, 60 min).

Addl. RFF: Additional Reduction From Feed - the additional nitrogen weight (% of the total nitrogen in the feedstock) removed with the addition of PT (e.g. *UGA Cons.*: 18.8% of feedstock nitrogen weight balanced to biocrude phase with HTL only; 12.3% with PT and HTL two-stage).

Table 5.1: Proximate and ultimate analysis, and higher heating value (HHV) of algae feedstocks and *UGA Consortium* liquefaction products.

Feedstock or Product	Proximate (% w/w)		Ultimate (dry basis) (% w/w)					HHV	N-Removal	Yield
	Moisture	Ash	C	H	N	S	O[a]	(MJ/kg)	(% w/w)	(% w/w)
UGA Consortium	4.8	10.1	40.8±1.0	5.4±0.2	7.6±0.5	ND	46.2±0.7	13.3	NA	NA
Nannochloropsis	1.3	7.4	51.2±0.1	7.4±0.1	10.1±0.3	0.8±0.8	30.4±0.6	22.5	NA	NA
Spirulina	6.6	8.5	43.1±1.0	5.8±0.1	10.8±0.2	ND	40.4±1.2	15.7	NA	NA
PT[b] - Solid	5.0	20.5	46.0±1.2	6.4±0.1	6.8±1.1	1.4±0.2	39.5±1.1	17.6	44.6	59.0
PT at DRI[c] - Solid	NP	NP	43.5±0.9	5.5±0.2	6.7±0.2	0.1±0.1	44.3±0.4	14.7	54.4	49.2
HTL - Biocrude	NA	NA	71.6±2.1	8.7±0.2	5.8±0.2	1.2±0.7	13.4±3.2	34.2	81.2	26.7
Two-Stage[b] HTL - Biocrude	NA	NA	71.4±0.4	8.8±0.1	5.9±0.1	ND	13.9±0.4	34.2	87.7	17.4

[a]Determined by difference; ND: not detected, NP: not performed, NA: not applicable.

[b]Low Temp. Liquefaction - 225 °C, 15 minutes.

[c]DRI two-chamber reactor; no heat-up time - 225 °C, 5 minutes.

Table 5.2: Biochemical composition of whole algae feedstocks (% w/w).

Algae Strain	Protein	Carbohydrate	Lipid
Spirulina	48	16	0.5-11
UGA Consortium	33	17	6
Nannochloropsis[a]	45.8	14	9-18

[a]Reported by Reed Mariculture.

Table 5.3: Total nitrogen (TN), ammonium (NH_4^+), total phosphorus (TP), and acetic acid (AA) concentrations, and pH of the aqueous co-product phase (PT at varying conditions) and several growth media.

Strain or Medium	Temperature (°C)	Reaction Time (min.)	TN (g L^{-1})	NH_4^+ (g L^{-1})	TP (mg L^{-1})	AA (g L^{-1})	pH
UGA Consortium	225	15	10.0±0.6	2.73	322	3.20±0.62	6.2
	225	5	9.5±0.3	2.50	437	3.02±0.52	5.9
	225	2.5	8.9±0.1	1.99	470	2.73±0.77	5.7
	225	0.5	8.7±0.2	1.75	550	2.67±0.87	5.5
	175	15	8.6±0.03	1.88	618	2.49±0.53	5.7
	125	15	3.6±0.0	0.58	688	1.63	4.7
Nannochloropsis	225	15	13.7±0.0	4.05	1055	1.92±0.14	6.8
Spirulina	225	15	14.6±0.7	3.73	605	1.74±0.27	6.7
UGA Consortium at DRI	225	5	0.341	NP	58.75	NP	7.2
	250	5	0.124	NP	13.43	NP	7.6
BG 11[a]	NA	NA	0.250	NA	10	0.0	7.5
COMBO[b]	NA	NA	0.013	0.0	1.55	0.0	7.4
3N-BBM+V[c]	NA	NA	0.124	0.0	153	0.0	6.8

Reported by: [a](Jena et al., 2011b); [b](Alba et al., 2013); [c](Biller et al., 2012). NP: not performed, NA: not available.

Table 5.4: Nutrient analysis (in ppm) of the aqueous co-product (*UGA Consortium*, 225 °C, 15 min.) compared to several standard growth media.

Element	Aqueous Co-Product	BG 11[a]	COMBO[b]	Erdschreiber[c]
Al	1.63	-	-	-
B	1.97	0.5	-	-
Ca	86.9	9.81	17.0	377.9
Cr	0.28	-	-	-
Cu	<0.50	0.023	-	-
Fe	52.5	1.27	-	0.93
K	2146.2	18	1290	-
Mg	145.4	7.4	29.3	-
Mn	1.08	0.5	-	927
Mo	<0.10	0.16	-	1.45
Na	518.3	414.5	334.5	-
Ni	0.14	-	-	-
P	322.3	7.11	-	22.91
Si	78.3	-	-	2.68
Zn	0.52	0.05	-	0.028

[a]Calculated based on reported compound concentrations (Jena et al., 2011b).

Reported by: [b](Alba et al., 2013); [c](Chen et al., 2011).

Chapter 6

Effect of Low Temperature Hydrothermal Liquefaction on Catalytic Hydrodeoxygenation/Hydrodenitrogenation of Algae Biocrude[1]

[1]Costanzo, William and Roger Hilten, Jim Kastner. To be submitted to *Bioresource Technology*.

Abstract

A selective hydrothermal liquefaction process was coupled with catalytic upgrading to generate a refinery-grade biocrude from algae biomass using heterogeneous catalysis. Low- and high-temperature subcritical liquefaction stages (PT: 225 °C, 15 min; HTL: 350 °C, 60 min) were first used to pretreat the biomass and generate an oil phase, primarily characterized by free fatty acids, unsaturated hydrocarbons, and long chain heteroatoms. Heterogeneous catalytic hydrodeoxygenation (HDO: 350 °C, 240 min) was conducted using ruthenium (5% Ru on carbon), several cobalt molybdenum forms (on aluminum oxide), and a hydrogen-reduced mixed metal oxide (mainly iron oxide) byproduct known as Red Mud. The extent of the HDO/HDN reaction was limited by low hydrogen concentrations stemming from the consumption of this reactant in a batch atmosphere, and thus the HDO stage was repeated twice per biocrude, with fresh hydrogen recharged. Implementing all four stages produced the most favorable biocrude, with minimal nitrogen levels and a chemical composition dominated by long chain and aromatic hydrocarbons. The Ru catalyst achieved the most favorable elemental composition, and heteroatom and hydrocarbon percentages.

6.1 Introduction

The demand for a sustainable, renewable, and domestic source for liquid fuel precursors has become increasingly apparent over the past decade. Algae have proven to be a viable biomass feedstock for conversion to fuel intermediates because of their high energy content (specifically as lipids) and their autotrophic and carbon dioxide fixing growth. HTL and pyrolysis are two thermochemical conversion processes that directly convert biomass such as algae into liquid hydrocarbons. Previous comparative evaluation of HTL and pyrolysis processes for bio-oil production from microalgae biomass indicate that HTL is energetically more efficient for liquid fuel production than the pyrolysis process, resulting in 29% higher bio-oil yield and 32% more energy recovery (Jena

and Das, 2011). Also, past studies indicate that HTL bio-oil is more energy dense and shows higher thermal and oxidative stability than the bio-oil produced from pyrolysis (Jena and Das, 2011). To reduce overall energy and cost input, it is necessary to process algae without complete drying (unlike the pyrolysis process), which can be accomplished by hydrothermal liquefaction (HTL) process.

HTL is performed using hot compressed water, since it is a highly reactive medium as it approaches its critical point (374 °C, 22.1 MPa) due to changes in properties such as solubility, density, dielectric constant and reactivity. The bio-oil is a dark viscous liquid with an energy value 70-95% of that of petroleum fuel oil (Brown et al., 2010; Dote et al., 1998; Minowa et al., 1998). Under subcritical conditions, the hydrothermal liquefaction of algae yields a multitude of products stemming from the hydrolysis/depolymerization of the algae macromolecules. These products include long-chain fatty acids (e.g. oleic acid), nitrogenated and oxygenated heterocyclics (e.g. pyrrolidine, phenol), and some long-chain hydrocarbons (e.g. pentadecane) (Biller and Ross, 2011). Thus, HTL converts organic constituents of algae into a liquid bio-oil that in theory can be refined to gasoline/diesel-like fuels via heteroatom removal mechanisms such as decarboxylation, decarbonylation, denitrogenation, and hydrodeoxygenation. The catalytic upgrading of several isolated HTL products to refinery inputs has been demonstrated (Duan and Savage, 2011; Santillan-Jimenez and Crocker, 2012; Srokol et al., 2004).

However, due to the large amount of proteins present in the starting algae biomass, the bio-oil has a large abundance of nitrogen heterocyclic compounds which poses potential problems in the subsequent upgrading processes; nitrogen has been shown to poison and deactivate biocrude-upgrading catalysts (Dong et al., 1997; Laurent and Delmon, 1993). The various nitrogenated compounds present in the HTL product bio-oil are nitrogen heterocyclics (pyridine, pyrrole, pyrrolidine, piperdine, and indole) and non-heterocyclics such as open-chain amines and amides (hexadecanenitrile, and hexadecanamides) (Anastasakis and Ross, 2011; Biller and Ross, 2011; Brown et al., 2010; Jena et al., 2011a; Ross et al., 2010; Toor et al., 2011). Also, the presence of polype-

tides and proteins lead to the high molecular weight compounds in the bio-oil in the range of 2,000-10,000 g mol^{-1} (Alba et al., 2012). The rest of the components result in low (100 to 300 g mol^{-1}) and medium (400 to 500 g mol^{-1}) molecular weight compounds. These nitrogenated compounds have negative effects on pollution production from the combustion of the subsequent fuels, catalytic activity, and overall bio-oil energy content. It is thus beneficial to create a biocrude low in its nitrogen content.

Previous work conducted (Chapter 5) demonstrated the implementation of a low temperature hydrothermal liquefaction pretreatment as a method of removing nitrogen from algae biomass prior to biocrude generation via high temperature liquefaction. In short, a range of temperatures (125 to 225 °C) and holding times (0.5 to 15 minutes) were tested on several strains of algae to determine their effects on the amount of nitrogen partitioning that occurred (out of the solid phase) and on the amount of solid biomass retained. Across the three algae strains tested, a direct correlation between reaction temperature and nitrogen partitioning was found, with a less extreme dependency on holding time. The highest amount of nitrogen partitioning was obtained using a pretreatment of 225 °C for 15 minutes (as seen on *UGA Consortium* in Figure 6.1). Even with the reduction in nitrogen from the pretreatment stage, the nitrogen content of the subsequent biocrude is too high for direct use as a refinery input. This, coupled with an abundance of oxygen in the biocrude, makes it unsuitable for co-processing with petroleum oil. Typically, refinery oils based from petroleum contain 0.5-6% oxygen and 0.1-1.5% nitrogen (Manning and Thompson, 1995; Mederos et al., 2012; Olsen, 2014). It is thus common practice to upgrade the biocrude generated through heterogeneous catalytic hydrodeoxygenation and hydrodenitrogenation (Galadima and Muraza, 2014; Tran et al., 2010).

Bai et al. (2014) performed a catalytic screening study in which algae oil generated from the liquefaction of *Chlorella* (350 °C, 60 min) was subjected to a two-stage upgrading process: a high-temperature upgrading stage using hydrogen gas without catalyst (350 °C, 4 hours), and a supercritical upgrading stage using hydrogen gas with varying types of heterogeneous catalysts

(400 °C, 4 hours; 10% catalyst loading by weight). It was determined that although the hydrogen treatment alone favorably reduced the nitrogen content of the bio-oil and increased its flowability, every catalyst tested achieved greater reduction in O and N, lower viscosity, and higher HHV. Specifically, across a range of 14 commercial catalysts, including precious metal catalysts, sulfided metal catalysts, zeolites, and varying supports, their work demonstrated that ruthenium (5% wt. on carbon) and Raney nickel, used in conjunction, produced the best results. Their two-stage process reduced the nitrogen content of the bio-oil from 8.0% to 2.0% (by mass). The catalysts examined showed signs of significant coking under these conditions (20% by weight), potentially due to the nitrogenated compounds present during upgrading.

Savage and Duan (2011) conducted a study on the relative importance of temperature (430 to 530 °C), time (2 to 6 hours), catalyst loading (5 to 20%), and catalyst type on the quality of algae bio-oil after the catalytic upgrading stage. Using either Mo_2C, HZSM-5, or Pt/C catalyst, they determined which parameter of the catalytic hydrodeoxygenation (HDO) stage had the most relevant effect on the elemental quality, the compound quality, and the higher heating value of *Nannochloropsis* hydrothermal liquefaction (HTL) biocrude upgraded in supercritical water. Their work demonstrated that temperature had the greatest relative importance for every biocrude characteristic analyzed, with higher temperatures (530 °C), times (6 hours) and catalyst loading (20%) correlating to more favorable quality (in terms of elemental and chemical composition). Their evidence showed that at an HDO temperature of 530 °C, more of the carbon was distributed to the gas and coke phases than to the oil phase. This suggested that 530 °C was likely too severe a treatment temperature if liquid fuel precursors are the desired product. Supercritical temperatures, in general, are inherently more energy demanding, requiring additional energy inputs to maintain.

This study was designed firstly to determine if subcritical HDO temperatures (350 °C) are suitable for generating refinery quality bio-oil if paired with low- and high-temperature hydrothermal liquefaction. Literary evidence suggests that using a lower temperature during HDO will maximize the bio-oil yield: a necessary qualification for the technology to be considered for scale-up

(Bai et al., 2014; Galadima and Muraza, 2014; Tran et al., 2010). To better mimic the continuous reaction setting likely to be utilized on the larger scale, catalytic HDO was performed on the entire HTL liquid and solid product (including the aqueous phase) (Elliott et al., 2013; Jazrawi et al., 2013). Moreover, Bai et al. (2014) and Savage and Duan (2011) both suggested that catalyst performance is heavily affected by the algae strain being used and the conditions of the upgrading stage. For that reason, multiple catalysts were evaluated in this study. Ruthenium (5% on carbon, Ru/C) was the control catalyst used, since its performance has already been demonstrated as a top candidate for this process (Bai et al., 2014). Cobalt molybdenum (CoMo) was evaluated in several forms, as it is a primary candidate for co-processing with petroleum oil. Sulfided CoMo is regularly used in petroleum refining, and was thus evaluated; since algae biocrude is naturally low in sulfur concentrations, a hydrogen-reduced CoMo was also be evaluated. In addition, a hydrogen reduced mixed metal oxide catalyst known as red mud (primarily iron oxide, RRM) was evaluated, as it is potentially an inexpensive alternative to precious metal catalysts since it is a waste product from the mining industry. Several explorative evaluations of its activity have been performed (Balakrishnan et al., 2011; Sushil and Batra, 2008).

6.2 Experimental

6.2.1 Materials

Freeze-dried *Spirulina platensis* was obtained from Earthrise Nutritionals LLC (Calipatria, CA), and *Nannochloropsis sp.* was obtained from Reed Mariculture (”Nanno 3600”, strain CCMP525). A consortium of three algal strains (*UGA Consortium* henceforth), namely *Chlorella sorokiniana*, *Chlorella minutissima*, and *Scenedesmus bijuga*, were grown and harvested for use in this study as well.

Ruthenium (5% on carbon w/w, 20 um particle size, *Ru/C*) was obtained from Sigma-Aldrich (MO, USA). A cobalt oxide (3.4-4.5%) molybdenum oxide (11.5-14.5%) on alumina (Al_2O_3) catalyst (2.5 mm trilobe, *CoMo*) was obtained from Alfa Aesar (MS, USA). The $CoMo/Al_2O_3$ catalyst was reduced in the presence of flowing hydrogen (100%) at 400 °C in a tubular packed bed reactor (1 in. ID); 100 mL min^{-1} of hydrogen gas was passed over the catalyst for 2 hours (*CoMo-H_2*). In addition, pre-sulfided $CoMo/Al_2O_3$ catalyst (2-7% Co-S and 5-25% Mo-S, trilobe 2.5 mm, *CoMo-S*) was obtained from EureCat (EU). A mixed metal oxide catalyst (Red Mud) was obtained from Rio Tinto (Alcan, Canada). This catalyst was dried (105 °C), crushed, and sieved ($0.5 < d_p < 2$, mm). The red mud particles were reduced in the presence of flowing hydrogen (100%) at 300 °C in a tubular packed bed reactor (1 in. ID); 90 mL min^{-1} of hydrogen gas was passed over the catalyst for 20 hours (*RRM*).

6.2.2 Algae Growth

A consortium of three algal strains (*UGA Consortium* henceforth), namely *Chlorella sorokiniana*, *Chlorella minutissima*, and *Scenedesmus bijuga*, were grown and harvested at The University of Georgia (USA). A monoculture inocula of the constituent strains were first grown in 20 L carboys under controlled conditions in a growth chamber at 25 $\pm$ 1 °C for 12 h with alternating light-dark cycles; the light intensity was 100 μmoles m^{-2} s^{-1} with continuous air bubbling. The final consortium was prepared by mixing equal proportions (v/v) of each individual strain and then using it as inoculum at 10% v/v for outdoor cultivation in raceway ponds under green house facilities at an algae bioenergy lab of the University of Georgia (UGA). The raceway ponds are constructed of HDPE plastic and are 1.32 m wide, 2.18 m long, and 0.61 m deep with a working volume of approximately 500 L at 0.17 m water depth. Standard algae growth medium BG 11 was used in fresh water for cultivation (Jena et al., 2011b). Supplemental CO_2 was derived from a commercial 10% CO_2 storage cylinder and used as a carbon source and for pH control. The UGA designed carbonation column (Putt et al., 2011) was used for CO_2 mass transfer. Once the cell den-

sity in raceways reached 500 mg/L, the biomass was harvested using a continuous centrifuge and dried at 55 °C until constant weight was observed after multiple weighing. The dried biomass was packed in zip-lock bags and stored at 4 °C until further use. Subsequently, the dried microalgae was ground to a fine powder using a heavy-duty laboratory knife mill (Retsch SM 2000, Germany) with a screen size of 0.5 mm. The knife mills cutting blade rotor (1690 rpm, 60 Hz) was powered by a 1.5 kW electric motor.

6.2.3 Liquefaction Apparatus and Experimental Procedure

Reactor Operation

Figure 6.2 illustrates the process flow of the entire 4-stage conversion process. The low temperature liquefaction pretreatment (*PT*, 125 to 225 °C) was performed in a batch reactor (Parr 5000 Multi Reactor System, 75 mL vessel). Vessels were charged with 7 g of algae and 32 g of deionized water, and were sealed using a PTFE gasket. The system contains six separate vessels, each with its own PTFE magnetic stir bar (300 RPM) and band heater in an aluminum block (250 W); the heating rate of each reactor is approximately 10 °C min^{-1}. The residence time is taken from the point the reactor reaches temperature. Vessels were pressurized with 300 psi (20.7 bar) helium prior to heating to ensure liquid water throughout the reaction. Once the residence time was complete (ranging from 0.5 to 30 minutes), the vessels were removed from the heating block, and the bottom sections of the vessels (below the screw cap) were submerged in a water bath. At ambient temperatures, the vessels were depressurized and weighed to determine the mass of gas produced from the reaction.

The whole product from the low temperature liquefaction stage was transferred without additional solvent into a 50 mL centrifuge tube and centrifuged in a Sorvall Super T21 centrifuge at 10000 RPM for 20 minutes. The aqueous phase was decanted off and weighed, and the remaining solids were resuspended in a fresh aliquot of deionized water (enough to make the slurry 47

g total). For solid analysis, solids were dried after centrifugation and decanting at 105 °C for 4 hours.

High temperature liquefaction (*HTL*, 350 °C) was performed in a different batch reactor (Parr 4598 Micro-Stirred Reactor, 100 mL vessel). Vessels were charged with either 7 g of algae and 40 g of deionized water, or with the resuspended solid slurry. Vessels were sealed using a consumable Parr Grafoil gasket (flat flexible graphite). The mixture was stirred using a 4-blade impeller powered by a magnetic stirrer (model no. A1120HC6, 100 W variable speed) at 300 RPM. Vessels are heated using a ceramic fiber external jacket (700 W); the heating rate is approximately 14 °C min^{-1}. The residence time is taken from the point of PID leveling that is characterized by a noticeable and sizable decrease in the heating rate, occurring approximately 10 degrees below the set point. High temperature liquefaction was performed at 350 °C for 60 minutes. Vessels were pressurized with 500 psi (34.5 bar) helium prior to heating to ensure liquid water throughout the reaction. Once the residence time was complete, the external jacket was lowered and removed, and the vessel was cooled using a fan. At ambient temperatures, the vessels were depressurized and weighed to determine the mass of gas produced from the reaction. The whole product was transferred without additional solvent into a 50 mL centrifuge tube for storage.

Catalytic hydrodeoxygenation and repeated batch catalysis (*HDO* and *RB*, 350 °C) were performed in the Parr 4598 Micro-Stirred Reactor following the procedure listed above. The vessels were charged with catalyst while being charged with the reaction slurry, and 750 psi (51.7 bar) of hydrogen gas was used to fill the headspace; reactions were conducted for 240 minutes, stirring at either 300 or 500 RPM.

Phase Separation and Biocrude Extraction Procedure

Following high temperature liquefaction or catalytic upgrading, 40 mL of dichloromethane (DCM) was added to the whole product and mixed. This solution was filtered under vacuum through Whatman #4 filter paper (pore size 20-25 um), and the cake was rinsed with 15 mL of

additional DCM. The cake was weighed wet, dried at 105 °C for 4 hours, and weighed again to determine wet and dry solid yield, and estimated solid water content. The filtrate was then transferred into a separatory funnel (150 mL) and was allowed to phase separate for 15 minutes. The bottom phase (oil solubilized in DCM) was decanted off, and 1 g of anhydrone (magnesium perchlorate) was added to the decanted phase. This phase was filtered again under vacuum with 10 mL DCM used to rinse the anhydrone cake. The filtrate was transferred to a rotary evaporator (Rotovap) flask. The flask was then rotated under vacuum pressure (40 mbar) in a 36 °C water bath for 30-45 minutes until all DCM was removed; the remaining product was weighed to determine the mass of bio-crude. Since the solvent-free bio-crude is very viscous, two different storage techniques were used: a subsample was scooped from the flask using a scoopula for analyses that require solvent-free product, and the remaining bio-crude in the flask was resuspended in DCM (approximately 6:1 DCM:oil by mass).

6.2.4 Sample Workup and Analysis

The elemental composition (C, H, N, and S) of the samples was measured using a Thermo-Scientific Flash 2000 elemental analyzer according to the ASTM D5291 standard method; solvent-free oils and dry solids were used in this analysis. Issues with the biocrude being overly volatile during sample weighing were overcome by using two tin capsules (instead of one) and by loading and analyzing each replicate individually (rather than loading the device carousel fully).

The concentration of whole proteins was found by performing Bradford Protein Assay using Coomassie Blue and UV-Vis spectroscopy (595 nm, measured on a Beckman DU 650 spectrophotometer).

Proximate analysis was performed using thermal gravimetric analysis (TGA) on a LECO TGA 701. The moisture step was performed with a 6 °C min^{-1} ramp from 25 to 107 °C in a nitrogen atmosphere, the volatiles step was performed with a 43 °C min^{-1} ramp from 107 to 950 °C in a

nitrogen atmosphere with crucible lids on, and the ash step was performed with a 15 °C min^{-1} ramp from 600 to 750 °C in an oxygen atmosphere.

Simulated Distillation was performed on a Mettler-Toledo TGA/SDTA851. The following temperature-programmed volatilization was used: 25 °C initially, followed by a 10 °C min^{-1} ramp to 625 °C. 40 uL aluminum crucibles containing approximately 2 mg of sample were used for analysis; the inert gas flow was 50 mL min^{-1} of nitrogen.

Gas Chromatography-Mass Spectrometry (GC/MS) was performed on an Agilent GC-MSD (Hewlett-Packard 5973 and 6890) with an HP5 MS Capillary Column (30 m x 0.25 um x 0.25 um). Separation was achieved using a temperature-programmed method of 40 °C, held for 4 minutes, with a 5 °C min^{-1} ramp until 275 °C was reached, held for 5 minutes; the inlet was held at 260 °C, the split ratio was 50:1, the injection volume was 1 uL, the helium carrier gas flow was 0.8 mL min^{-1}, and the MS scan was 30-400 m.u. Standard curves were constructed using model compounds and 1-hexanol as an internal standard, in triplicate.

High Pressure Liquid Chromatography (HPLC) was performed on a Shimadzu LC-20 AT equipped with a RID-10A refractive index detector and a Coragel 64-H transgenomic analytical column (7.8 x 300 mm); the flow was 0.6 mL min^{-1} for a 55 minute run time, the sample volume was 5 uL, the mobile phase was 4 mN sulfuric acid, and the samples were analyzed at 6.89 MPa and 60 °C. About 2 mL of the oil was diluted with DI water at 1:1 ratio and centrifuged at 5000 rpm for 30 min, and then decanted. The supernatant was filtered through a 0.45 m filter into 2 mL auto-sampling vials. The sample was injected into the column using the LC-20 AT Shimadzu auto-injector. Samples were identified using standard curves constructed on isolated model compounds.

The higher heating value (HHV) of bio-crude was estimated using the elemental composition and the Dulong formula [Eq. 6.1] (Corbitt, 1999). The nitrogen removal was calculated on a weight basis based on the initial amount of nitrogen in the dry/ash-free feedstock, according to Eq. 6.2. Total Acid Number was determined according to the ASTM D974-12 standard method,

in which sample dissolved in a solution of toluene, isopropanol, and water (500:495:5, by mass) is titrated with potassium hydroxide titrant (dissolved in isopropanol, molarity approx. 0.11 M) until the indicator solution (p-naphtholbenzein) drastically changes color. Total Acid Number (TAN) is typically reported as milligrams of KOH required to neutralize one gram sample (mg KOH (g oil)$^{-1}$). pH was determined using potentiometry performed on an Orion 520A Digital pH meter (Orion Research Inc., USA). Water content was determined using a Mettler Toledo DL31 Karl Fischer Titrator. Water content was measured on a weight percentage basis using sample suspended in Hydranal, titrated with CombiTitrant 5 Keto.

$$0.3383 * \%C + 1.422 * (\%H - (\%O/8)) \quad [MJ/kg] \tag{6.1}$$

$$\%Nitrogen\ Removal = \frac{(\%N * DAF\ wt.)_{feedstock} - (\%N * wt.)_{product}}{(\%N * DAF\ wt.)_{feedstock}} * 100 \tag{6.2}$$

Tar bound to the catalysts after reaction was weighed via rinsing. A known mass of used catalyst was rinsed with a 1:1:1 (by volume) mixture of toluene, acetone, and methanol, and was filtered under vacuum through Whatman #4 filter paper (pore size 20-25 um) until the rinsate became clear in color. The rinsed catalyst was then dried at 105 °C for 1 hour, and the mass lost through the rinsing is considered tar. Tar is reported as a percent based per gram of catalyst, as shown in Equation 6.3.

$$Tar\ Removal(\%) = \frac{mass_{tar\ removed}}{mass_{catalyst}} \tag{6.3}$$

Surface area of the catalysts were measured by N_2 adsorption over a relative pressure range (P/P_0) of 0.05-0.35 using a 7-point BET analysis equation (Quantachrome AUTOSORB-1C; Boynton Beach, Fl, US). Pore size distribution, average pore radius, and total pore volume were esti-

mated from N_2 desorption curves using BJH analysis. All samples were degassed ranging from 250 to 300 °C for 3-4 hours prior to analysis.

Catalyst coke weight was determined using a Mettler Toledo TGA/SDTA 851e. The temperature-programmed method was 25 °C, followed by a 10 °C min^{-1} ramp to 800 °C. 5 mg of sample was used, and the temperature profile occurred in an air atmosphere.

6.3 Results and Discussion

6.3.1 Effect of Catalytic Upgrading Parameters on Bio-oil Quality

Table 6.1 illustrates the effect of varying stage combinations, catalyst loading, and HDO agitation parameters on the quality and yield of biocrude produced from the conversion of *UGA Consortium* using Ru/C. Quality is partially determined based upon the nitrogen content of the biocrude. Performing catalytic hydrodeoxygenation (HDO) alone, without prior liquefaction, gave the least favorable results, with a nitrogen content of 6.4% at a biocrude yield of 20.6%; high-temperature liquefaction (HTL) alone produced biocrude with a nitrogen content of 5.8% at a yield of 26.7%. The addition of the low-temperature pretreatment liquefaction (PT) reduced the nitrogen content across any stage combination, with the most effective nitrogen reduction being obtained using all three conversion stages. Implementing the pretreatment stage, however, reduced the biocrude yield an average of 14% (from approx. 20% to 6%). This is likely due to the loss in hydrolyzed material stemming from the subsequent separation that occurs after the pretreatment stage, through which degraded proteins are partitioned out of the solid phase prior to generation of biocrude. Increasing the catalyst loading from 10% to 30% favorably decreased the nitrogen content across all stage combinations. Moreover, the most effective nitrogen reduction was obtained using all three conversion stages with a higher agitation during HDO (2.4% nitrogen at a biocrude yield of 22.2%). The agitation rate having an effect on the quality of the biocrude provides more evidence that the

batch reaction taking place may be mass transfer limited or kinetic limited. Industrially, this process would be performed in a continuous reactor so as to maintain a constant initial concentration of hydrogen and other reactants.

There was not a strong correlation between stage combination and oxygen content of the biocrude. Trials containing the catalytic treatment stage performed better than HTL alone in reducing the oxygen content. For example, the two-stage HTL/HDO trial produced a biocrude containing 10.4% oxygen (by weight), down from 13.4% from HTL alone (a 22% improvement). For identical catalyst loading and agitation trials, the oxygen content in the biocrude was highly variable. Potentially, this could be due to kinetic limitations stemming from the consumption of the finite amount of hydrogen present in the reaction space.

The hydrodeoxygenation reaction is conducted by having hydrogen chemically replace oxygen and nitrogen in compounds. For this reason, the hydrogen consumption measured is said to correlate directly to the effective HDO of the stage. There appeared to be no trend in hydrogen consumption across varying stage combinations. However, increasing the catalyst loading, although lowering the hydrogen consumption rate, increased the total consumption of hydrogen for congruent periods of time. Increasing the agitation rate further increased the total hydrogen consumption, but asymptotically. An increase in agitation from 300 to 500 RPM had a profound effect on the amount of hydrogen consumed, but no statistical effect was found from increasing from 500 to 700 RPM. This provided evidence that mass transfer limitations were not preventing further upgrading of the biocrude, and instead, a separate limitation could have potentially been occurring.

Figures 6.3a-6.3c clearly illustrate an improvement in the composition quality of the biocrude with the addition of the pretreatment (PT) and catalytic upgrading (HDO) stages, as compared to high-temperature liquefaction alone (HTL). The improvements stemming from the addition of the pretreatment stage (as compared to HTL alone) were discussed in previous work, and will thus not be repeated here (Chapter 5). When comparing the 3-stage conversion process involving PT, HTL, and HDO to the 2-stage process without HDO, it is clear that there are a multitude of cat-

alytic mechanisms through which compounds were upgraded, manly into straight chain saturated hydrocarbons. Free fatty acids (hexadecanoic acid) were decarboxylated to form long chain hydrocarbons; unsaturated free fatty acids (oleic acid) were hydrogenated and decarboxylated so that the hydrocarbons formed were saturated. Any unsaturated hydrocarbons formed from the initial two stages (1-pentadecene) are hydrogenated into hydrocarbons. Ruthenium appeared unable to fully deaminate the biocrude compounds. Long chain amides and pyrridines, unaffected by the pretreatment stage, are only partially upgraded. Figure 6.3c shows these long chain amides (hexadecanamide) remain, even after catalytic HDO. Speculatively, these compounds were formed by cross reactions occurring between fatty acids and protein-based ammonia generated during protein hydrolysis.

6.3.2 Implementation of Repeated Batch Upgrading

In order to overcome hydrogen consumption limitations inherent to the nature of batch reactors, a 4-stage process was implemented. Low- and high-temperature liquefaction (PT and HTL) and catalytic upgrading (HDO) were performed. The reactor headspace was then purged and repressurized with hydrogen gas, and the HDO stage was repeated (hence, repeated batch, RB). The purpose of this repeated batch stage was to alleviate reaction restrictions stemming from limiting catalytic mechanisms through low hydrogen concentrations. Adding more hydrogen to the reactor system would drive the HDO/HDN reactions further, creating a higher quality bio-oil. In industrial practice, this type of hydrogen recharge would not be necessary, as continuous reactors inherently have a constant reactant concentration entering.

Table 6.2 contains the biocrude quality characteristics of 4-stage oils generated through use of different catalysts on different algal strains. Across all three strains, ruthenium on carbon (Ru/C) achieved the most favorable results in all measured characteristics (total acid number [TAN], water content [%W], pH, percent heteroatoms [%HA], nitrogen and oxygen content, and higher heating value [HHV]). Ru/C was the most effective at producing a low-nitrogen biocrude, with the

best results being with a 4-stage conversion of *UGA Consortium* (3.2% nitrogen). Comparatively, sulfided cobalt molybdenum (CoMo-S) produced a biocrude with 4.1% nitrogen under the same conditions. Reduced red mud (RRM) and hydrogen reduced cobalt molybdenum (CoMo-H_2) were both less effective at nitrogen removal that Ru/C, producing a biocrude from *Nannochloropsis* with 4.9% nitrogen (compared to 3.8% with Ru/C under the same conditions). In addition, the pretreatment temperature (225, compared to 175 °C) had no effect on generating a low-nitrogen oil. This is potentially due to the initial removal of nitrogen occurring in the pretreatment stage, which enables more efficient nitrogen removal through catalysis during HDO and RB in a process that is not kinetically limited in its ability to remove nitrogen. Refineries require their input streams to possess a nitrogen content between 0.1 and 1.5% (Manning and Thompson, 1995; Mederos et al., 2012; Olsen, 2014).

Surprisingly, catalyst type had no statistically significant effect on the oxygen content of the biocrude produced from the 4-stage conversion process. Several pieces of evidence indicate that this variance is likely due to factors external to the catalysts themselves; specifically, hydrogen limitations may still be present, even with a full hydrogen recharge occurring between the HDO and RB stages. One indication of this limitation is the hydrogen consumption measured during both HDO and RB (Table 6.4). Across all catalysts, algae strains, and conditions, the hydrogen consumption measured in RB was only approx. 8% less than that of HDO. If the biocrude upgrading reactions were nearing completion, the hydrogen consumption rate should drastically decrease; however, this rate decrease was not observed, indicating the reaction was being limited by some other factor. Further analysis revealed that of all the hydrogen that would be consumed in 240 minutes of the repeated batch, 92% had already been consumed after 90 minutes (Figure 6.4). This, again, points to the reactant-limiting nature of batch reactors, and further provides evidence that continuous reactor configurations may be more successful for this type of process.

Table 6.2 also describes the acidity and water content properties of oils generated from 4-stage repeated batch upgrading of several strains. Across all three strains, Ru/C produced oil with the

lowest total acid number (TAN). *UGA Consortium* had a TAN of 11.6 and *Nannochloropsis* of 47.1. Some petroleum oils have reported total acid numbers as low as 0.2 (Laredo et al., 2004). The water content of 4-stage algae bio-oil was relatively consistent (approx. $1.2\pm1\%$) between all catalysts, strains, and conditions. This consistency is likely due to our extraction process being responsible for any residual water present in the oil phase.

Comparatively, Figure 6.3 does not reveal a significant level of quality improvement between 3-stage and 4-stage generation of biocrude. Especially between Figures 6.3c and 6.3d, little to no compositional improvements were observed between 3- and 4-stage conversion, even if ultimate analysis did reveal marginal nitrogen content improvements (approx. 0.5% nitrogen content decrease). However, Table 6.2 describes the distinct heteroatom peak area percentage (%HA) differences between catalysts found through GC/MS. Ru/C achieved the most favorable results, with %HA levels as low as 0.0% (in *UGA Consortium*). With *Nannochloropsis*, CoMo-S generated oil with %HA levels of 53%, with CoMo-H_2 and RRM performing less favorable (70 and 61%, respectively).

A catalyst longevity study was conducted on Ru/C, in which the catalyst used in both HDO and RB of *UGA Consortium* was directly reused (without pre-processing, rinsing, or reactivating) in a second HDO and second RB upgrading of fresh, un-upgraded *UGA Consortium* biocrude. The nitrogen content in the catalyst reuse oil was 3.9%, higher than its fresh catalyst counterpart (at 3.2%). The oxygen content was not statistically different, for hydrogen limitation reasons discussed earlier; the hydrogen consumption rate, however, was only about half that of the fresh Ru/C hydrogen consumption. The total acid number of the catalyst reuse oil was 171, compared to 11.6 of the fresh catalyst; the catalyst reuse had the highest total acid number of all trials conducted, potentially indicating poisoned catalysts first lose their ability to catalyze acidic compound fixation and upgrading. The %HA levels from catalyst reuse oils were 23%, compared to 0.0% in oil upgraded using fresh catalyst under the same conditions. Overall, the reused Ru/C catalyst showed

evidence of activity loss performing catalytic hydrodeoxygenation of algae oil after 600 minutes "on stream".

6.3.3 Effect of Catalyst Type on Bio-oil Composition

Figure 6.5 shows the percent peak area (in GC/MS) for each compound group produced during 4-stage repeat batch conversion of *Nannochloropsis* using 4 different catalysts (Ru/C, CoMo-H_2, CoMo-S, RRM reduced at 300 °C). This figure was generated based upon the relative percent peak area for each compound group, and no internal standard quantification was performed. Ru/C achieved the most favorable composition of upgraded biocrude, with approx. 90% of the total peak area consisting of long chain and aromatic hydrocarbons. All fatty acids present were converted, and no ketones or nitrogenated aromatics remained. Some residual phenolics and long chain amides persisted (2 and 3%, respectively), indicating incomplete extents of reaction. CoMo-S performed less effectively than Ru/C, but much more so than CoMo-H_2 or RRM. CoMo-S generated biocrude containing approx. 65% long chain and aromatic hydrocarbons. Some residual fatty acids remained (2%), and no ketones remained. However, nearly 15% of the total peak area consisted of nitrogenated aromatics, with an additional 15% consisting of phenolics and long chain amides. This suggests Ru/C has a higher activity for denitrogenation than CoMo-S, and that nitrogenated compounds may have poisoned CoMo-S, preventing it from complete deoxygenation. Algae biocrude does not contain ample sulfur to maintain the activity of a sulfided catalyst. Both CoMo-H_2 and RRM showed poor activity towards decarboxylation of fatty acids, denitrogenation, and deoxygenation. Heteroatoms (phenolics, ketones, nitrogenated aromatics, long chain amides) comprised approx. 55% of the total peak area in biocrude generated from each catalyst. The total area % of hydrocarbons was less than that of nitrogenated aromatics for each of these two catalysts, suggesting the Mars van Krevelen mechanism (activated by hydrogen-generated oxygen vacancy cites) may not be active for the heteroatoms typically present in algae liquefaction biocrude (Sushil and Batra, 2008).

Figures 6.6 and 6.7 illustrate the boiling point distribution of bio-oils (along with a gas oil standard) which help characterize which type of liquid fuels these bio-oils would most readily generate. Through extrapolation from GC/MS chromatograms, the bio-oil can be fractioned into distillation classes (Table 6.3) characterized by boiling point; the progression of this extrapolation can be seen in Figure 6.6. Figure 6.7 illustrates the distillation classes and amounts for *Nannochloropsis* repeated batch oils generated using four different catalysts (Ru/C, CoMo-H_2, CoMo-S, and RRM). Between the four algae oils, there is a relationship between the hydrocarbon compositional content and the boiling point distribution: as the hydrocarbon content increased, the boiling point distribution shifted towards higher BP classifications, such as kerosine and DFO. RRM and CoMo-H2 both had the lowest hydrocarbon content, and thus had the lowest average boiling point. CoMo-S was next highest, with Ru/C having both the highest hydrocarbon content and average boiling point classification. Simulated distillation of the gas oil standard revealed that in petroleum oil, the fractions contained in each distillation class are approximately equal in cumulative peak area (for boiling points between 100 and 350 °C). This is different than algae oil, in which each of the four bio-oils had a primary fraction that contained a majority of the cumulative peak area. For Ru/C and CoMo-S, this range was Distillate Fuel Oil (DFO), and was kerosine for both RRM and CoMo-H_2. In catalysts besides Ru/C, a decrease in the average boiling point of the oil is likely a result of the presence of additional heteroatoms such as phenolics and nitrogenated aromatics. Even though RRM and CoMo-H2 did not generate a significant amount of hydrocarbons in the biocrude phase, high boiling point compounds are still present in the distillation curve. These are likely long-chain amide and nitrile cross-products stemming from the incomplete upgrading of lipid and protein interactions.

6.3.4 Catalyst Characterization and Comparison

Table 6.4 shows several catalyst characteristics (surface area, average pore size, average pore volume) that were measured, both before and after repeated batch upgrading of the three algae

strains. In all trials, the surface area and average pore volume decreased after use in algae biocrude upgrading. Ru/C, which possessed the highest fresh surface area (721 m^2 g^{-1}), had its surface area decrease by at least 50% for all three strains, with the largest decrease occurring in *UGA Consortium* (to 110 m^2 g^{-1}); *Nannochloropsis* decreased to 181 m^2 g^{-1} and *Spirulina* to 347 m^2 g^{-1}. Often, the surface area of a catalyst correlates to its overall activity, which suggested that the catalysts experienced significant losses in activity after a single use in 4-stage repeated batch upgrading. This was confirmed by the catalyst reuse study conducted, in which the surface area of Ru/C decreased from 110 to 56 m^2 g^{-1} after being used a second time. Moreover, the catalyst reuse oil suggested lower catalyst activity than its fresh catalyst counterpart (discussed previously). CoMo experienced a decrease in surface area upon sulfidation (from 253 to 194 m^2 g^{-1}), with no surface area change observed through hydrogen reduction. Similar to Ru/C, CoMo-S showed a decrease in surface area (from 194 to approx. 120 m^2 g^{-1}) when used in repeated batch upgrading, in all three strains.

Figure 6.8 illustrates the percent change of several physical parameters (coking and taring, surface area, and pore volume) occurring after the catalysts were used. As stated, all catalysts showed a decrease in surface area and pore volume after use, with the largest initial surface areas (Ru/C and CoMo-S) showing the most substantial percent decrease in surface area (75 and 35%, respectively). There appeared to be no correlation between the percent decrease in surface area and in average pore volume; the most substantial decrease in pore volume occurred in Ru/C. In addition, the catalyst reuse study revealed that Ru/C showed further decrease in surface area and pore volume after additional use (although to a significantly lesser extent than the initial decrease observed between the fresh and the single-use catalyst). Figure 6.8 also indicates the accumulation of tar and coke on the catalyst surface. In all cases, this weight was below 0.1 gram per gram of catalyst. This accumulation can be removed by rinsing with solvent (toluene, acetone, and methanol were used in this study), and the industrial practice of reactivating catalysts may need to include catalyst rinsing if economic catalyst longevity is to be feasible.

6.4 Conclusion

A four-stage conversion process was implemented to make a refinery-grade intermediate feedstock from algae more effectively than any other stage combination. Low- and high-temperature hydrothermal liquefaction with catalytic hydrodeoxygenation produced a low nitrogen biocrude. Ruthenium on carbon achieved the greatest desired results, reducing heteroatom levels and producing oil with the highest long chain and aromatic hydrocarbon content. Significant decreases in catalyst surface area and pore volume were observed with use in catalytic HDO, more so on catalysts with greater initial values of these characteristics. The extent of reaction was limited by low hydrogen concentrations stemming from the consumption of this reactant in a batch atmosphere.

6.5 Figures and Tables

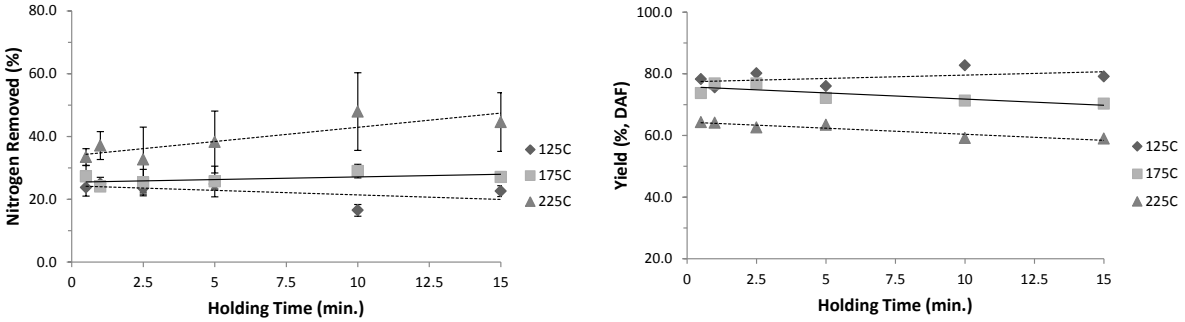

(a) Nitrogen partitioning.

(b) Solid retention.

Figure 6.1: Effects of temperature and reaction duration of PT stage on nitrogen partitioning (% removal from solid phase) and solid retention (daf yield %) in *UGA Consortium*.

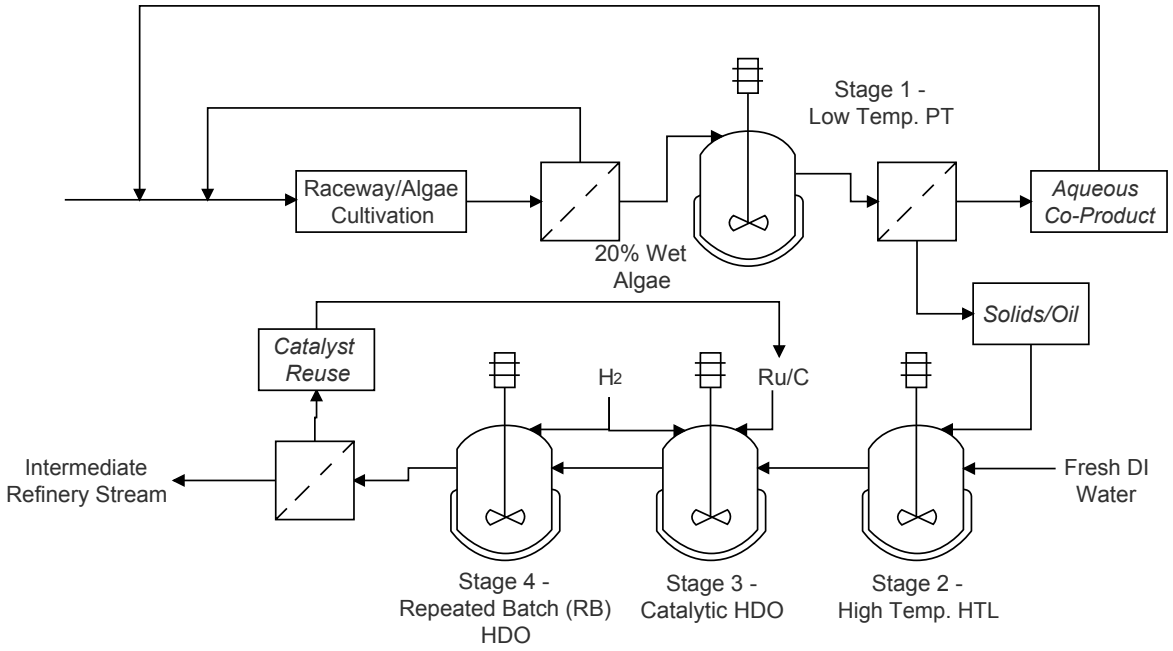

Figure 6.2: Process flow diagram for the experimental steps in the 4-stage conversion of algae to liquid fuels.

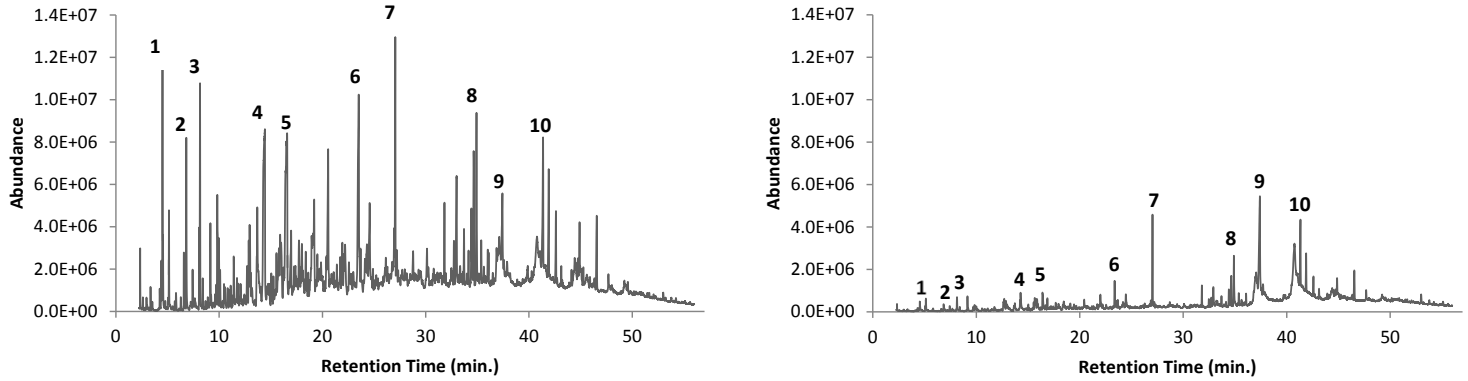

(a) HTL only.

(b) PT and HTL.

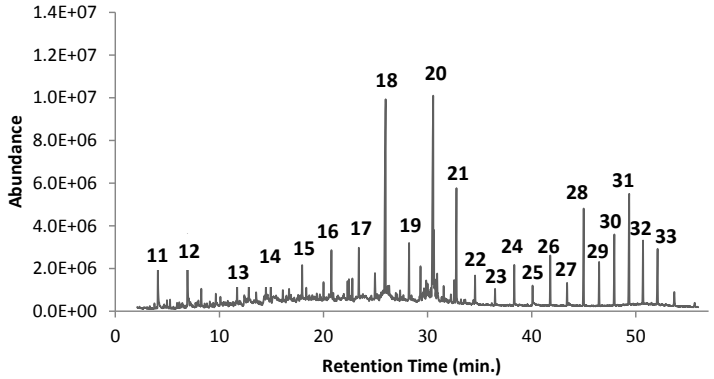

(c) PT, HTL, and HDO.

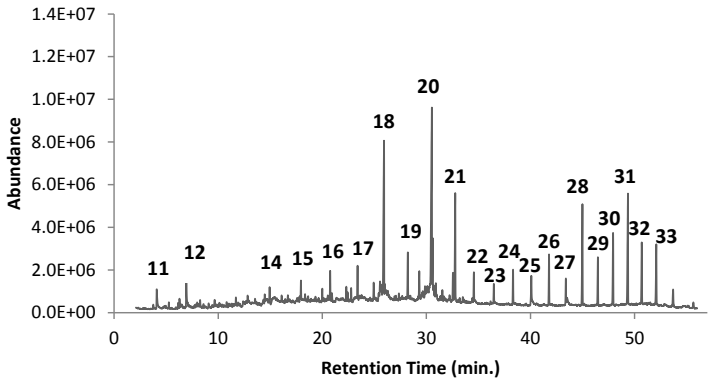

(d) PT, HTL, HDO, and RB.

Figure 6.3: GC/MS analysis of *UGA Consortium* biocrude using Ru/C [PT: 225 °C, 15 min; HTL: 350 °C, 60 min; HDO and RB: 350 °C, 240 min].

Identified compounds are (1) pyrazine, (2) methyl-pyrazine, (3) ethyl benzene, (4) 1-methyl-2-pyrrolidinone, (5) 1-ethyl-2-pyrrolidinone, (6) 1-methyl-piperidine, (7) 1-pentadecene, (8) 3,7,11,15-tetramethyl-2-hexadecene, (9) hexadecanoic acid, (10) hexadecanamide, (11) toluene, (12) ethyl benzene, (13) decane, (14) undecane, (15) dodecane, (16) tridecane, (17) tetradecane, (18) pentadecane, (19) hexadecane, (20) heptadecane, (21) phytane, (22) nonadecane, (23) eicosane, (24) heneicosane, (25) docosane, (26) tricosane, (27) tetracosane, (28) pentacosane, (29) hexacosane, (30) heptacosane, (31) octacosane, (32) nonacosane, (33) triacontane.

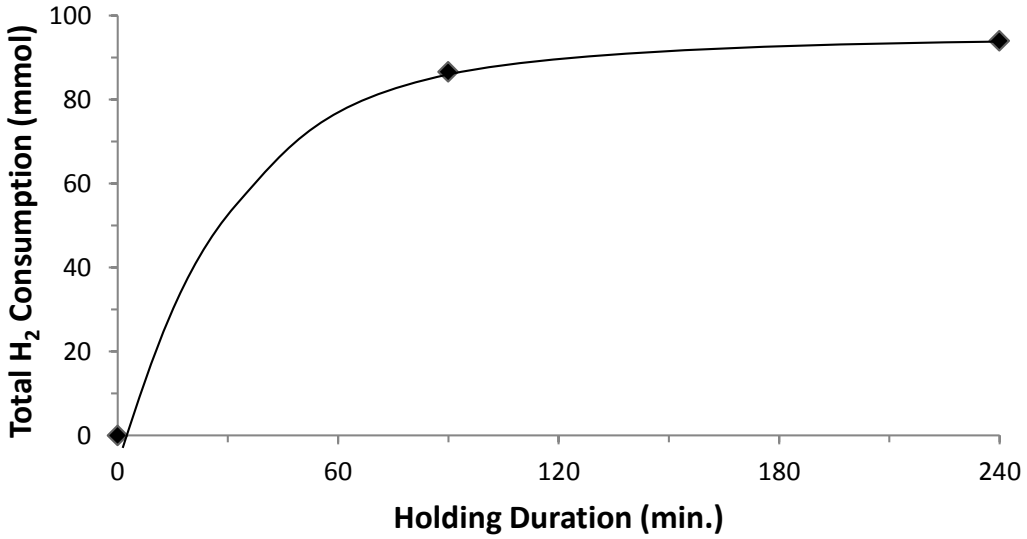

Figure 6.4: Total hydrogen consumption vs holding duration for 4-stage repeated batch upgrading of *UGA Consortium* [PT: 225 °C, 15 min; HTL: 350 °C, 60 min; HDO: 350 °C, 240 min; RB: 350 °C].

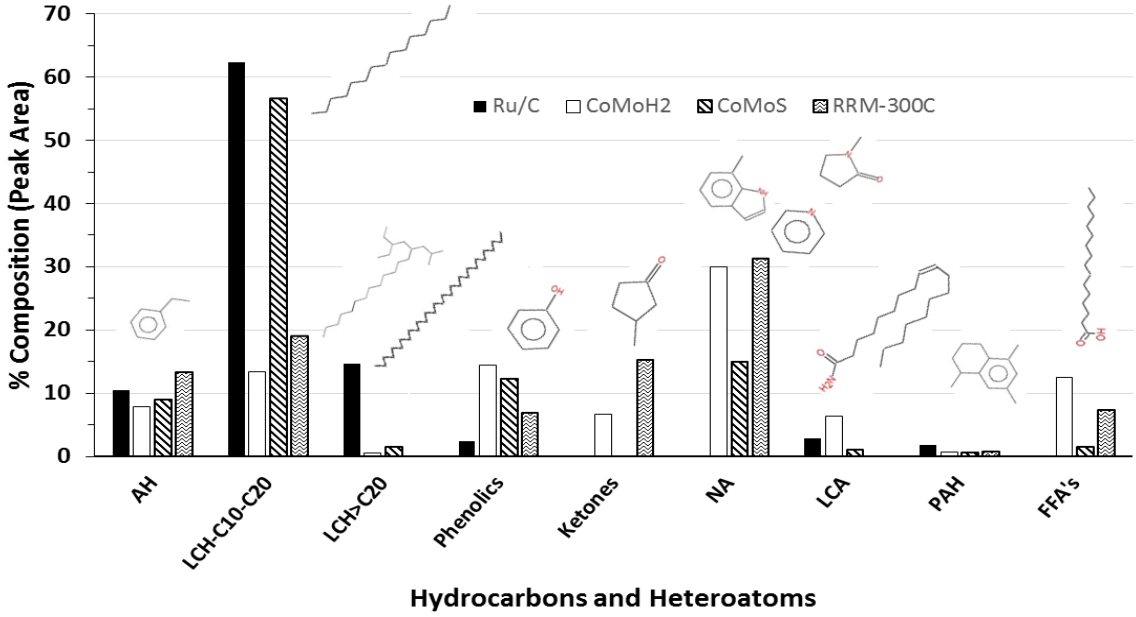

Figure 6.5: Compositional analysis of algal oil, from *Nannochloropsis*, after repeated batch upgrading (RB) using several catalysts, based on GC/MS analysis and % peak area [PT: 225 °C, 15 min; HTL: 350 °C, 60 min; HDO and RB: 350 °C, 240 min].

AH - aromatic hydrocarbons, LCH - long chain hydrocarbons, NA - nitrogenated aromatics, LCA - long chain amides, PAH - polycyclic aromatics, FFA's - fatty acids.

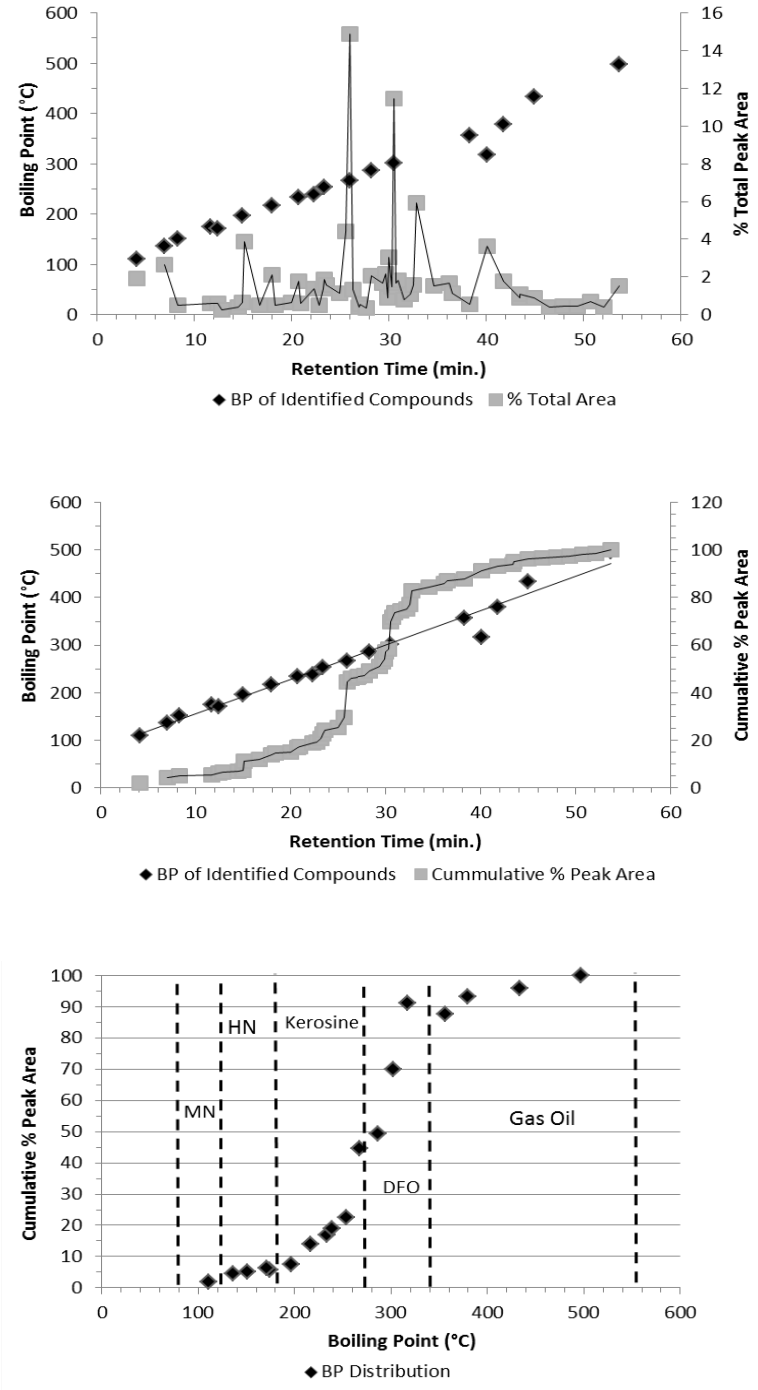

Figure 6.6: Simulated distillation analysis and GC/MS work-up of 4-stage RB algal oil generated from *Nannochloropsis* using Ru/C catalyst [PT: 225 °C, 15 min; HTL: 350 °C, 60 min; HDO: 350 °C, 240 min, 30% cat. loading].

See Table 6.3 for distillation cut classifications.

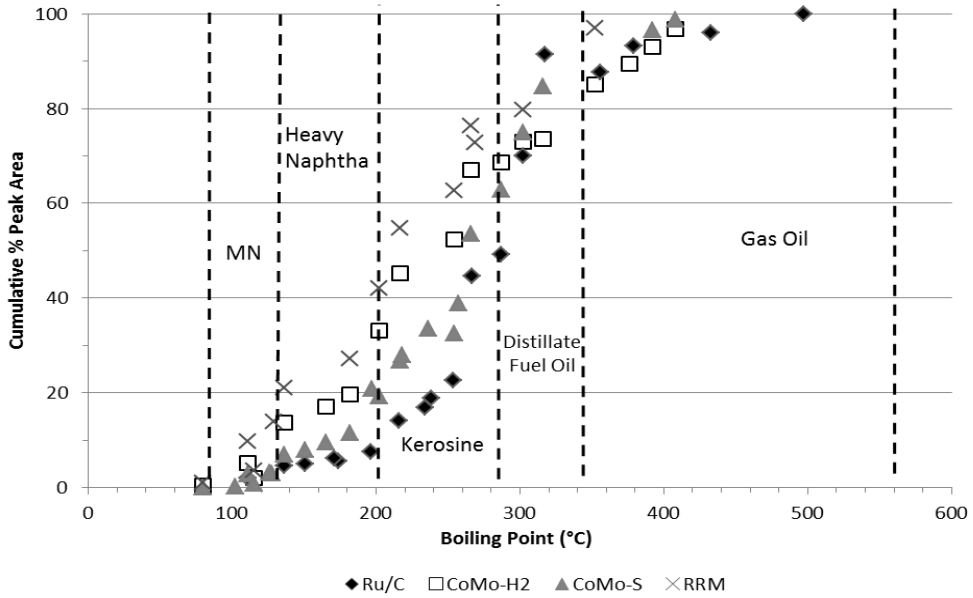

(a) 4-stage RB algal oil from *Nannochloropsis* using varying catalysts [PT: 225 °C, 15 min; HTL: 350 °C, 60 min; HDO: 350 °C, 240 min, 30% cat. loading].

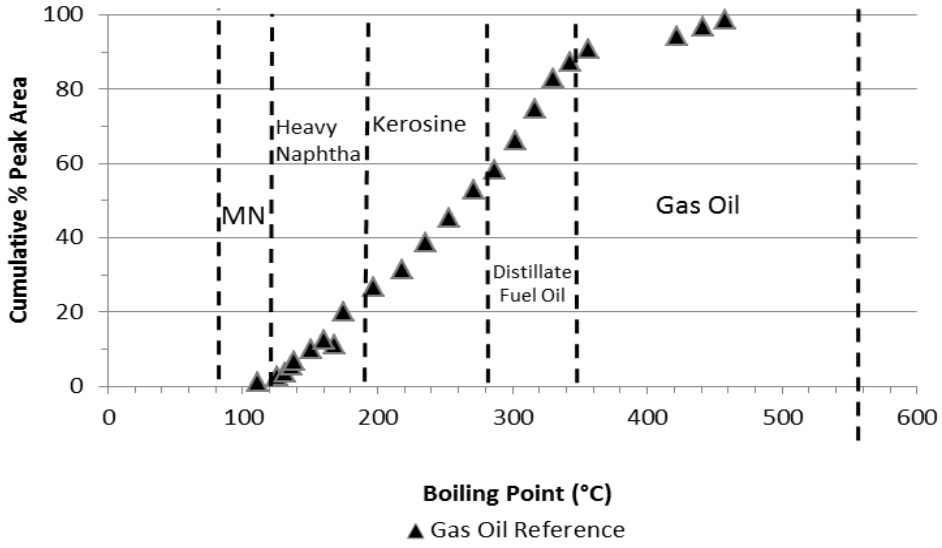

(b) Petroleum gas oil standard.

Figure 6.7: Simulated distillation analysis of biocrude and petroleum gas oil via GC/MS extrapolation.

See Table 6.3 for distillation cut classifications.

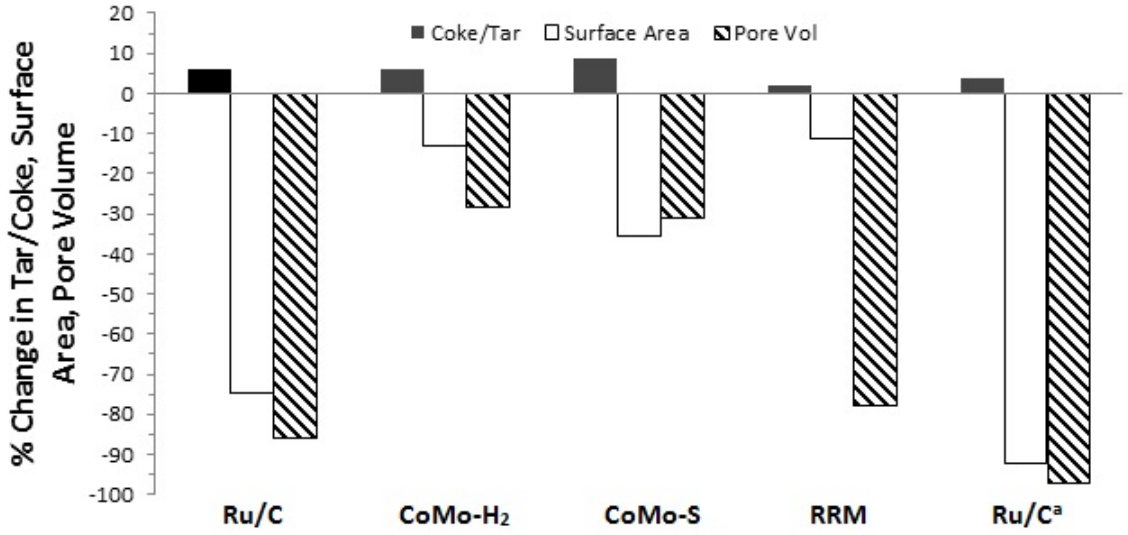

Figure 6.8: Tar accumulation, % change in surface area and pore volume for recovered catalysts used in the repeated batch HDO experiments of *Nannochloropsis* [PT: 225 °C, 15 min; HTL: 350 °C, 60 min; HDO: 350 °C, 240 min, 30% cat. loading].

([a]Catalyst reuse experiment, using *UGA Consortium*. Measured against fresh catalyst).

Table 6.1: Effect of HDO parameters on ultimate analysis and HHV of biocrude, and hydrogen consumption (in HDO) from 3-stage conversion of *UGA Consortium* using Ru/C [PT: 225 °C, 15 min; HTL: 350 °C, 60 min; HDO: 350 °C, 240 min].

Stage Combination			Cat. Loading	HDO Agitation	Ultimate (dry basis) (% w/w)				HHV	Yield	H_2 Consumption
PT	HTL	HDO	(%, w/w)	(RPM)	C	H	N	O[a]	(MJ/kg)	(% DAF feed)[b]	(mmol hr $^{-1}$ g_{cat}^{-1})
	x		NA	NA	71.6±2.1	8.7±0.2	5.8±0.2	13.4±3.2	34.2	26.7	NA
		x	10	300	74.3±0.3	9.4±0.1	6.4±0.1	9.2±1.1	36.8	20.6	25.5
	x	x	10	300	74.6±0.1	9.3±0.2	5.8±0.2	10.4±0.1	36.6	22.1	22.1
x		x	10	300	74.4±0.1	9.4±0.1	5.0±0.1	11.2±0.7	36.6	9.5	25.9
x	x	x	10	300	74.5±0.7	9.3±0.1	4.8±0.1	12.2±0.9	36.3	6.2	25.4
	x	x	30	300	75.6±0.3	10.6±0.1	4.9±0.1	8.9±0.4	39.0	24.3	11.9
x		x	30	300	77.4±0.4	11.7±0.1	3.4±0.1	7.5±0.5	41.5	13.8	11.9
x	x	x	30	300	79.0±1.1	12.0±0.2	3.0±0.2	6.1±0.9	42.7	17.3	12.0
x	x	x	30	500	66.8±3.6	8.6±0.6	2.4±0.2	20.2±4.3	29.9	22.2	13.8
x	x	x	30	700	72.6±0.7	10.6±0.2	3.1±0.1	13.8±0.1	37.2	17.2	13.6

[a]Determined by difference. [b]% w/w of dry/ash-free feedstock fed initially. NA: Not applicable.

Table 6.2: Properties of oil generated by repeated batch catalysis [PT: 15 min; HTL: 350°C, 60 min; HTL and RB: 350°C, 240 min].

Algae Strain	Catalyst	PT Temperature	Acidity/Water (% w/w)		Heteroatoms (% w/w)			HHV
		(°C)	TAN	%Water	%HA[a]	%N[b]	%O[c]	(MJ/kg)
UGA Consortium								
	Ru/C	225	11.6±1.4	1.3±0.6	0.0	3.2±0.2	9.3±0.7	39.8
	CoMo-S	225	63.1±3.9	0.8±0.1	53	4.1±0.1	12.5±0.9	36.1
	Ru/C	175	20.8	NP	14	3.2±0.2	19.5±2.4	33.1
	Ru/C Reuse[d]	225	171±0.9	NP	23	3.9±0.1	7.7±0.2	40.2
Nannochloropsis								
	Ru/C	225	47.1±4.7	3.6±1.5	5.3	3.8±0.5	9.6±1.7	39.7
	CoMo-H_2	225	70.8±1.8	1.2±0.2	70	4.9±0.1	7.4±0.5	39.0
	CoMo-S	225	65.8±8.7	1.0±0.2	53	3.8±0.1	6.0±0.3	41.4
	RRM	225	67.8±1.2	1.4±0.3	61	4.9±0.1	9.9±0.6	37.6
	Ru/C	175	6.3±0.4	0.3±0.1	31	3.9±0.1	15.1±0.5	35.5
Spirulina								
	Ru/C	225	NP	0.3±0.3	40	NP	NP	NP
	CoMo-S	225	74.0±5.5	0.8±0.1	50	4.8±0.4	14.2±0.2	35.0
	Ru/C	175	18.8±0.6	0.2±0.1	NP	NP	NP	NP

[a]Percent heteroatoms based on % peak area in GC/MS analysis - includes phenolics, ketones, nitrogenated aromatics, amides, fatty acids.

[b]CHNS using two tin holders and single sample analysis, which solved volatility issues and gave consistent results.

[c]Oxygen found by subtraction. [d]Catalyst from ”reuse” study. NP: not performed.

Table 6.3: Distillation cut classifications used in simulated distillation analysis of catalytic HDO samples.

Fraction		Lower BP (°C)	Higher BP (°C)
Light Naphtha	LN	25	79
Medium Naphtha	MN	79	121
Heavy Naphtha	HN	121	191
Kerosine	Kerosine	191	277
Distillate Fuel Oil	DFO	277	343
Gas Oil	GO	343	566
Residuum	Residuum	566	1000

Table 6.4: Catalyst properties after repeated batch HDO of HTL-generated algal oil [PT: 15 min; HTL: 350 °C, 60 min; HDO and RB: 350 °C, 240 min].

Algae Strain	Catalyst	PT Temperature (°C)	Surface Area ($m^2\ g^{-1}$)	Avg. Pore Size (diameter, Å)	Avg. Pore Volume ($cm^3\ g^{-1}$)	H_2 Consumption (mmol $hr^{-1}\ g_{cat}^{-1}$)	
						HDO	RB
Fresh Catalyst[a]							
	Ru/C	NA	721	14.4	0.52	NA	NA
	CoMo	NA	253	46.0	0.29	NA	NA
	CoMo-H_2	NA	258	46.0	0.30	NA	NA
	CoMo-S	NA	194	111	0.53	NA	NA
	RRM	NA	31	25.0	0.04	NA	NA
UGA Consortium							
	Ru/C	225	110	47.2	0.13	12.2	11.2
	CoMo-S	225	73	56.3	0.10	12.1	11.6
	Ru/C	175	122	44.0	0.13	12.0	10.9
	Ru/C Reuse[b]	225	56	53.0	0.08	6.1	6.5
Nannochloropsis							
	Ru/C	225	181	41.2	0.19	12.5	9.5
	CoMo-H_2	225	224	46.8	0.26	12.3	11.1
	CoMo-S	225	125	47.1	0.15	12.3	11.5
	RRM	225	27	6.0	0.0041	12.3	11.8
	Ru/C	175	200	40.2	0.20	12.8	11.5
Spirulina							
	Ru/C	225	347	33.7	0.29	12.2	11.6
	CoMo-S	225	102	56.3	0.10	12.1	12.0
	Ru/C	175	405	112	0.32	12.4	11.6

[a]Catalysts analyzed prior to use. [b]Catalyst from ”reuse” study. NA: Not applicable.

Chapter 7

Effect of Macromolecular Ratios on Biofuel Precursor Formation and Catalytic Activity

7.1 Introduction

Algae possess a multitude of varying macromolecular compositions, in terms of the type and amount of each of lipids, proteins, and carbohydrates. It can be assumed the interactions between these macromolecular compounds and their degradation products have a substantial effect on the quality and composition of the biocrude subsequently generated. Since algal strains are relatively set in their biochemical compositions (noting that nutrient deficient growth can trigger lipid accumulation, for example), a method is needed for systematically determining the effect of these macromolecular ratios on the biocrude generated and on the activity of the heterogeneous catalysts used in upgrading.

Hydrothermal liquefaction and catalytic hydrodeoxygenation were performed on varying ratios of macromolecules in accordance with Table 4.4 on page 64 under reaction conditions that mimic those used on whole algae cells. The products from these macromolecular mixtures were extracted and analyzed in a manner that enabled comparison to whole algae cells.

7.2 Isolated Model Macromolecule Pathway Investigation

7.2.1 Lipid Triglyceride to Saturated Hydrocarbons

Algae lipids are normally generated metabolically in the form of triglycerides: a glycerol backbone containing three fatty acid chains. As stated in Section 3.2, many algal strains produce lipids containing fatty acids in the range of 14 to 20 carbons (see Table 3.1 on page 38). Heated subcritical water possesses the capability to act as an acid catalyst that catalyzes the hydrolysis of many types of bonds. In particular, hydrolysis of triglycerides occurs under these conditions on the bond that joins the carboxylic acid of each fatty acid to the glycerol backbone, thus generating a free fatty acid. For example, hydrolysis of a typical *Spirulina platensis* triglyceride may yield n-hexadecanoic acid (a saturated 16-carbon fatty acid) and oleic acid (a monounsaturated 18-carbon fatty acid).

Free fatty acids such as these have high affinities for decarboxylating catalysts (such as ruthenium). Figure 7.1a illustrates a potential pathway via decarboxylation through which n-hexadecanoic acid could be upgraded heterogeneously (in the presence of hydrogen gas under HDO conditions) to pentadecane, a saturated hydrocarbon. Similarly, dehydration potentially could occur under HTL conditions that utilize free radical hydrogen ions in the heated subcritical water solvent. Figure 7.1b illustrates the pathway through which n-hexadecanoic acid could be twice dehydrated and hydrogenated to form hexadecane.

HTL and HDO experimentation was conducted on palm oil (rich in C16:0 and C18:1$\triangle$9 fatty acids) under the conditions described in Section 4.2. GC/MS performed on the isolated biocrude generated from HTL revealed an abundance of free fatty acids, providing evidence of triglyceride hydrolysis as predicted (Figure 7.2a). Mainly, C16:0 and C18:1$\triangle$9 fatty acids were identified. The biocrude yield from this experimentation was above 100% (with the residual weight from the separation of the aqueous phase), indicating that nearly all of the lipid mass charged to the reactor

was converted to free fatty acids via HTL hydrolysis (Table A.10). Further, HDO on this biocrude fraction demonstrated decarboxylation of the fatty acids to hydrocarbons (Figure 7.2b). GC-TCD analysis of the gas phase revealed substantial carbon dioxide generation: evidence of decarboxylation occurring. 27% of the total head space volume was composed of CO_2. The primary peaks in the HDO biocrude identified by GC/MS were saturated straight-chain hydrocarbons, primarily in the 15-17 carbon range. Hydrocarbons as short as methane (a single carbon compound identified in the gas phase by GC-TCD) and as long as 20+ carbons were identified, signifying cracking and reforming of hydrocarbon chains occurs under these reaction conditions; similarly, branched straight-chain hydrocarbons were observed. In addition, GC/MS identified toluene generation, potentially due to the cyclization of unsaturated shorter-chain hydrocarbons that are intermediates of decarboxylation.

7.2.2 Protein Polypeptide Hydrolysis and Ammonia Generation

Proteins typically found in algal cells are composed of large polypeptide chains composed of amino acids (see Figure 3.5 on page 42). These polypeptide chains are formed through peptide bonds between the carboxylic acid of one amino acid and the amine group of another. Under HTL conditions, subcritical water has an affinity to hydrolyze this peptide bond, generating radical amino acids (Figure 7.3 illustrates this reaction). Further, these amino acids can be deaminated (again, by heated subcritical water) to yield a reactive anion carboxylic acid with its amino acid sidechain, and ammonia: an active reactant that interacts with many of the other compounds present in algae biocrude.

Specifically, GC/MS of biocrude generated from HTL of albumin identified that this ionized carboxylic acid group further reacts with other degradation products and ammonia to form nitrogenated compounds such as pyrrolidinone, piperdine, and propanamine (Figure 7.4a). Moreover, Duan and Savage (2011) demonstrated the conversion of cyclic nitrogenates (specifically pyridine and piperdine) to butane and pentane via catalytic hydrogenolysis and hydrolysis using Pt/γ-Al_2O_3.

GC/MS of upgraded biocrude from albumin after catalytic HDO/HDN using ruthenium identified long chain hydrocarbons, in addition to long-chain amides and nitriles, indicating ammonia present in the reaction mixture interacts strongly with the ion sites mechanized by the catalyst (Figure 7.4b). Several types of nitrogenated aromatics, in addition to traditional aromatics such as styrene, were also formed, likely from the amine disproportionation reaction (Duan and Savage, 2011).

7.2.3 Carbohydrate Polysaccharide Hydrolysis

Carbohydrates found in whole algae cells are typically stored as polysaccharides, mainly starches and starch-derived glucose (see Figure 3.4 on page 41). An oligomeric chain of glucose monomers form starch via α-1,4 glycosidic bonds; under HTL conditions, it is this bond that is first hydrolyzed by subcritical water acting as an acid catalyst (Funazukuri and Nagamori, 2004). Since amylose and amlyopectin starches both are not reducing sugars, no glucose that is a part of the chain can be opened to its straight-chain form. Hydrolyzing and isolating these glucose monomers, however, frees the cyclic molecule for equilibration with its open-chain form. Open-chain glucose is in equilibrium with fructose (an isomer) via the 1,2-enediol anion pathway (Hakim et al., 2013). Figure 7.5 illustrates a potential pathway through which fructose is dehydrated and decarboxylated to form cyclopentanone: a product identified via GC/MS of biocrude generated from HTL of potato starch (Luijkx et al., 1993). Other HTL products identified via GC/MS from HTL of starch include unsaturated hydrocarbons and aromatic hydrocarbons (Figure 7.6a).

Ruthenium catalysts have a high activity towards deoxygenation of ketones, specifically in a hydrogen gas atmosphere. The biocrude from potato starch HTL, when subjected to HDO conditions with Ru/C, reacts favorably with this catalyst to produce a suite of hydrocarbons. Compounds such as n-pentadecane, cyclohexane, BTEX (e.g. benzene), and methyl-naphthalene comprise the majority of the peak area percentage measured via GC/MS (Figure 7.6b).

7.3 Cross Products from Macromolecular Interactions

7.3.1 Fatty Acid and Carbohydrate Hydrolysate Interaction

In addition to the fatty acids, cyclopenten-ones, long chain alkanes, and mono-unsaturated alkenes stemming from the individual model compounds, performing HTL on palm oil and starch together produced a new suite of cross products most easily grouped as long chain cyclic hydrocarbons (such as undecyl-cyclohexane). Upon cleavage of the fatty acid from its glycerol backbone, the carboxylic acid structure is unhydrogenated; an alternative pathway to simple hydrogenation via consumption of water ions involves the redox reaction that could occur between this carboxylic acid and an unsaturated aromatic, such as benzene or cyclohexene. In addition, the relative concentration of unsaturated hydrocarbons in HTL biocrude appears to have increased, according to the GC/MS relative peak areas (Figure 7.7a).

Performing coupled HTL and HDO on this same reaction mixture generated a suite of long-chain ketones (e.g. 9-heptadecanone) in addition to the saturated hydrocarbons found from the model compounds alone. Ruthenium has a high activity to deoxygenate this type of compound, suggesting stereo reactivity restrictions exist between the mid-chain ketone and the oxygen binding site on the catalyst surface. The full suite of compounds generated were identified via GC/MS in Figure 7.7b.

7.3.2 Fatty Acid and Protein Hydrolysate Interaction

The ammonia and ionic amino acid products generated from the hydrolysis and hydrogenolysis of protein and amino acids showed a very high activity for reacting with the cleavage site of fatty acids during glyceride hydrolysis. GC/MS of biocrude generated from HTL of palm oil and albumin protein revealed that, in addition to the expected fatty acid and nitrogenated aromatics generated from isolated macromolecules, a new suite of long-chain nitrogenates was formed (Figure

7.8a). The relative peak area of fatty acids decreased, as fatty acids interacted to form long-chain amides and nitriles. Other cross-products identified include branched pyridines, pyrroles, and indoles.

Performing HDO on this biocrude revealed the catalyst complex being used does not have a high affinity for denitrification of this type; many of the nitrogenated compounds present in the HTL biocrude persisted through the HDO stage and were identified again via GC/MS after the stage was conducted (Figure 7.8b). In addition, some long-chain alcohols were formed during HDO (1-pentadecanol). This compound is likely an intermediate from the decarboxylation of a free fatty acid, suggesting the presence of protein inhibits the catalytic activity for decarboxylation of compounds of this type. Further indications of this inhibition are provided from the catalyst characterization reported in Section 7.4 and in Table 7.1.

7.3.3 Amino Acid and Carbohydrate Hydrolysate Interaction (Maillard)

The pathway through which many cyclic nitrogenates are formed from protein and carbohydrates is complicated and not well understood. Andrew A. Peterson (2010) performed some experimentation on a reaction scheme called the Maillard Reaction, through which amino acids and sugars react to form high molecular weight polymers (melanoidins) in addition to the suite of low weight compounds. In his work, he showed that D-glucose and glycine react to ultimately form melanoidins, most easily identified by their brown color, nutty odor, and UV photometric absorption (approx. 250 nm). The beginning of the melanoidin pathway investigated by Andrew A. Peterson (2010) is shown in Figure 7.9. D-glucose and glycine first dehydrate and bond to form N-substituted glycosamine. Glycosamine is then isomerated to form the Amadori compound, which acts a precursor for further dehydration to furfurals, aldehydes, reductones, and melanoidins. In addition, performing HTL on these two macromolecules generates cyclic nitrogenates, such as pyridine and pyrazine, as identified by GC/MS (Figure 7.10). The generation pathway for these types of compounds requires further investigation, but one potential pathway resulting in pyri-

dine from carbohydrate and amino acid degradation products is proposed in Figure 7.11 via the Bohlmann-Rahtz reaction pathway. Condensation of enamines with ethynylketones leads to an aminodiene intermediate that undergoes a cyclodehydration to yield 2,3,6-trisubstituted pyridines.

HDO performed on this mixture was unsuccessful. The biocrude product generated from coupling HDO with HTL was highly miscible with the water present in the reaction medium, and was inseparable by typical extraction means. Additional organic solvents (e.g. hexane) did not improve this issue. Difficulties in separation techniques may provide evidence for biocrude composition composed mainly of water soluble compounds, indicating incomplete deoxygenation and upgrading. Perhaps the Maillard compounds formed during HTL are not active on ruthenium; further, perhaps the compounds that are catalytically active ultimately end up interacting to form different melanoidin compounds.

7.3.4 Interaction of Three Macromolecules

In addition to the compounds generated through HTL of either isolated or paired macromolecules, performing the conversion of lipid, protein, and carbohydrate in one reaction mixture produced long chain fatty acid methyl esters (C16:0 *FAME*). No additional products were seen following HDO, suggesting the fatty acid methyl esters can be decarboxylated and upgraded to saturated hydrocarbons via a similar mechanism as traditional fatty acids (see Figure 7.12).

It can be noted in Figure 7.12b, that illustrates the biocrude composition after coupled HTL and HDO, that the long chain amides have been removed or upgraded. This is likely due to the effect the macromolecular ratio has on the HTL biocrude composition. For example, increasing the initial lipid ratio generates more free fatty acids following HTL, which are available for cross-reactions with ammonia generated from the hydrolysis of proteins. Ruthenium may only have a partial affinity for deamination of compounds of this type, meaning it would be more favorable to fully convert and eliminate the amide cross products if their starting concentrations were lessened.

7.4 Catalytic Activity and Characterization from Varying Macromolecular Ratios

The full characterization of the catalysts utilized for this series of experimentation can be found in Table 7.1. In this table, catalyst coking, taring, and characterization (via Quantachrome analytics) are shown. Since coking was measured via TGA combustion in the presence of air on a catalyst with a carbon-based support, a temperature-programmed control run was performed on untreated Ru/C to determine the mass loss from the catalyst support alone. This measurement was then used to extrapolate the true coking weight and percentage from the total mass loss measured on the catalyst samples via TGA (which also have carbon supports).

The highest coke percentage was found to have been generated by conversion of isolated carbohydrates, at 5.34%. This is agreeable with the solid yield found from this same reaction mixture (Table A.10), indicating carbohydrates such as starch are not ideally suitable for direct conversion to liquid fuels. The next largest coking amount was found in isolated proteins (2.59%), possibly leading to catalyst deactivation and explaining the decrease in catalytic deoxygenation and denitrogenation properties (thus leading to a less quality biocrude). Further, the amide and nitrile cross-products stemming from the interaction between lipids and proteins also caused a significant amount of coking (2.03%), indicating that catalyst deactivation occurs from the cross-products involving proteins as well as the isolated protein compounds. Many of the mixtures showed no coking, indicating any residual mass added to the catalyst surface from the conversion could be removed by solvent rinsing, and is thus considered tar.

The highest tar percentages were found in representations involving mixtures of lipids and proteins, with the lipid content more closely correlating (proportionally) to the tar amount. The representation involving equal parts of each macromolecule had a tar content of 26%, followed by the *Nannochloropsis sp.* representation at 17.7%. The lowest tar content was measured in paired

mixtures without protein (lipids and carbs., 4.1%) and without lipids (proteins and carbs., 3.6%), suggesting interactions with carbohydrates can actually reduce the amount of tar present on the catalyst surface (as compared to 6.8 and 9.6% in lipid only and protein only, respectively). On the catalyst used for the repeated batch conversion of whole *Nannochloropsis* cells, only 6% tar (by weight) was observed. Perhaps the individual model compounds interact in a way that is more susceptible to taring since they do not have cell wall inhibitions. It is unlikely, but perhaps the cell walls themselves interact with the bio-oil to prevent taring by driving the reaction composition towards the biocrude phase.

Table 7.1 also provides the catalyst characterization data, including average pore size, total pore volume, and surface area: all key indicators of catalytic activity. Unsurprisingly, all used catalysts showed a decrease in surface area as compared to the unused control. Isolated lipids retained the highest amount of surface area, showing a decrease of only 12.4%. All other catalysts observed showed a decrease in surface area of at least 67%, with isolated carbohydrates causing the most significant decrease in surface area (a decrease of 81.2%). There was no significant correlation between coking, taring, and surface area.

7.5 Figures and Tables

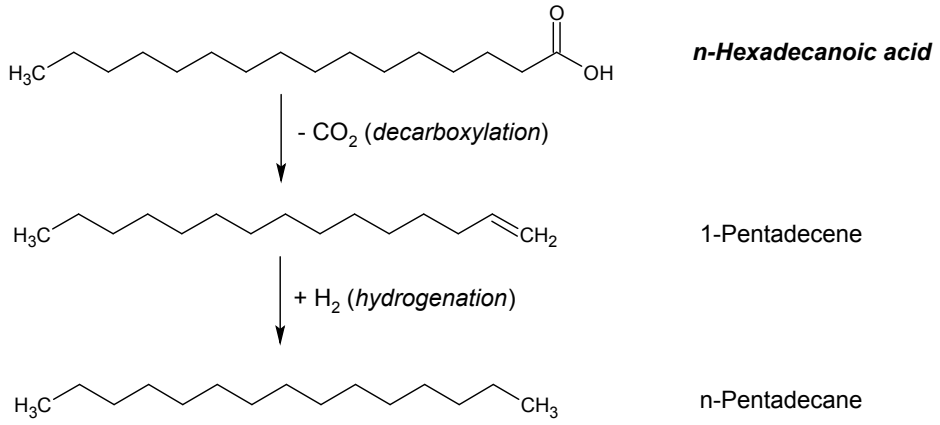

(a) Conversion via decarboxylation.

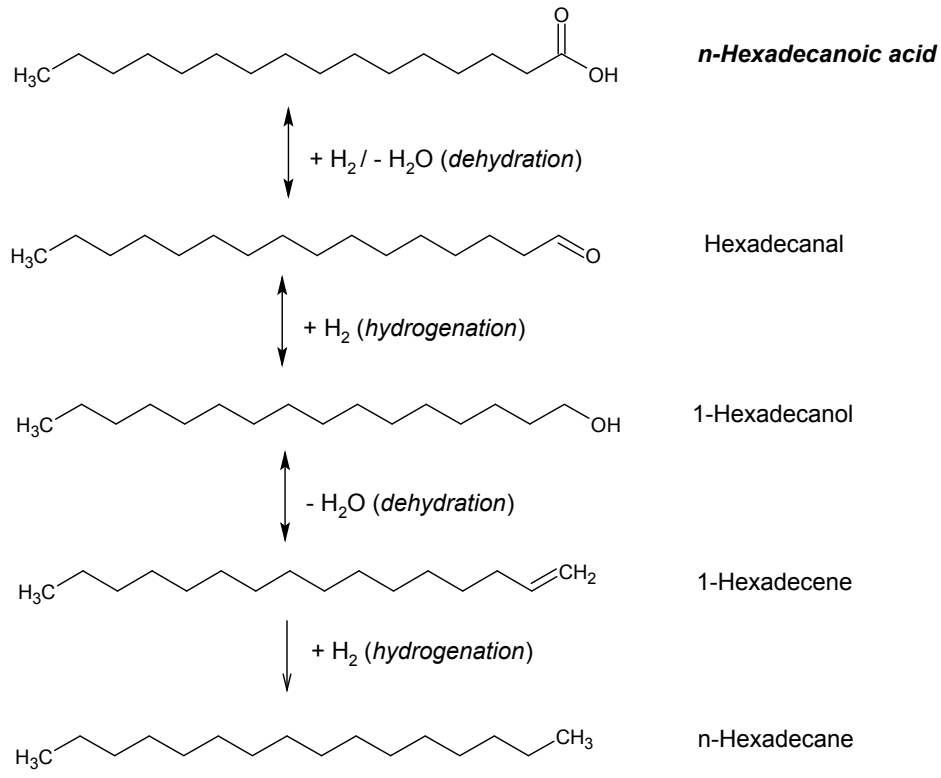

(b) Conversion via dehydration.

Figure 7.1: Potential pathways for conversion of n-hexadecanoic acid to saturated hydrocarbons.

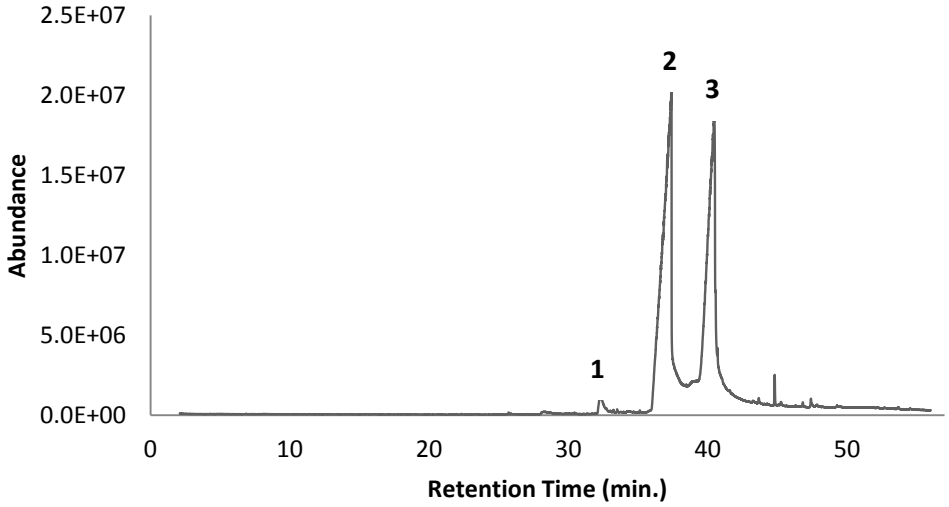

(a) Conversion via HTL only.

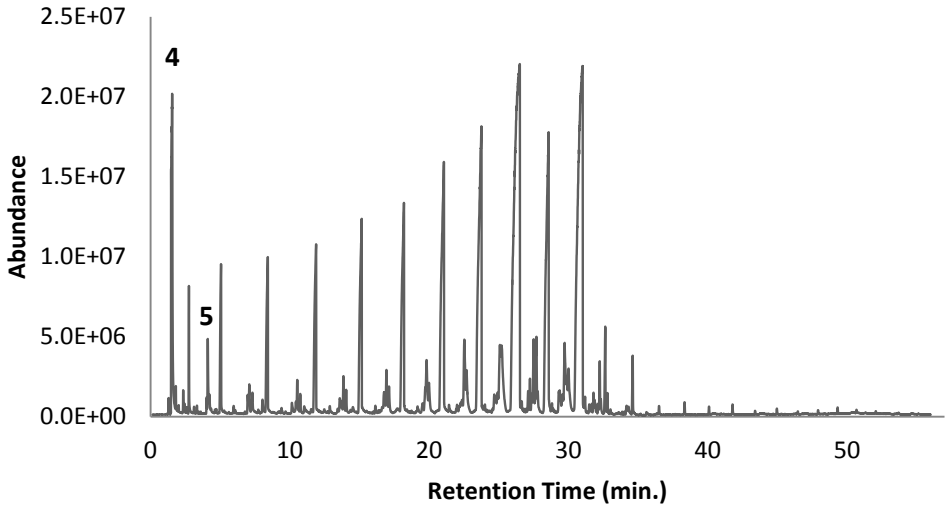

(b) Conversion via coupled HTL and HDO. Unlabeled, isolated, sharp peaks are n-C# hydrocarbons (C7-C26+), with the largest three being C15-C17. Low peak formations are mainly branched hydrocarbons and long-chain cyclopentanes or benzenes.

Figure 7.2: GC/MS chromatograms for biocrude generated from conversion of lipids.

Identified compounds are (1) myristic acid (C14:0), (2) palmitic acid (C16:0), (3) oleic acid (C18:1$\triangle$9), (4) carbon dioxide, (5) toluene.

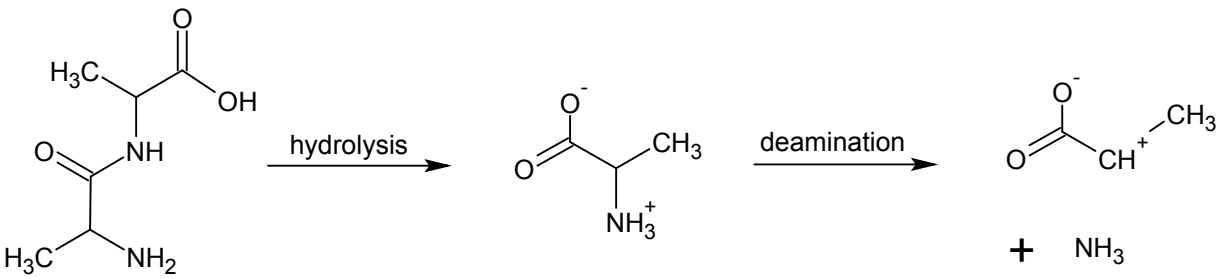

Figure 7.3: Dipeptide (two alanine amino acids) hydrolysis and deamination.

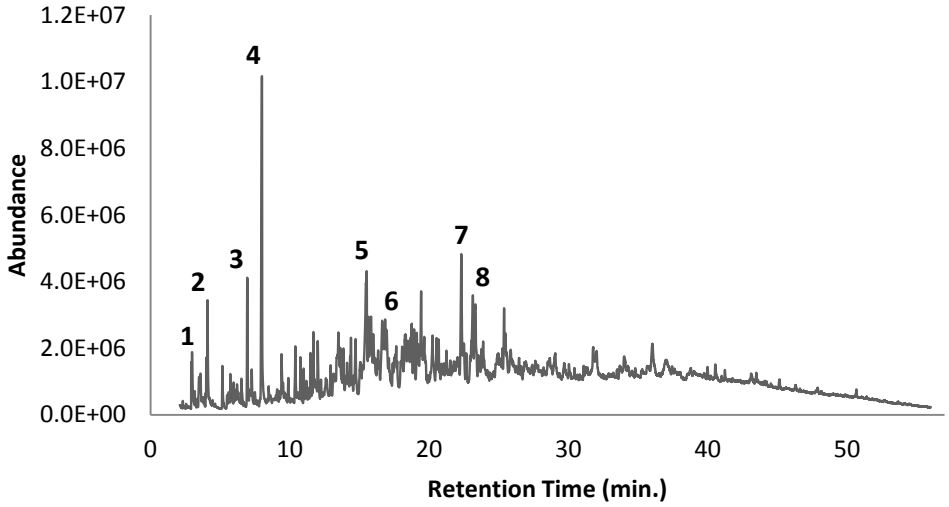

(a) Conversion via HTL only.

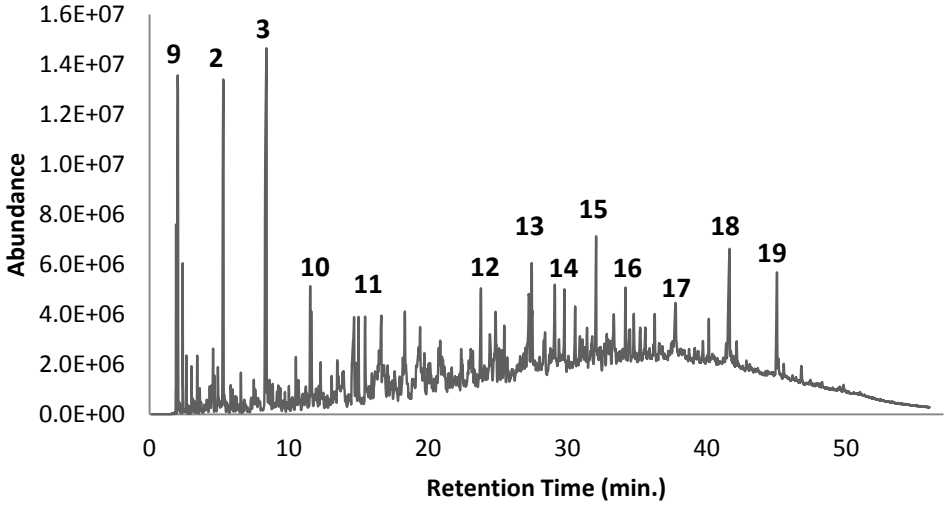

(b) Conversion via coupled HTL and HDO.

Figure 7.4: GC/MS chromatograms for biocrude generated from conversion of proteins.

Identified compounds are (1) 2-methyl-butylamine, (2) toluene, (3) ethyl benzene, (4) styrene, (5) 1-propyl-2-pyrrolidinone, (6) methylbutanamide, (7) methyl-piperidine, (8) 1-propyl-pyrrolidin-2,5-dione, (9) carbon dioxide, (10) 1-methyl-2-pyrrolidinone, (11) 4-methylphenol, (12) N-containing polyaromatic, (13) pentadecane, (14) hexadecane, (15) heptadecane, (16) octadecane, (17) hexadecanenitrile, (18) hexadecanamide, (19) octadecanamide.

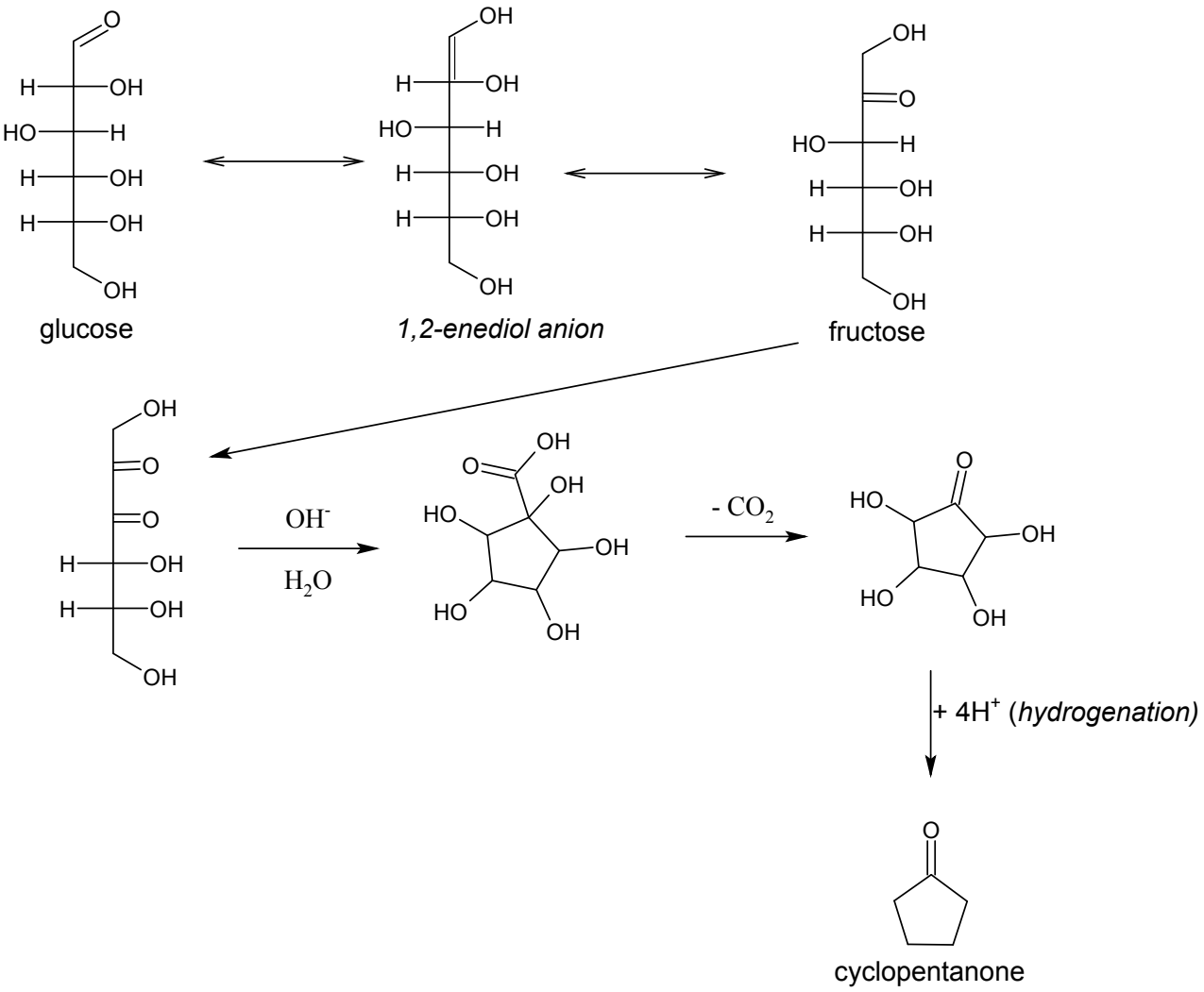

Figure 7.5: Potential pathway for glucose conversion to cyclopentanone via isomerization, dehydration, and decarboxylation.

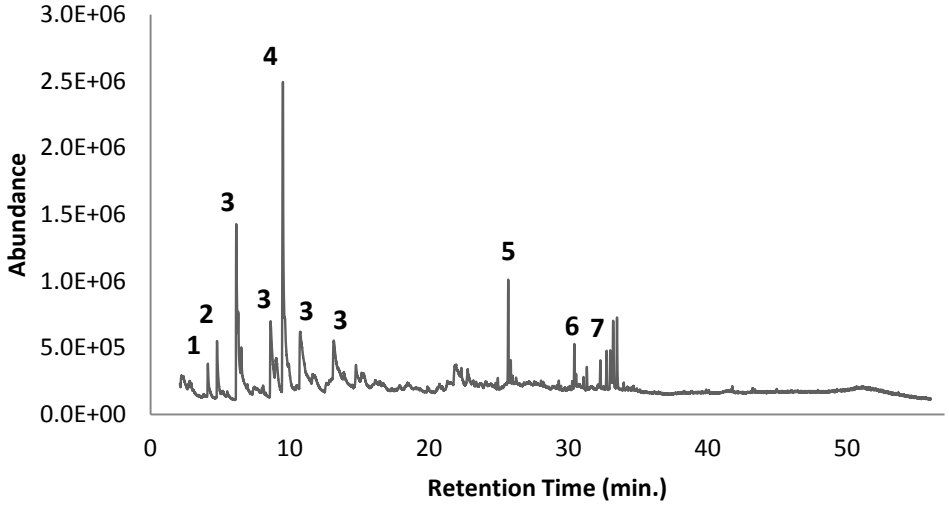

(a) Conversion via HTL only.

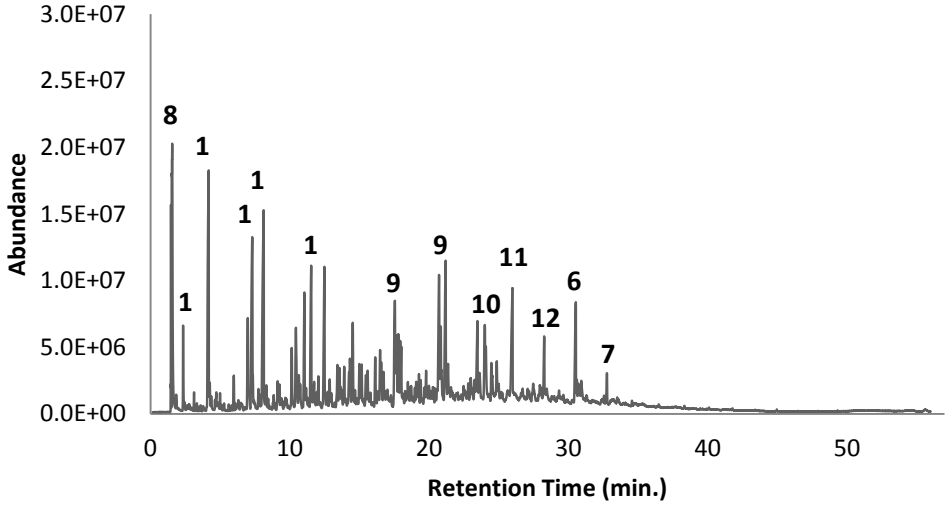

(b) Conversion via coupled HTL and HDO.

Figure 7.6: GC/MS chromatograms for biocrude generated from conversion of carbohydrates.

Identified compounds are (1) BTEX, (2) cyclopentanone, (3) (methyl)-cyclopentene-1-one, (4) acetonyl acetone, (5) 1-pentadecene, (6) heptadecane, (7) phytane, (8) acetone, (9) (methyl)-naphthalene, (10) tetradecane, (11) pentadecane, (12) hexadecane.

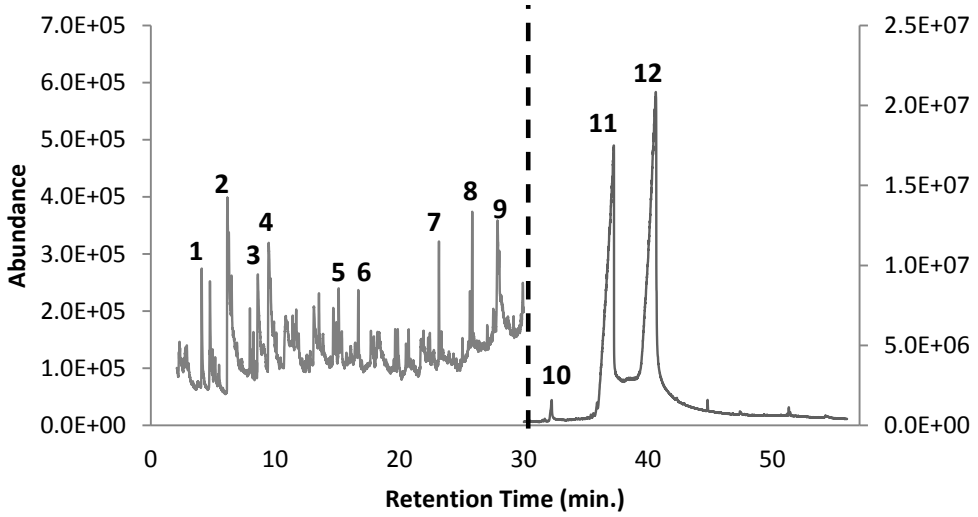

(a) Conversion via HTL only.

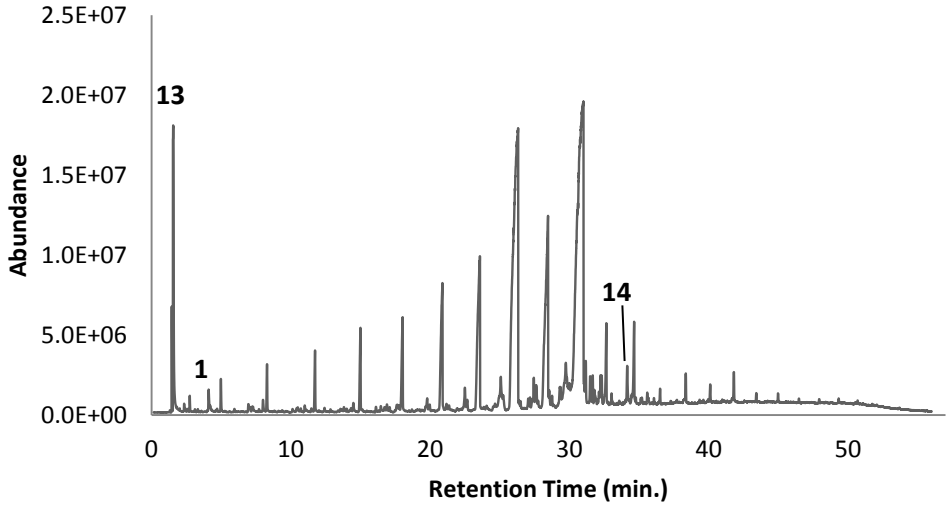

(b) Conversion via coupled HTL and HDO. Unlabeled, isolated, sharp peaks are n-C# hydrocarbons (C7-C26+), with the largest three being C15-C17. Low peak formations are mainly branched hydrocarbons and long-chain cyclopentanes or benzenes.

Figure 7.7: GC/MS chromatograms for biocrude generated from conversion of lipids and carbohydrates.

Identified compounds are (1) toluene, (2) cyclopentanone, (3) cyclopentene-one, (4) acetonyl acetone, (5) 5-undecene, (6) pentylbenzene, (7) 2-tetradecane, (8) pentadecane, (9) lauric acid (C12:0), (10) myristic acid (C14:0), (11) palmitic acid (C16:0), (12) oleic acid (C18:1△9), (13) carbon dioxide, (14) 9-heptadecanone.

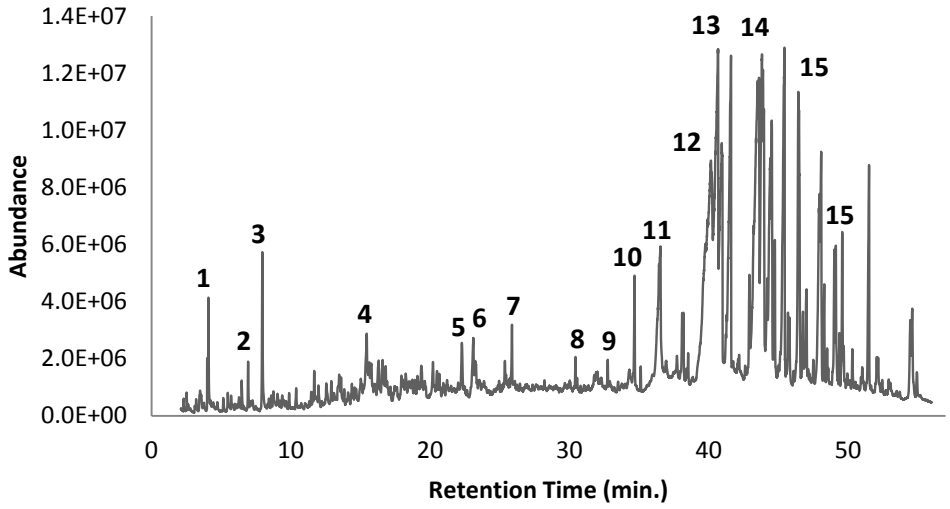

(a) Conversion via HTL only.

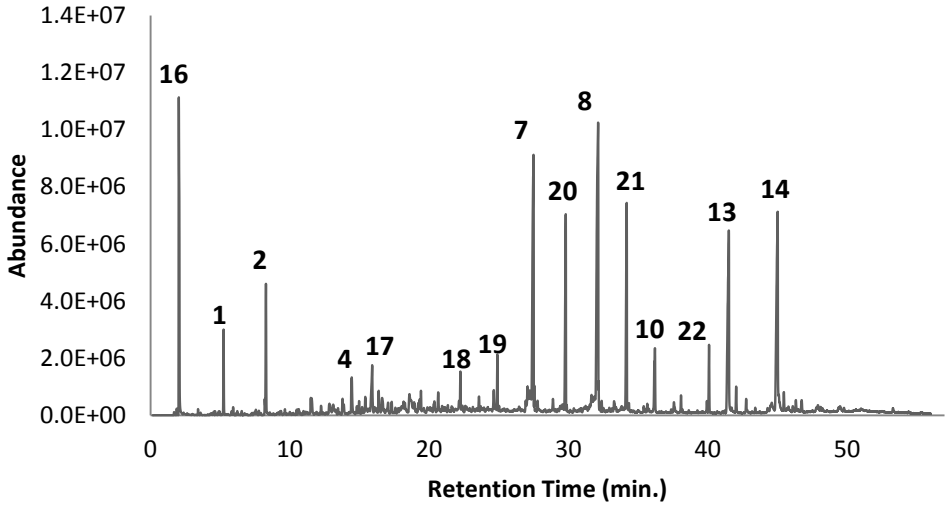

(b) Conversion via coupled HTL and HDO.

Figure 7.8: GC/MS chromatograms for biocrude generated from conversion of lipids and proteins.

Identified compounds are (1) toluene, (2) ethyl benzene, (3) cyclooctatetraene, (4) pyrrolidinone, (5) pyrrole, (6) indole, (7) pentadecane, (8) heptadecane, (9) phytane, (10) pentadecanenitrile, (11) palmitic acid (C16:0), (12) oleic acid (C18:1△9), (13) hexadecanamide, (14) octadecanamide, (15) C18 oxo-pyrrolidine, (16) carbon dioxide, (17) methylphenol, (18) tridecane, (19) tetradecane, (20) hexadecane, (21) octadecane, (22) octadecanenitrile.

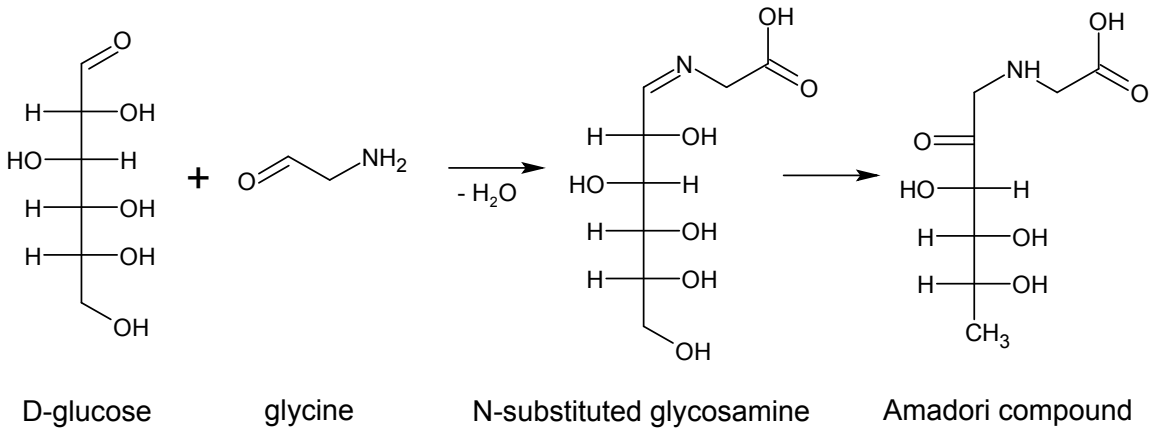

Figure 7.9: Proposed reaction between D-glucose and glycine to form Maillard reaction intermediates (adapted from Andrew A. Peterson (2010)).

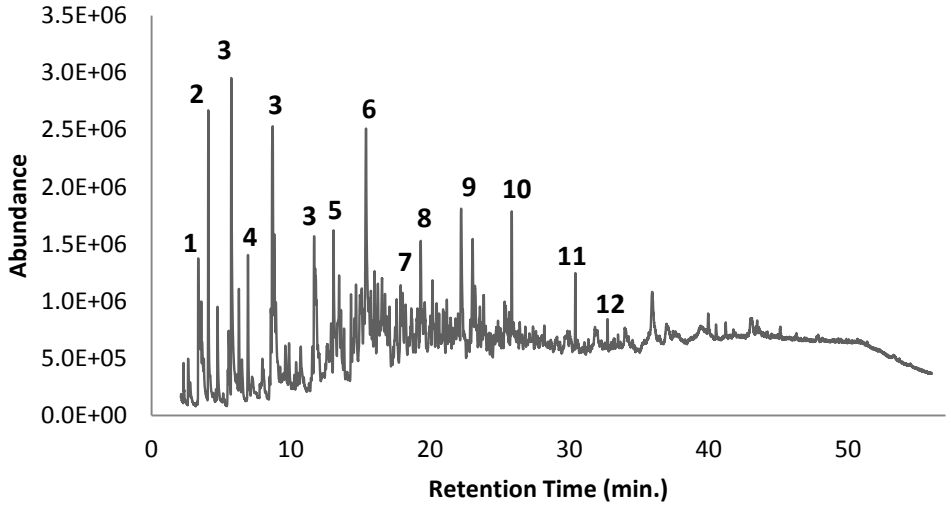

Figure 7.10: GC/MS chromatograms for biocrude generated from HTL only conversion of carbohydrates and proteins.

HDO was unsuccessful for this reaction mixture. Identified compounds are (1) pyrazine, (2) toluene, (3) branched pyrazine, (4) ethyl benzene, (5) methyl-cyclopentanone, (6) 1-propyl-2-pyrrolidinone, (7) 2-ethyl-3,4,5-trimethyl-1H-pyrrole, (8) 1-methylpiperidine, (9) 1-ethyl-6-methyl-3-piperidinone, (10) pentadecane, (11) heptadecane, (12) phytane.

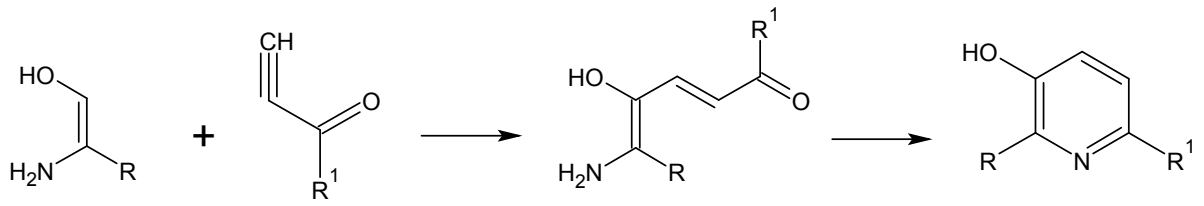

Figure 7.11: Bohlmann-Rahtz reaction pathway from carbohydrate and protein hydrolysates to pyridine.

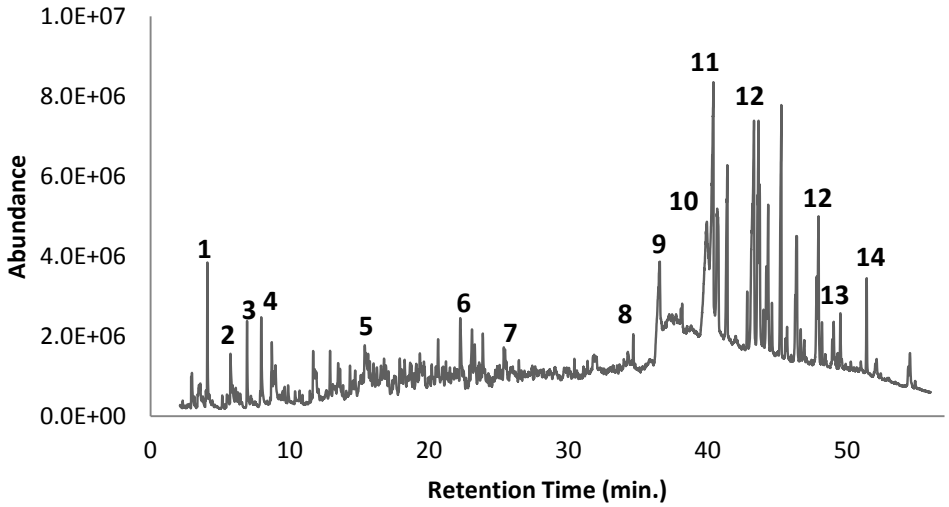

(a) Conversion via HTL only.

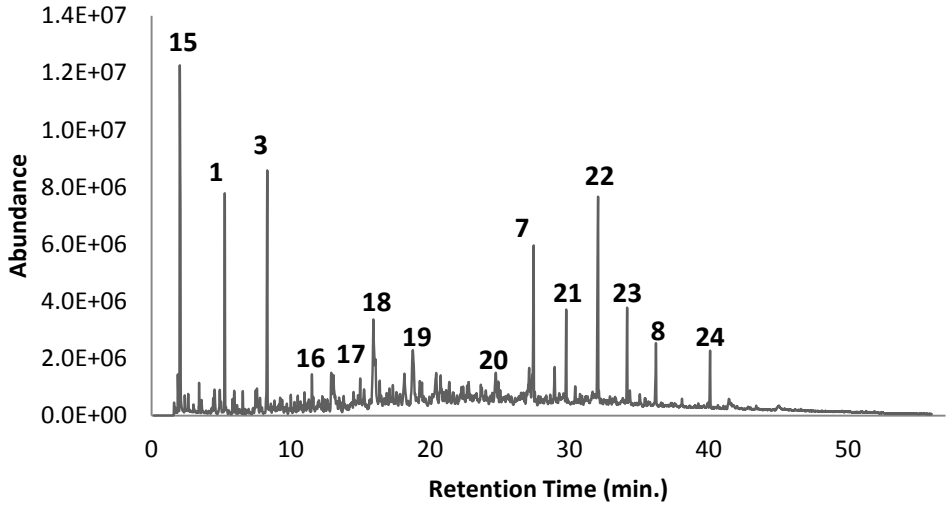

(b) Conversion via coupled HTL and HDO.

Figure 7.12: GC/MS chromatograms for biocrude generated from conversion of lipids, carbohydrates, and proteins.

Identified compounds are (1) toluene, (2) 2-methylpyrazine, (3) ethyl benzene, (4) styrene, (5) 1-propyl-2-pyrrolidinone, (6) methylpiperidine, (7) pentadecane, (8) pentadecanenitrile, (9) palmitic acid (C16:0), (10) oleic acid (C18:1△9), (11) hexadecanamide, (12) octadecanamide, (13) C18 oxo-pyrrolidine, (14) phenylethyl ester fatty acid, (15) carbon dioxide, (16) branched pyridine, (17) branched pyrrolidinone, (18) methylphenol, (19) ethylphenol, (20) tetradecane, (21) hexadecane, (22) heptadecane, (23) octadecane, (24) octadecanenitrile.

Table 7.1: Catalyst coking, taring, and characterization for two-stage conversion (HTL and HDO) using model compound mixtures.

Representation	Coking[a] (%, w/w)	Tar (%, w/w)	Average Pore Size (Radius, Å)	Total Pore Volume ($cm^3\ g^{-1}$)	Surface Area ($m^2\ g^{-1}$)
Untreated Ru/C Control	NA	NA	11.37	0.4100	721.4
Only Lipid	0.59	6.80	15.27	0.2410	631.6
Only Carb.	5.34	8.87	18.50	0.0625	135.3
Only Protein	2.59	9.57	13.46	0.0807	239.8
No Protein	-7.82	4.12	13.44	0.0694	206.6
No Carb.	2.03	11.94	ND	ND	ND
No Lipid	1.18	3.57	ND	ND	ND
Equal Parts	-0.71	25.95	ND	ND	ND
Spirulina platensis	-0.87	6.91	11.98	0.0514	171.6
Nannochloropsis sp.	0.41	17.71	ND	ND	ND

[a]Determined compared to the mass loss of the control catalyst. NA: Not applicable, ND: Not determined.

Chapter 8

Conclusions and Recommendations

8.1 Conclusions

The work presented here demonstrates the capacity for algae to be used as a widescale feedstock for liquid fuel production. The biocrude nitrogen content, which is a critical barrier in the production of algae-based fuel intermediates because of the high protein content algae naturally possesses, was overcome using a low temperature liquefaction technique that excluded the use of external materials that would potentially require additional separation techniques. This low temperature pretreatment partitioned nitrogen out of the solid phase, which would ultimately be converted to biocrude, in a manner that enabled nutrient recycling through separation and recovery of the aqueous phase. Further, the biocrude resulting from HTL of the pretreated biomass was successfully upgraded using varying types of catalysts, with the highest quality and most favorable elemental composition being achieved through ruthenium (5%, on carbon). Results indicated that refreshing the reaction headspace with an additional aliquot of hydrogen gas drove the kinetics of heterogeneous catalysis further towards a high quality biocrude, characterized in its composition mainly by straight-chain hydrocarbons (e.g. n-pentadecane). These hydrocarbons, comprising the

vast majority of the total peak area found via GC/MS of the upgraded biocrude, were suitable for direct distillation and co-processing with gas oils normally used by liquid fuel refineries.

Chapter 5: Evaluation of Low Temperature Hydrothermal Liquefaction of Algae for Low Nitrogen Biocrude Generation and Nutrient Recycling Potential

The results indicate that nitrogen removal can be achieved through low temperature hydrothermal liquefaction. An increase in temperature and in the heating rate corresponded to an increase in nitrogen partitioning across all strains; the amount partitioned was moderately independent of reaction duration, with higher durations corresponding to increased partitioning. The amount of solids retained was inversely related to the amount of nitrogen partitioned. It was demonstrated that the addition of the pretreatment caused a quality improvement in the composition of the biocrude subsequently produced via HTL. In addition, the aqueous co-product generated from the pretreatment stage contains ample nutrients and minimal inhibitory compounds, making it suitable for algae cultivation.

Chapter 6: Effect of Low Temperature Hydrothermal Liquefaction on Catalytic Hydrodeoxygenation/Hydrodenitrogenation of Algae Biocrude

A four-stage conversion process was implemented to make a refinery-grade intermediate feedstock from algae more effectively that any other stage combination. Low- and high-temperature hydrothermal liquefaction with catalytic hydrodeoxygenation produced a low nitrogen biocrude. Ruthenium on carbon achieved the greatest desired results, reducing heteroatom levels and producing oil with the highest long chain and aromatic hydrocarbon content. Significant decreases in catalyst surface area and pore volume were observed with use in catalytic HDO, more so on catalysts with greater initial values of these characteristics. The extent of reaction was limited by low hydrogen concentrations stemming from the consumption of this reactant in a batch atmosphere.

8.2 Recommendations

The biocrude as a whole, however, did not meet the elemental requirements for nitrogen and oxygen required by refineries. One potential reason for the limits of hydrodeoxygenation is the concentration of hydrogen that can be presented to the reaction mixture in a batch configuration. In addition, having batch reactors in series is not a valid approach for industrial scale generation of algae biocrude due to the time-limited nature of reactant and product removal and reactor cleaning and setup.

A solution to these issues would be to perform the four-stage conversion process described on a continuous basis (Elliott et al., 2013; Jazrawi et al., 2013). Figure 8.1 illustrates all of the required stages through which algae can be feasibly grown, harvested, and converted to liquid fuel precursors. It can be seen that there are a multitude of unit operations that must work in tandem in order for the process as a whole to be smooth and effective. A continuous process may look like the following:

Algae is grown continuously through raceway ponds operating similar to a CSTR, or with several raceway ponds in parallel on different points in the growth cycle. The algae slurry is then passed through a continuous centrifuge used to both reduce the water content of the slurry to approximately 20% and to recycle the water not needed for conversion solvents. The slurry is then converted to biocrude using two continuous tubular reactors operating at high temperature and pressure, with a continuous centrifuge in between (for separating the nitrogen-rich aqueous phase from the pretreatment stage). The biocrude slurry is then passed through a tubular packed bed reactor that has a bed packed with catalyst in order to be upgraded. The product from this reactor is then phase separated using solvent extraction, filtration, centrifugation, and solvent evaporation (all on a continuous basis). The isolated upgraded biocrude is then ready for storage or for co-processing with existing refinery feedstocks.

8.3 Figures and Tables

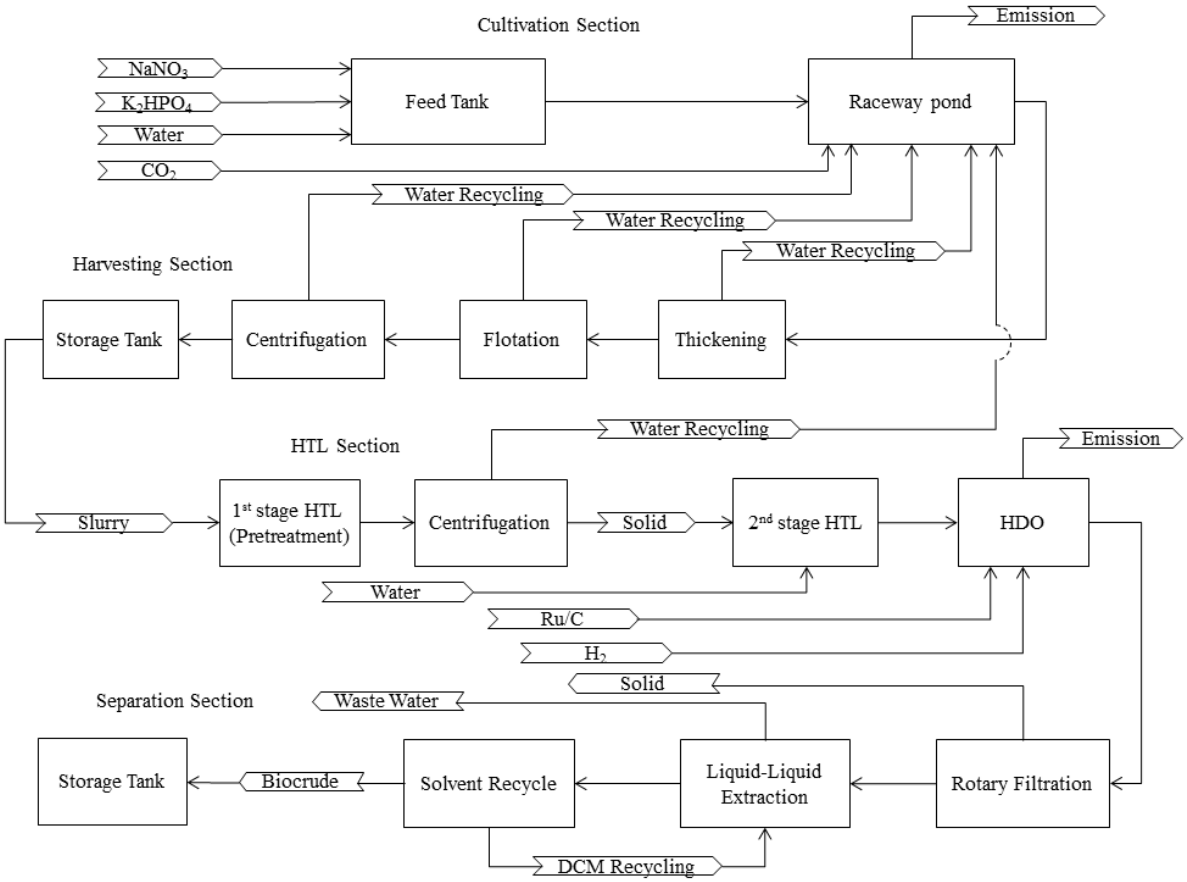

Figure 8.1: Simplified process schematic for the overall growth and conversion process of algae to liquid fuel precursors.

Appendix A

Yield Data

Table A.1: Yield data for stage 1 pretreatment (PT) of *Nannochloropsis*.

Yields given as percentage of initial slurry, unless specified.

Stage 1 Conditions		Gas Phase		Aqueous Phase		Solid Phase						Losses	
Temp	Duration	Wt	Yield	Wt	Yield	Wet Solid		Dry Solid			Est. Water Content[a]	Wt	Yield
(°C)	(min)	(g)	(%)	(g)	(%)	Wt (g)	Yield (%)	Wt (g)	Yield (%)	Yield (% DAF feed)	(%)	(g)	(%)
125	0.5	0	0	19.6	50.3	16.9	43.3	5.5	14.1	79.6	67.5	2.5	6.4
125	1	0	0	16.6	42.5	18.5	47.3	5.3	14.2	76.0	71.6	4	10.2
125	2.5	0	0	18.8	48.1	17.1	43.7	5.3	13.6	76.6	69.1	3.2	8.2
125	5	0	0	19.1	48.8	17.1	43.7	5.2	13.4	75.7	69.4	2.9	7.4
125	10	0	0	19.6	50.1	16.8	43.0	5.3	13.5	76.1	68.7	2.7	6.9
125	15	0	0	19.3	49.5	16.7	42.8	5.1	13.1	74.0	69.4	3	7.7
175	0.5	0.6	1.5	21.6	55.7	13.9	35.8	4.1	10.0	59.3	70.5	3.3	8.5
175	1	0.9	2.3	20.3	51.7	16	40.7	4.6	11.8	66.0	71.5	3	7.6
175	2.5	1.1	2.8	20.5	52.4	15.2	38.9	4.4	11.5	63.8	71.0	3.4	8.7
175	5	1	2.6	21.7	55.5	14.5	37.1	4.1	10.6	59.6	71.6	2.9	7.4
175	10	0.9	2.3	20.6	52.8	14.4	36.9	3.8	9.8	54.4	73.9	4	10.3
175	15	0.8	2.0	21	53.7	15.3	39.1	4.0	10.2	57.6	74.0	2.8	7.2
225	0.5	0	0	26.9	68.8	10.3	26.3	3.9	10.1	55.7	62.6	1.9	4.9
225	1	0	0	26	66.5	10.5	26.9	3.6	9.4	52.4	65.5	2.6	6.6
225	2.5	0.1	0.3	27.3	69.8	9.9	25.3	3.2	8.5	46.9	67.3	1.8	4.6
225	5	0	0	27.6	69.0	11.2	28.0	3.4	9.1	49.1	69.7	1.2	3.0
225	10	0	0	29.4	75.4	8.3	21.3	3.3	8.7	47.2	60.7	1.3	3.3
225	15	0.1	0.3	31.4	80.5	5.7	14.6	2.8	6.9	39.9	51.6	1.8	4.6

[a] 1-(dry solid weight / wet solid weight).

Table A.2: Yield data for stage 1 pretreatment (PT) of *UGA Consortium*.

Yields given as percentage of initial slurry, unless specified.

Stage 1 Conditions		Gas Phase		Aqueous Phase		Solid Phase					Losses	
Temp	Duration	Wt	Yield	Wt	Yield	Wet Solid		Dry Solid		Est. Water Content[a]	Wt	Yield
(°C)	(min)	(g)	(%)	(g)	(%)	Wt (g)	Yield (%)	Wt (g)	Yield (% DAF feed)	(%)	(g)	(%)
125	0.5	0	0	9.7	24.9	24.7	63.3	5.5	91.4	77.8	4.6	11.8
125	1	0.1	0.3	12	32.4	24	64.9	5.3	88.3	78.0	0.9	2.4
125	2.5	0	0	11	28.2	24.6	63.1	5.6	93.6	77.2	3.4	8.7
125	5	0	0	10.7	27.4	24.2	62.1	5.3	88.8	78.0	4.1	10.5
125	10	0	0	9.9	25.4	25.4	65.1	5.8	96.6	77.2	3.7	9.5
125	15	0.1	0.3	10.3	26.4	24.6	63.1	5.5	92.4	77.5	4.0	10.3
175	0.5	ND	ND	11.2	27.3	24.2	58.9	5.2	86.1	78.7	5.6	13.9
175	1	ND	ND	11.9	30.9	24.3	63.1	5.4	89.8	77.9	2.3	6.0
175	2.5	ND	ND	11.5	29.9	24.4	63.5	5.4	89.8	78.0	2.5	6.5
175	5	ND	ND	12	30.9	23.5	60.6	5.1	84.3	78.5	3.3	8.5
175	10	ND	ND	11.5	30.0	23.5	61.4	5.0	83.3	78.8	3.3	8.6
175	15	ND	ND	12.8	32.8	23	59.0	4.9	82.1	78.6	3.2	8.2
225	0.5	0.7	1.8	14.9	39.0	20.7	54.2	4.5	75.1	78.3	1.9	5.0
225	1	0.5	1.3	17.2	44.4	20.2	52.2	4.5	74.9	77.8	0.8	2.1
225	2.5	1	2.6	16.5	43.5	20.1	53.0	4.4	73.1	78.2	0.3	0.8
225	5	0.5	1.3	17.4	46.5	19.3	51.6	4.4	74.1	77.0	0.6	0.5
225	10	0.7	1.9	18.7	49.7	17.6	46.8	4.1	69.1	76.5	0.6	1.6
225	15	1	2.5	20.8	51.7	16.9	42.0	4.1	68.9	75.6	1.5	3.7

[a]1-(dry solid weight / wet solid weight).

Table A.3: Yield data for stage 1 pretreatment (PT) of *Spirulina*.

Yields given as percentage of initial slurry, unless specified.

Stage 1 Conditions		Gas Phase		Aqueous Phase		Solid Phase					Losses	
Temp	Duration	Wt	Yield	Wt	Yield	Wet Solid		Dry Solid		Est. Water Content[a]	Wt	Yield
(°C)	(min)	(g)	(%)	(g)	(%)	Wt (g)	Yield (%)	Wt (g)	Yield (%)	(%)	(g)	(%)
125	1	ND	ND	17.5	43.8	20.3	50.8	6.5	16.1	68.2	2.2	5.5
125	2.5	ND	ND	18.3	47.8	18.5	48.3	6.2	16.3	66.3	1.5	3.9
125	5	0.1	0.3	9.4	25.1	24	64.2	4.7	12.6	80.3	3.9	10.4
125	10	ND	ND	7.1	18.9	26.6	70.9	5.4	14.3	79.8	3.8	10.1
125	15	0.4	1.0	13.5	34.5	21.1	54.0	5.1	13.1	75.7	4.1	10.5
125	30	ND	ND	11.8	30.3	24.3	62.3	5.9	15.0	75.9	2.9	7.4
175	1	1.6	4.1	13.3	34.1	24.6	63.1	5.7	14.6	76.8	0.5	1.2
175	2.5	ND	ND	17.9	45.9	20.4	52.3	5.1	13.0	75.2	0.7	1.8
175	5	0.2	0.5	15.7	41.8	20	53.2	4.5	11.9	77.6	1.7	4.5
175	10	0	0.0	16.7	43.6	20.1	52.5	3.8	10.0	81.0	1.5	3.9
175	15	0.1	0.3	15.8	40.5	21	53.8	4.8	12.3	77.1	2.1	5.4
175	30	ND	ND	18.1	46.2	18.8	48.0	4.2	10.8	77.6	2.3	5.9
225	1	ND	ND	20.8	53.3	16.3	41.8	3.9	9.9	76.4	1.9	4.9
225	2.5	ND	ND	23	59.0	14.9	38.2	3.6	9.1	76.2	1.1	2.8
225	5	ND	ND	24.1	65.0	11.2	30.2	2.9	7.8	74.0	1.8	4.9
225	10	0.3	0.8	26.1	69.8	10.3	27.5	2.7	7.2	74.0	1	2.7
225	15	0.5	1.3	28.4	72.8	8.9	22.8	2.8	7.1	69.0	1.2	3.1
225	30	0.4	1.0	30.6	78.7	6.1	15.7	2.1	5.5	65.1	1.8	4.6

[a] 1-(dry solid weight / wet solid weight).

Table A.4: Yield data for two-stage PT/HTL of three algal strains after HTL stage.

Yields given as percentage of initial slurry, unless specified.

Stage 1 Conditions		Oil Phase			Gas Phase and Losses		Aqueous Phase		Solid Phase				
Temp	Duration	Wt	Yield		Wt	Yield	Wt	Yield	Wet Solid		Dry Solid		Est. Water Content[a]
(°C)	(min)	(g)	(%)	(% DAF feed)	(g)	(%)	(g)	(%)	Wt (g)	Yield (%)	Wt (g)	Yield (% DAF feed)	(%)
UGA Consortium													
125	0.5	1.2	4.6	19.9	2.5	5.3	39.6	84.5	3.6	14.0	0.8	16.7	78.8
125	1	1.1	2.4	17.5	2.7	6.1	38.0	85.5	2.7	10.6	0.7	15.8	73.8
125	2.5	0.7	1.4	11.8	2.9	5.8	41.8	83.3	4.8	19.4	1.0	22.8	78.5
125	5	0.6	1.3	10.5	2.3	4.8	41.8	87.9	2.9	12.3	0.9	21.5	69.5
125	10	0.8	1.7	13.7	1.5	3.1	42.4	87.5	3.8	14.5	1.1	23.0	71.0
125	15	1.0	1.9	15.9	2.2	4.5	42.1	85.8	3.8	15.2	1.0	21.7	74.3
175	0.5	1.0	2.3	15.9	2.2	5.2	35.1	83.3	3.9	16.5	1.0	26.2	73.1
175	1	1.0	2.2	16.7	2.5	5.4	40.2	86.6	2.7	11.2	0.8	19.3	69.5
175	2.5	1.2	2.8	20.5	1.6	3.7	36.2	82.8	4.7	19.9	1.2	29.8	73.9
175	5	0.9	2.2	15.7	2.7	6.4	31.0	73.5	7.5	31.9	1.2	30.5	83.7
175	10	1.0	2.1	17.0	2.0	4.1	42.4	86.3	3.7	15.9	1.0	26.1	72.4
175	15	1.3	2.8	21.9	2.1	4.5	36.8	79.4	6.1	27.1	1.0	26.9	83.4
225	0.5	1.2	2.2	20.0	2.2	4.1	46.4	86.5	3.8	15.4	1.0	18.4	74.0
225	1	1.0	1.9	17.2	2.5	4.6	47.3	87.2	3.4	14.1	1.0	19.0	70.1
225	2.5	1.2	2.3	20.2	1.7	3.3	43.7	84.9	4.9	19.8	1.2	21.9	75.9
225	5	1.0	1.8	15.9	2.2	4.3	44.0	85.6	4.3	20.6	1.1	22.7	74.6
225	10	1.1	2.3	18.0	1.9	4.0	40.3	84.4	4.5	19.9	1.1	20.0	76.3
225	15	1.0	2.3	17.4	1.8	3.9	38.7	83.9	4.6	23.7	0.9	19.3	80.1
Nannochloropsis													
225	15	1.4	2.7	48.2	94.0	1.0	1.9	13.7	0.7	0.3	0.5	7.1	64.9
Spirulina													
225	15	0.5	1.3	8.6	1.8	4.5	36.3	90.0	1.7	24.9	0.3	15.3	83.9

[a] 1-(dry solid weight / wet solid weight).

Table A.5: Yield data for single-stage HTL of three algal strains.

Yields given as percentage of initial slurry, unless specified.

Stage 2 Conditions		Oil Phase		Gas Phase and Losses		Aqueous Phase		Solid Phase			
Temp	Duration	Wt	Yield	Wt	Yield	Wt	Yield	Wet Solid	Dry Solid		Est. Water Content[a]
(°C)	(min)	(g)	(% DAF feed)	(g)	(%)	(g)	(%)	Wt (g)	Wt (g)	Yield (% DAF feed)	(%)
UGA Consortium											
350	15	1.6	27.1±3.9	2.1	4.7	38.9	83.2	4.0	1.1	17.6	ND
350	30	1.8	30.4±2.2	3.3	7.1	37.0	80.1	4.5	1.1	17.6	ND
350	60	1.6	26.9±3.5	2.5	5.3	36.5	79.0	5.9	1.1	17.6	ND
350	90	1.6	26.2±5.6	2.6	5.6	38.4	83.2	4.1	1.0	16.7	ND
350	120	1.5	25.6±2.7	2.7	5.8	38.4	83.1	4.5	1.1	17.6	ND
Spirulina											
350	15	1.9	31.0±1.0	2.1	4.5	42.4	89.8	0.8	0.3	4.6	ND
350	30	1.9	31.3±1.9	3.1	6.9	40.4	88.3	ND	0.3	4.6	ND
350	60	1.8	29.3±8.3	3.0	6.6	40.5	87.6	ND	0.5	7.6	ND
350	90	1.7	29.1±5.4	2.5	5.4	41.7	90.0	ND	0.4	6.7	ND
350	120	2.2	37.4±3.5	3.4	7.4	40.2	87.1	ND	0.3	4.6	ND
275	90	1.3	22.5	3.3	7.2	40.6	88.5	0.6	0.3	4.6	ND
300	90	2.0	33.5	2.8	6.1	39.9	86.8	0.6	0.1	2.2	ND
325	90	1.9	29.8	2.7	5.8	40.1	86.1	1.0	0.3	4.6	ND
Nannochloropsis											
350	60	1.6	23.7	2.3	4.9	42.2	89.9	0.8	0.2	2.9	75.6

[a]1-(dry solid weight / wet solid weight).

Table A.6: Yield data for multi-stage PT/HTL/HDO of *Nannochloropsis* after HDO stage.

Yields given as percentage of initial slurry, unless specified.

Stage Combination			Catalyst		HDO Agitation	Oil Phase		Gas Phase[b]		Aqueous Phase		Solid Phase			
PT	HTL	HDO	Loading	Identity		Wt	Yield	Wt	Yield	Wt	Yield	Wet Solid	Dry Solid[c]		Est. WC[a]
			(% w/w)		(RPM)	(g)	(% DAF feed)	(g)	(%)	(g)	(%)	Wt (g)	Wt (g)	Yield (% DAF feed)	(%)
		x	10	Ru/C	300	1.9	27.1	2.8	6.0	40.6	86.5	1.7	0.9	12.7	47.6
		x	10	RRM	300	1.7	24.6	2.8	6.0	41.6	88.5	0.9	0.5	6.8	48.9
x		x	10	Ru/C	300	0.7	10.7	2.1	5.4	34.5	89.1	1.4	0.6	8.5	56.6
x		x	10	RRM	300	0.7	10.1	2.0	5.0	35.9	90.3	1.2	0.5	7.5	55.2
	x	x	10	Ru/C	300	1.3	18.4	1.9	4.3	40.2	90.4	1.1	0.6	8.2	47.7
	x	x	10	RRM	300	1.6	22.7	2.0	4.6	39.2	89.3	1.1	0.7	9.6	42.1
x	x	x	10	Ru/C	300	0.6	9.0	0.3	0.7	42.1	93.6	2.0	0.7	9.4	66.8
x	x	x	10	RRM	300	1.9	27.2	0.5	1.1	41.6	91.5	1.5	0.6	8.1	62.7
x		x	30	Ru/C	300	0.8	12.0	2.2	4.5	41.7	85.3	4.2	2.0	29.1	51.8
x		x	30	RRM	300	1.5	22.0	1.6	3.4	40.4	86.6	3.1	1.8	25.6	43.3
	x	x	30	Ru/C	300	2.0	28.9	0.9	2.0	37.1	83.0	4.7	2.2	31.5	53.6
	x	x	30	RRM	300	2.2	31.5	1.2	2.7	39.0	86.8	2.5	1.6	22.9	37.8
x	x	x	30	Ru/C	300	0.9	12.3	0.9	2.0	39.9	86.5	4.5	2.0	28.2	56.5
x	x	x	30	RRM	300	1.4	19.8	0.6	1.3	42.0	89.6	2.9	1.6	22.4	46.9
x	x	x	30	CoMo	300	ND	ND	0.2	0.5	44.3	99.5	ND	ND	ND	ND
x	x	x	30	CoMo-H2	300	ND	ND	0.1	0.2	44.2	99.8	ND	ND	ND	ND
x	x	x	30	Ru/C	500	1.6	22.7	0.2	0.4	33.7	76.8	8.4	2.4	34.3	71.9
x	x	x	30	Ru/C	700	1.6	22.6	0.7	1.6	37.9	84.5	4.7	1.8	25.6	62.1

[a]Water Content: 1-(dry solid weight / wet solid weight). [b]Includes losses from reactor transfer. [c]Includes catalyst weight.

Table A.7: Yield data for multi-stage PT/HTL/HDO of *UGA Consortium* after HDO stage.

Yields given as percentage of initial slurry, unless specified.

Stage Combination			Catalyst		HDO Agitation	Oil Phase		Gas Phase[b]		Aqueous Phase		Solid Phase			
PT	HTL	HDO	Loading	Identity		Wt	Yield	Wt	Yield	Wt	Yield	Wet Solid	Dry Solid[c]		Est. WC[a]
			(% w/w)		(RPM)	(g)	(% DAF feed)	(g)	(%)	(g)	(%)	Wt (g)	Wt (g)	Yield (% DAF feed)	(%)
		x	10	Ru/C	300	1.2	20.6	2.3	5.9	31.7	81.0	3.2	1.2	20.6	61.1
		x	10	RRM	300	1.5	25.3	2.7	6.8	31.1	78.1	3.8	1.2	19.8	69.1
x		x	10	Ru/C	300	0.6	9.5	1.8	4.5	31.0	77.5	5.9	1.2	ND	80.1
x		x	10	RRM	300	0.6	10.6	2.4	5.3	35.0	78.0	6.1	0.3	ND	95.3
	x	x	10	Ru/C	300	1.3	22.1	1.0	2.2	37.4	82.9	4.7	1.0	ND	78.7
	x	x	10	RRM	300	1.6	26.2	1.1	2.4	36.3	80.1	5.7	-0.5	ND	109.6
x	x	x	10	Ru/C	300	0.4	6.1	1.7	4.5	32.6	85.6	2.7	0.6	ND	79.1
x	x	x	10	RRM	300	1.0	16.3	1.2	2.8	36.6	84.4	3.9	0.6	ND	85.1
x		x	30	Ru/C	300	0.8	13.8	3.4	7.4	34.2	74.4	5.5	0.4	ND	92.3
x		x	30	RRM	300	2.3	37.7	2.6	5.6	32.3	69.4	7.3	0.5	ND	93.2
	x	x	30	Ru/C	300	1.5	24.3	1.2	2.7	34.1	75.9	6.1	1.1	ND	81.2
	x	x	30	RRM	300	1.8	30.6	1.3	2.9	34.5	76.5	5.4	1.1	ND	79.1
x	x	x	30	Ru/C	300	1.0	17.3	0.7	1.6	36.4	84.0	4.5	0.6	ND	87.4
x	x	x	30	RRM	300	3.2	53.7	1.2	2.5	39.7	83.1	3.0	0.2	ND	94.6
x	x	x	30	Ru/C	500	1.3	22.2	1.1	2.3	37.0	80.3	6.7	2.5	41.4	62.9
x	x	x	30	Ru/C	700	1.0	17.2	1.0	2.3	35.7	81.8	5.9	2.4	40.5	59.0

[a]Water Content: 1-(dry solid weight / wet solid weight). [b]Includes losses from reactor transfer. [c]Assumes full catalyst recover, calc. by subtraction.

Table A.8: Yield data for multi-stage PT/HTL/HDO of *Spirulina* after HDO stage.

Yields given as percentage of initial slurry, unless specified.

Stage Combination			Catalyst		HDO Agitation	Oil Phase		Gas Phase[b]		Aqueous Phase		Solid Phase			
PT	HTL	HDO	Loading	Identity		Wt	Yield	Wt	Yield	Wt	Yield	Wet Solid	Dry Solid[c]		Est. WC[a]
			(% w/w)		(RPM)	(g)	(% DAF feed)	(g)	(%)	(g)	(%)	Wt (g)	Wt (g)	Yield (% DAF feed)	(%)
		x	10	Ru/C	300	1.2	20.1	3.1	7.9	33.0	84.3	1.1	0.2	4.0	78.9
		x	10	RRM	300	1.7	28.3	2.3	5.8	34.2	85.9	0.9	0.1	1.2	92.5
x		x	10	Ru/C	300	0.5	8.4	1.1	2.7	37.0	90.4	1.6	0.4	ND	75.5
x		x	10	RRM	300	0.9	14.4	1.0	2.5	36.5	91.7	0.7	0.0	ND	94.5
	x	x	10	Ru/C	300	1.2	19.3	0.8	1.8	41.0	91.0	1.4	0.3	ND	77.6
	x	x	10	RRM	300	1.5	25.3	2.1	4.6	40.6	89.2	0.6	0.1	ND	80.6
x	x	x	10	Ru/C	300	0.4	6.9	0.4	1.0	36.7	91.3	2.0	0.3	ND	83.0
x	x	x	10	RRM	300	0.7	11.4	0.4	1.0	37.8	94.5	0.4	-0.1	ND	117.1

[a]Water Content: 1-(dry solid weight / wet solid weight). [b]Includes losses from reactor transfer. [c]Assumes full catalyst recover, calc. by subtraction.

Table A.9: Yield data for four-stage repeated batch (PT/HTL/HDO/RB) of three algal strains after RB stage.

Yields given as percentage of initial slurry, unless specified.

Catalyst	Pretreatment	Oil Phase		Gas Phase and Losses		Aqueous Phase		Solid Phase			
Identity	Temperature	Wt	Yield	Wt	Yield	Wt	Yield	Wet Solid	Dry Solid[b]		Est. Water Content[a]
	(°C)	(g)	(% DAF feed)	(g)	(%)	(g)	(%)	Wt (g)	Wt (g)	Yield (% DAF feed)	(%)
Nannochloropsis											
Ru/C	225	0.9	14.9	1.5	3.4	37.0	83.3	5.0	2.0	33.0	60.6
Ru/C	175	3.6	52.0	0.9	2.0	37.1	80.2	4.6	1.9	27.6	58.6
CoMo-H2	225	1.2	17.2	1.0	2.2	38.4	84.8	4.7	2.2	32.4	52.3
CoMo-S	225	0.7	9.8	1.5	3.2	41.1	88.2	3.3	2.4	34.3	28.4
RRM	225	1.6	22.4	1.0	2.3	37.0	84.8	4.1	1.6	22.4	62.3
UGA Consortium											
Ru/C	225	1.3	20.9	2.4	5.3	35.0	79.0	5.7	2.0	33.4	64.8
Ru/C	175	2.5	35.5	2.2	4.5	35.4	74.4	7.6	2.5	36.3	66.9
CoMo-S	225	1.5	21.3	0.2	2.3	35.5	81.0	5.9	3.2	46.5	45.2
Ru/C Reuse	225	1.4	23.9	0.6	1.4	34.4	79.0	7.1	2.4	39.5	66.6
Spirulina											
Ru/C	225	1.2	17.4	2.0	4.5	36.6	83.2	4.2	1.5	21.7	64.5
Ru/C	175	2.0	28.8	1.9	4.2	38.1	82.4	4.2	1.5	22.0	64.0
CoMo-S	225	1.4	20.0	0.4	2.3	37.5	85.9	3.8	2.5	35.5	34.8

[a]1-(dry solid weight / wet solid weight). [b]Includes catalyst weight.

Table A.10: Yield data for single-stage and two-stage conversion (HTL and HDO) of varying model compound arrangements after the final stage.

Yields given as percentage of initial slurry, unless specified.

Representation	Oil Phase		Gas Phase and Losses		Aqueous Phase		Solid Phase			
	Wt	Yield	Wt	Yield	Wt	Yield	Wet Solid	Dry Solid		Est. Water Content
	(g)	(% dry feed)	(g)	(%)	(g)	(%)	Wt (g)	Wt (g)	Yield (% dry feed)	(%)
Single-stage HTL										
Only Lipid	10.4	104.1	0.8	1.6	38.5	76.9	0.3	0.0	0.2	93.8
Only Carb.	1.4	13.5	5.3	10.6	33.8	67.4	9.7	3.3	32.8	66.0
Only Protein	2.9	28.7	3.9	7.8	41.6	83.2	1.6	0.1	1.4	91.3
No Protein	5.9	58.5	3.4	6.8	35.3	70.7	5.4	2.4	24.3	54.7
No Carb.	3.1	31.2	4.2	8.4	41.0	81.9	1.7	0.1	1.1	93.6
No Lipid	3.2	32.3	4.9	9.8	40.6	81.1	1.3	0.5	5.0	62.7
Equal Parts	9.0	90.4	3.7	7.4	35.1	70.3	2.1	0.6	6.0	71.8
Spirulina platensis	6.8	67.8	2.6	5.2	40.4	80.4	0.5	0.1	0.7	85.7
Nannochloropsis sp.	8.2	81.8	4.8	9.6	36.7	73.3	0.4	0.0	0.4	89.5
Two-stage HTL and HDO										
Only Lipid	7.1	70.5	ND	ND	35.7	72.5	6.2	2.0	20.0	67.6
Only Carb.	1.3	12.8	0.3	0.7	26.4	59.0	16.8	5.0	50.1	70.1
Only Protein	3.9	39.1	3.4	7.4	30.7	66.6	8.1	2.8	27.7	65.7
No Protein	4.6	45.9	2.6	5.6	29.1	62.5	10.3	3.4	33.7	67.3
No Carb.	19.5	194.8	0.6	1.3	9.3	20.2	16.5	5.0	49.5	69.9
No Lipid	1.5	15.4	1.6	3.5	33.6	74.4	8.4	3.4	33.6	60.0
Equal Parts	ND	ND	3.0	6.5	29.5	63.8	13.8	2.9	28.5	79.3
Spirulina platensis	11.9	119.2	3.7	7.8	24.5	51.6	7.3	2.8	27.7	62.1
Nannochloropsis sp.	15.7	156.9	2.9	6.4	14.1	31.3	12.5	3.7	37.3	70.1
Only Lipid[a]	ND	ND	1.4	3.1	44.8	96.9	ND	ND	ND	ND
No Protein[a]	ND	ND	0.2	0.5	43.5	99.5	ND	ND	ND	ND
Equal Parts[a]	ND	ND	1.3	3.1	42.1	96.9	ND	ND	ND	ND

[a]HDTC catalyst used instead of Ru/C.

Bibliography

Abdelmoez, W., Nakahasi, T., and Yoshida, H. (2007). Amino acid transformation and decomposition in saturated subcritical water conditions. *Industrial and Engineering Chemistry Research*, 46:5286–5294.

Alba, L. G., Torri, C., Fabbri, D., Kersten, S. R., and Brilman, D. W. W. (2013). Microalgae growth on the aqueous phase from hydrothermal liquefaction of the same microalgae. *Chemical Engineering Journal*, 228:214–223.

Alba, L. G., Torri, C., Samori, C., van der Spek, J., Fabbri, D., Kersten, S. R. A., and Brilman, D. W. F. W. (2012). Hydrothermal treatment (htt) of microalgae: Evaluation of the process as conversion method in an algae biorefinery concept. *Energy and Fuels*, 26:642–657.

Anastasakis, K. and Ross, A. (2011). Hydrothermal liquefaction of the brown macro-alga laminaria saccharina: Effect of reaction conditions on product distribution and composition. *Bioresource Technology*, 102:4876–4883.

Andrew A. Peterson, Russell P. Lachance, J. W. T. (2010). Kinetic evidence of the maillard reaction in hydrothermal biomass processing: Glucose-glycine interactions in high-temperature, high-pressure water. *Industrial and Engineering Chemistry Research*, 49:2107–2117.

Babadzhanov, A. S., Abdusamatova, N., Yusupova, F. M., Faizullaeva, N., Mezhlumyan, L. G., and Malikova, M. K. (2004). Chemical composition of spirulina platensis cultivated in uzbekistan. *Chemistry of Natural Compounds*, 40(3):276–279.

Bai, X., Duan, P., Xu, Y., Zhang, A., and Savage, P. E. (2014). Hydrothermal catalytic processing of pretreated algal oil: A catalyst screening study. *Fuel*, 120:141–149.

Balakrishnan, M., Batra, V. S., Hargreaves, J. S. J., and Pulford, I. D. (2011). Waste materials catalytic opportunities: an overview of the application of large scale waste materials as resources for catalytic applications. *Green Chemistry*, 13:16–24.

Barreiro, D. L., Samori, C., Terranella, G., Hornung, U., Kruse, A., and Prins, W. (2014). Assessing microalgae biorefinery routes for the production of biofuels via hydrothermal liquefaction. *Bioresource Technology*, 174:256–265.

Becker, E. (2007). Micro-algae as a source of protein. *Biotechnology Advances*, 25:207–210.

Behrendt, F., Neubauer, Y., Oevermann, M., Wilmes, B., and Zobel, N. (2008). Direct liquefaction of biomass. *Chemical Engineering Techology*, 31(5):667–677.

Biller, P., Riley, R., and Ross, A. (2011). Catalytic hydrothermal processing of microalgae: decomposition and upgrading of lipids. *Bioresource Technology*, 102:4841–4848.

Biller, P. and Ross, A. (2011). Potential yields and properties of oil from the hydrothermal liquefaction of microalgae with different biochemical content. *Bioresource Technology*, 102:215–225.

Biller, P., Ross, A., Skill, S., Lea-Langton, A., Balasundaram, B., Hall, C., Riley, R., and Llewellyn, C. (2012). Nutrient recycling of aqueous phase for microalgae cultivation from the hydrothermal liquefaction process. *Algal Research*, 1:70–76.

Bradford, M. M. (1976). A rapid and sensitive method for the quantitation of microgram quantities of protein utilizing the principle of protein-dye binding. *Analytical Biochemistry*, 72:248–254.

Brown, M. R. (1991). The amino-acid and sugar composition of 16 species of microalgae used in mariculture. *J. Exp. Mar. Biol. Ecol.*, 145:79–99.

Brown, T., Duan, P., and Savage, P. (2010). Hydrothermal liquefaction and gasication of nannochloropsis sp. *Energy and Fuels*, 24:3639–3646.

Carpenter, D. L., Lehmann, J., Mason, B. S., and Slover, H. T. (1976). Lipid composition of select vegetable oils. *Journal of the American Oil Chemists' Society*, 53(12):713–718.

Chakraborty, M., Miao, C., McDonald, A., and Chen, S. (2012). Concomitant extraction of bio-oil and value added polysaccharides from chlorella sorokiniana using a unique sequential hydrothermal extraction technology. *Fuel*, 95:63–70.

Changi, S. M. (2012). *Hydrothermal Reactions of Algae Model Compounds*. Thesis.

Chen, C.-Y., Zhao, X.-Q., Yen, H.-W., Ho, S.-H., Cheng, C.-L., Lee, D.-J., Bai, F.-W., and Chang, J.-S. (2013). Microalgae-based carbohydrates for biofuel production. *Biochemical Engineering Journal*, 78:1–10.

Chen, M., Tang, H., Ma, H., Holland, T. C., Ng, K. S., and Salley, S. O. (2011). Effect of nutrients on growth and lipid accumulation in the green algae dunaliella teriolecta. *Bioresource Technology*, 102:1649–1655.

Chisti, Y. (2013). Constrains to commercialization of algal fuels. *Journal of Biotechnology*, 167:201–214.

Corbitt, R. A. (1999). *Standard Handbook of Environmental Engineering*. McGraw-Hill Inc., New York, 2nd edition.

Demirbas, A. (2010). Use of algae as biofuel sources. *Energy Conversion and Management*, 51:2738–2749.

Devi, M. A., Subbulakshmi, G., Devi, K. M., , and Venkataraman, L. V. (1981). Studies on the proteins of mass-cultivated, blue-green alga (spirulina platensis). *J. Agric. Food Chem*, 29:522–525.

Dong, D., Jeong, S., and Massoth, F. (1997). Effect of nitrogen compounds on deactivation of hydrotreating catalysts by coke. *Catalysis Today*, 37:267–275.

Dote, Y., Inoue, S., Ogi, T., and ya Yokoyama, S. (1998). Distribution of nitrogen to oil products from liquefaction of amino acids. *Bioresource Technology*, 64:157–160.

Duan, P. and Savage, P. (2010). Hydrothermal liquefaction of a microalga with heterogeneous catalysts. *Industrial and Engineering Chemistry Research*, pages 1899–1906.

Duan, P. and Savage, P. E. (2011). Catalytic hydrothermal hydrodenitrogenation of pyridine. *Applied Catalysis B: Environmental*, 108-109:54–60.

Elliott, D. C., Hart, T. R., Schmidt, A. J., Neuenschwander, G. G., Rotness, L. J., Olarte, M. V., Zacher, A. H., Albrecht, K. O., Hallen, R. T., and Holladay, J. E. (2013). Process development for hydrothermal liquefaction of algae feedstocks in a continuous-ow reactor. *Algal Research*.

Fujii, T., Khuwijitjaru, P., Kimura, Y., and Adachi, S. (2006). Decomposition kinetics of monoacyl glycerol and fatty acid in subcritical water under temperature-programmed heating conditions. *Food Chemistry*, 94:341–347.

Funazukuri, T. and Nagamori, M. (2004). Glucose production by hydrolysis of starch under hydrothermal conditions. *Journal of Chemical Technology and Biotechnology*, 79:229–233.

Galadima, A. and Muraza, O. (2014). Biodiesel production from algae by using heterogeneous catalysts: a critical review. *Energy*, 78:72–83.

Garcia, J. R., Fernandez, F. A., and Sevilla, J. F. (2012). Development of a process for the production of l-amino-acids concentrates from microalgae by enzymatic hydrolysis. *Bioresource Technology*, 112:164–170.

Garcia-Moscoso, J. L., Obeid, W., Kumar, S., and Hatcher, P. G. (2013). Flash hydrolysis of microalgae (scenedesmus sp.) for protein extraction and production of biofuels intermediates. *The Journal of Supercritical Fluids*, 82:183–190.

Grima, E. M., Sevilla, F., Mara, J., Fernndez, A., Gabriel, F., and Flickinger, M. C. (2009). *Microalgae, Mass Culture Methods*. Encyclopedia of Industrial Biotechnology. John Wiley and Sons, Inc.

Gunawan, R., Li, X., Lievens, C., Gholizadeh, M., Chaiwat, W., Hu, X., Mourant, D., Bromly, J., and Li, C.-Z. (2013). Upgrading of bio-oil into advanced biofuels and chemicals. part i. transformation of gc-detectable light species during the hydrotreatment of bio-oil using pd/c catalyst. *Fuel*, 111:709–717.

Gungor, A., Onenc, S., Ucar, S., and Yanik, J. (2012). Comparison between the one-step and two-step catalytic pyrolysis of pine bark. *Journal of Analytical and Applied Pyrolysis*, 97:39–48.

Hakim, S. H., Shanks, B. H., and Dumesic, J. A. (2013). Catalytic upgrading of the light fraction of a simulated bio-oil over cezrox catalyst. *Applied Catalysis B: Environmental*, 142-143:368–376.

Jazrawi, C. et al. (2013). Pilotplant testing of continuous hydrothermal liquefaction of microalgae. *Algal Research*.

Jena, U. and Das, K. (2011). Comparative evaluation of thermochemical liquefaction and pyrolysis for bio-oil production from microalgae. *Energy and Fuels*, 25:5472–5482.

Jena, U., Das, K., and Kastner, J. (2011a). Effect of operating conditions of thermochemical liquefaction on biocrude production from spirulina platensis. *Bioresource Technology*, 102:6221–6229.

Jena, U., Vaidyanathan, N., Chinnasamy, S., and Das, K. (2011b). Evaluation of microalgae cultivation using recovered aqueous co-product from thermochemical liquefaction of algal biomass. *Bioresource Technology*, 102:3380–3387.

Jones, S., Zhu, Y., Anderson, D., Hallen, R., Elliot, D., Schmidt, A., Albrecht, K., Hart, T., Butcher, M., Drennan, C., Snowden-Swan, L., Davis, R., and Kinchin, C. (2014). Process design and economics for the conversion of algal biomass to hydrocarbons: Whole algae hydrothermal liquefaction and upgrading.

Karimi, E., Gomez, A., Kycia, S. W., , and Schlaf, M. (2010). Thermal decomposition of acetic and formic acid catalyzed by red mud; implications for the potential use of red mud as a pyrolysis bio-oil upgrading catalyst. *Energy and Fuels*, 24:2747–2757.

Laird, D. A., Brown, R. C., Amonette, J. E., and Lehmann, J. (2009). Review of the pyrolysis platform for coproducing bio-oil and biochar. *Biofuels, Bioproducts and Biorefining*, 3(5):547–562.

Lamoolphak, W., Goto, M., Sasaki, M., Suphantharika, M., Muangnapoh, C., Prommuag, C., and Shotipruk, A. (2006). Hydrothermal decomposition of yeast cells for production of proteins and amino acids. *Journal of Hazardous Materials*, B137:1643–1648.

Laredo, G. C., López, C. R., Alvarez, R. E., and Cano, J. L. (2004). Naphthenic acids, total acid number and sulfur content profile characterization in isthmus and maya crude oils. *Fuel*, 83(11):1689–1695.

Laurent, E. and Delmon, B. (1993). Influence of oxygen-, nitrogen-, and sulfur-containing compounds on the hydrodeoxygenation of phenols over sulfided como/y-al2o3 and nimo/y-al2o3 catalysts. *Industrial and Engineering Chemistry Research*, 32:2516–2524.

Leckel, D. (2009). Diesel production from fischer-trophsch: The past, the present, and new concepts. *Energy and Fuels*, 23(2342-2358).

Loureno, S. O., Barbarino, E., Marquez, U. M. L., and Aidar, E. (1998). Distribution of intracellular nitrogen in marine microalgae: Basis for the calculation of specific nitrogen-to-protein conversion factors. *J. Phycol.*, 34:798–811.

Luijkx, G. C., van Rantwijk, F., and van Bekkum, H. (1993). Hydrothermal formation of 1,2,4-benzenetriol from 5-hydroxymethyl-2-furaldehyde and d-fructose. *Carbohydrate Research*, 242:131–139.

Man, Y. C., Haryati, T., Ghazali, H., and Asbi, B. (1999). Composition and thermal profile of crude palm oil and its products. *JAOCS*, 26(2):237–242.

Manning, F. S. and Thompson, R. E. (1995). Oilfield processing of petroleum: Crude oil.

Maschio, G., Koufopanos, C., and Lucchesi, A. (1992). Pyrolysis, a promising route for biomass utilization. *Bioresource Technology*, 42(219-231).

Mazaheri, H., Lee, K. T., Bhatia, S., and Mohamed, A. R. (2010). Subcritical water liquefaction of oil palm fruit press fiber for the production of bio-oil: Effect of catalysts. *Bioresource Technology*, 101(2):745–751.

McGarry, M. G. and Tongkasame, C. (1971). Water reclamation and algae harvesting. *Water Pollution Control Federation*, 43(5):824–835.

Mederos, F. S., Ancheyta, J., and Elizalde, I. (2012). Dynamic modeling and simulation of hydrotreating of gas oil obtained from heavy crude oil. *Applied Catalysis A: General*, 425-426:13–27.

Miao, C., Chakraborty, M., Dong, T., Yu, X., Chi, Z., and Chen, S. (2014). Sequential hydrothermal fractionation of yeast cryptococcus curvatus biomass. *Bioresource Technology*, 164:106–112.

MILNER, H. A. S. and HAROLD, W. (1948). The chemical composition of chlorella; effect of environmental conditions. *American Society of Plant Biologists*, pages 120–149.

Minowa, T., Kondo, T., and Sudirjo, S. T. (1998). Thermochemical liquefaction of indonesian biomass residues. *Biomass and Bioenergy*, 14(5/6):517–524.

Minowa, T. and Sawayama, S. (1999). A novel microalgal system for energy production with nitrogen cycling. *Fuel*, 78:1213–1215.

Na, J.-G., Yi, B. E., Han, J. K., Oh, Y.-K., Park, J.-H., Jung, T. S., Han, S. S., Yoon, H. C., Kim, J.-N., Lee, H., and Ko, C. H. (2012). Deoxygenation of microalgal oil into hydrocarbon with precious metal catalysts: Optimization of reaction conditions and supports. *Energy*, 47:25–30.

o Matsui, T., Nishihara, A., Ueda, C., Ohtsuki, M., , oki Ikenaga, S. N., and Toshimitsu (1997). Liquefaction of micro-algae with iron catalyst. *Fuel*, 76(11):1043–1048.

Olcese, R. N., Francois, J., Bettahar, M. M., Petitjean, D., and Dufour, A. (2013). Hydrodeoxygenation of guaiacol, a surrogate of lignin pyrolysis vapors, over iron based catalysts: Kinetics and modeling of the lignin to aromatics integrated process. *Energy and Fuels*, 27:975–984.

Oliveira, M. D., Monteiro, M.P.C., Robbs, P.G., and Leite, S.G.F (1999). Growth and chemical composition of spirulina maxima and spirulina platensis biomass at different temperatures. *Aquaculture International*, 7:261–275.

Olsen, T. (2014). An oil refinery walk-through. *Chemical Engineering Process*, (May 2014):34–40.

Peng, B., Zhao, C., Kasakov, S., Foraita, S., and Lercher, J. A. (2013). Manipulating catalytic pathways: Deoxygenation of palmitic acid on multifunctional catalysts. *Chem. Eur. J.*, 19:4732 – 4741.

Putt, R., Singh, M., Chinnasamy, S., and Das, K. (2011). An efficient system for carbonation of high-rate algae pond water to enhance co2 mass transfer. *Bioresource Technology*, 102:3240–3245.

Richmond, S. B. and E., A. (1979). Isolation and characterization of phycocyanins from the blue-green alga spirulina platensis. *Arch. Microbiol.*, 120:155–159.

Rogalinski, T., Herrmann, S., and Brunner, G. (2005). Production of amino acids from bovine serum albumin by continuous sub-critical water hydrolysis. *J. of Supercritical Fluids*, 36:49–58.

Rogalinski, T., Liu, K., Albrecht, T., and Brunner, G. (2008). Hydrolysis kinetics of biopolymers in subcritical water. *J. of Supercritical Fluids*, 46:335–341.

Ross, A., Biller, P., Kubacki, M., Li, H., Lea-Langton, A., and Jones, J. (2010). Hydrothermal processing of microalgae using alkali and organic acids. *Fuel*, 89:2234–2243.

Salimath, K. M., Shekharam, L. V., and Venkataraman, P. V. (1987). Carbohydrate composition and characterization of two unusual sugars from the blue green alga, spirulina platensis. *Phytochemistry*, 26(8):2267–2269.

Sandbank, E. and Shelef, G. (1987). Harvesting of algae from high rate ponds by flocculation flotation. *Wat. Sci. Tech.*, 19(12):257–263.

Santillan-Jimenez, E. and Crocker, M. (2012). Catalytic deoxygenation of fatty acids and their derivatives to hydrocarbon fuels via decarboxylation/decarbonylation. *J Chem Technol Biotechnol*, 87:1041–1050.

Sato, N., Quitain, A. T., Kang, K., Daimon, H., and Fujie, K. (2004). Reaction kinetics of amino acid decomposition in high-temperature and high-pressure water. *Industrial and Engineering Chemistry Research*, 43(13):3217–3222.

Savage, P. E. and Duan, P. (2011). Catalytic treatment of crude algal bio-oil in supercritical water: optimization studies. *Energy and Environmental Science*, 4:1447–1456.

Shende, R. and Tungal, R. (2013). Subcritical aqueous phase reforming of wastepaper for biocrude and h2 generation. *Energy Fuels*, 27:3194–3203.

Simo, C., Herrero, M., Neusub, C., Pelzing, M., Kenndler, E., Barbas, C., Ibanez, E., and Cifuentes, A. (2005). Characterization of proteins from spirulina platensis microalga using capillary electrophoresis-ion trap-mass spectrometry and capillary electrophoresis-time of flight-mass spectrometry. *Electrophoresis*, 26:2674–2683.

S.P. Slocombe, e. a. (2013). A rapid and general method for measurement of protein in micro-algal biomass. *Bioresource Technology*, 129:51–57.

Srokol, Z., Bouche, A.-G., van Estrik, A., Strik, R. C. J., Maschmeyer, T., and Peters, J. A. (2004). Hydrothermal upgrading of biomass to biofuel; studies on some monosaccharide model compounds. *Carbohydrate Research*, 339:1717–1726.

Stein, W. H. (1949). Amino acid composition of b-lactoglobulin and bovine serum albumin. *The Journal of Biological Chemistry*, 178:79–91.

Sushil, S. and Batra, V. S. (2008). Catalytic applications of red mud, an aluminium industry waste: A review. *Applied Catalysis B: Environmental*, 81:64–77.

Taimoor, A. A., Favre-Reguillon, A., Vanoye, L., and Pitault, I. (2012). Upgrading of biomass transformation residue: inuence of gas ow composition on acetic acid ketonic condensation. *Catalysis Science and Technology*, 2:359–363.

Toor, S., Rosendahl, L., and Rudolf, A. (2011). Hydrothermal liquefaction of biomass: a review of subcritical water technologies. *Energy*, 36:2328–2342.

Torzillo, G., Pushparaj, B., Bocci, F., Balloni, W., Materassi, R., and Florenzano, G. (1986). Production of spirulina biomass in closed photobioreactors. *Biomass*, 11:61–74.

Tran, N., Bartlett, J., Kannangara, G., Milev, A., Volk, H., and Wilson, M. (2010). Catalytic upgrading of biorefinery oil from micro-algae. *Fuel*, 89:265–274. Review article, mostly on cracking and transesterification upgrades.

Valdez, P. J., Dickinson, J. G., and Savage, P. E. (2011). Characterization of product fractions from hydrothermal liquefaction of nannochloropsis sp. and the influence of solvents. *Energy Fuels*, 25:3235–3243.

Valdez, P. J., Nelson, M. C., Wang, H. Y., Lin, X. N., and Savage, P. E. (2012). Hydrothermal liquefaction of nannochloropsis sp.: Systematic study of process variables and analysis of the product fractions. *Biomass and Bioenergy*, 46:317–331.

Valdez, P. J. and Savage, P. E. (2013). A reaction network for the hydrothermal liquefaction of nannochloropsis sp. *Algal Research*, 2:416–425.

Van Eykelenburg, C. (1977). On the morphology and ultrastructure of the cell wall of spirulina platensis. *Antonie van Leeuwenhoek*, 43(2):89–99.

Yin, S., Dolan, R., Harris, M., and Tan, Z. (2010). Subcritical hydrothermal liquefaction of cattle manure to bio-oil: Effects of conversion parameters on bio-oil yield and characterization of bio-oil. *Bioresource Technology*, 101(10):3657–3664.

Zacher, A. H., Olarte, M. V., Santosa, D. M., Elliott, D. C., and Jones, S. B. (2014). A review and perspective of recent bio-oil hydrotreating research. *Green Chemistry*, 16:491–515.

Zhanga, J., Chen, W.-T., Zhang, P., Luo, Z., and Zhang, Y. (2013). Hydrothermal liquefaction of chlorella pyrenoidosa in sub- and supercritical ethanol with heterogeneous catalysts. *Bioresource Technology*, 133:389–397.